In the Name of Allah

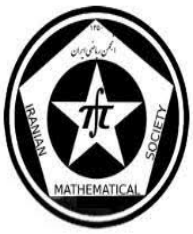

Proceedings of the 1st Annual National Conference on Biomathematics

12-13 March 2019

University of Neyshabur

Neyshabur, Iran

Preface

In the Name of Allah, the merciful and compassionate

We found the success of holding the first National Conference on biomathematics at the University of Neyshabur with the great effort of professors and students and supporting of the Department of Mathematics and Statistics, as well as the authorities of the University of Neyshabur and various organizations of the country. By presenting the latest scientific achievements and creating an atmosphere of discussion between academics, researchers and experts in this field, a stronger relationship between the academics of the Ministries of Science, Research and Technology and Health, Treatment and Medical Education has provided which will led to a more favourable quality of people's life. In this conference 3 key lectures "On optimal prescribing of Tamoxifen in controlling bone metastases", "Modelling the outcome of AIDS patients infected by differential equations" and "Analyzing single cells" were presented by the invited professors. Applicants attending the conference sent 62 papers to the secretariat, among which the scientific committee of the conference along with judges, accepted 24 articles as lectures, 27 papers as poster presentation and 1 subject as presenting workshop.

We sincerely appreciate the professors of universities throughout the country, especially members of the executive and scientific committees which their collaboration in proposing the useful suggestions has been a great help to make better the conference and the scientific texts of this book. In the end, the scientific committee deeply appreciate the honest efforts of all the officials, faculty and students of the department of mathematics and statistics, faculty of sciences and the staff of various parts of the University of Neyshabur.

Academic Committee
March 2019

Excutive Committee

Dr. Reza Mohammadi	University of Neyshabur
Dr. Mojhgan Afkhami Goli	University of Neyshabur
Dr. Ehsan Anjidani	University of Neyshabur
Dr. Bahareh Khatib Astaneh	University of Neyshabur
Dr. Mohammad Hossein Rahmani Doust	University of Neyshabur
Dr. Mohammad Shirazian	University of Neyshabur
Dr. Seyyed Mohsen Saleh	University of Neyshabur
Dr. Seyyed Mahdi Salehi	University of Neyshabur
Dr. Davoud Emarati Moghaddam	University of Neyshabur

Academic Committee

Dr. Seyyed Mohsen Saleh	University of Neyshabur
Dr. Rouzbeh Abedini Nasab	University of Neyshabur
Dr. Habibollah Esmaily	Mashhad University of Medical Sciences
Dr. Abbas Fakhari Ghouchani	Shahid Beheshti University
Dr. Ali Reza Fakharzadeh Jahromi	Shiraz University of Technology
Dr. Fatemeh Helen Ghane Ostadghasemi	Ferdowsi University of Mashhad
Dr. Atenna Ghasemabadi	Esfarayen Univercity of Technology
Dr. Mahdieh Ghasemi	University of Neyshabur
Dr. Mahmoud Hesaraki	Sharif University of Technology
Dr. Javad Jamalzadeh	University of Sistan and Baluchestan
Dr. Hosein Kheiri	University of Tabriz
Dr. Mohammad Reza Mahmoudi	Fasa University
Dr. Mohammad Reza Molaei	Shahid Bahonar University of Kerman
Dr. Omid Rabiei Motlagh	University of Birjand
Dr. Mohammad Hosein Rahmani Doust	University of Neyshabur
Dr. Ghasem Sadeghi Bajestani	Imam Reza International University
Dr. Alireza Sepasian	Fasa University
Dr. Mohammad Taghi Shakeri	Mashhad University of Medical Sciences
Dr. Mosa Al Reza Shamsieh Zahedi	Payame Noor University
Dr. Mohammad Shirazian	University of Neyshabur
Dr. Ali Vahidian Kamyad	Ferdowsi University of Mashhad

Contents

Picard iteration method for ecological models; growth rate
(*Ehsan Ameli, Mohammad Hosein Rahmani Doust and Ehsan Anjidani*) . 1

Meshless method for solving a equation arisen form the spatial spread of an epidemic
(*Fatemeh Asadi-Mehregan and Pouria Assari*) 8

Minimum number of fixed points in parallel dynamical systems
(*Ali Barzanouni, Ghazaleh Malekbala and Leila Sharifan*) 15

The next generation matrix and the stability analysis of a mathematical model of cancer virotherapy
(*Masume Behruzie and Ehsan Anjidani*) 21

The modelling of advection-dispersion by fractional differential equations
(*Nader Biranvand, Esmaeil babolian and Alireza Vahidi*) 26

On a New Biological Fractional-order Lotka-Voltra Predator-Prey Model and Its Dynamical Behaviors
(*Nader Biranvand, Esmaeil babolian and Alireza Vahidi*) 34

Analysis of a disease model with two susceptible groups
(*Atena Ghasemabadi*) 41

Modelling a disease with a nonlinear incidence function
(*Atena Ghasemabadi*) 47

Backward bifurcations in epidemiological models
(*Azizeh Jabbari, Hossein Kheiri, Mohsen Jafari and Fatemeh Iranzad*) . . 55

Application of the optimal q-homotopy analysis method for solving a model for HIV infection of $CD4^+$T-cells
(*Fatemeh Kazemi and Maryam Alipour*) 63

Estimating Gompertz Survival and Hazard Functions
(*Bahareh Khatib Astaneh*) 70

Role of fractional derivative order in a model for the spread of HIV/AIDS epidemic
(***Hossein Kheiri, Mohsen Jafari, Azizeh Jabbari and Fatemeh Iranzad***) . . **76**

Persistent homology for protein folding analysis
(***Hanieh Mirebrahimi and Ameneh Babaee***) **82**

Persistent homology for prediction of protein folding
(***Hanieh Mirebrahimi and Ameneh Babaee***) **88**

Modified variational iteration method to solve a model for HIV infection of $CD4^+$T-cells
(***Pooneh Omidiniya and Maryam Alipour***) **95**

The role of disease in the prey-predator model
(***Marzieh shamsabadi, M. H. Rahmani Doust and M. Shirazian***) **100**

Comparison of the Euler and Adaptive Runge-Kutta Methods for Solving a HTLVI Mathematical Model
(***Rezaei. Zeynab, Karami. Saeed and Dadi. Zohreh***) **107**

Optimal control of chemotherapy on a cancer-obesity model
(***Mohammad Shirazian and Somayyeh Beheshti***) **114**

Numerical solutions of mathematical model on fractional Lotka-Volterra equations
(***Haleh Tajadodi***) **120**

1st Annual National Conference on Biomathematics ..... h

همایش ملی ریاضیات زیستی
اولین همایش ملی ریاضیات زیستی
۲۱ و ۲۲ اسفندماه ۱۳۹۷
دانشگاه نیشابور

Picard iteration method for ecological models; growth rate

Ehsan Ameli*, Mohammad Hosein Rahmani Doust and Ehsan Anjidani
Department of Mathematics, Neyshabur University, Neyshabur, IRAN

Abstract:

The present paper deals with the growth rates such as exponential growth rate, harvest exponential growth rate and allometric growth rate equations. First, these models are introduced and then, their solutions are investigated by picard iteration method.

Keywords: Growth Rate, Differential Equation, Ecological Modeling, Picard Iteration Method **Mathematics Subject Classification (2010):** 92D40, 45E10

1 Introduction

Ecology, basically studies the relationship between species and their environment.This study is in such areas as population changes, predator-prey and competition interactions, multi-species societies, renewable resource management and etc. The study of population changes has a very long history: Fibonacci, in his arithmetic book in 1202 set a model involving an hypothetical growing rabbit population (3).
Thomas Malthus published a book in 1798 stating that populations with unlimited natural resources grow very rapidly, after which population growth decreases as resources become depleted. This accelerating pattern of increasing population size is called exponential growth (4).

*Speaker: ameliehsan73@gmail.com

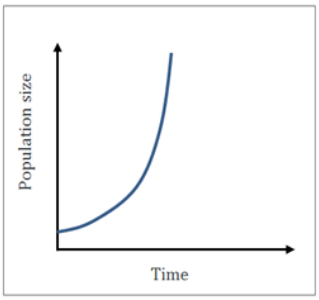

Figure 1: The exponential growth rate

Julian Huxley and Georges Teissier coined the term ″allometry″ in 1936. Allometry designates the changes in relative dimensions of parts of an organism that are correlated with changes in overall size (1).

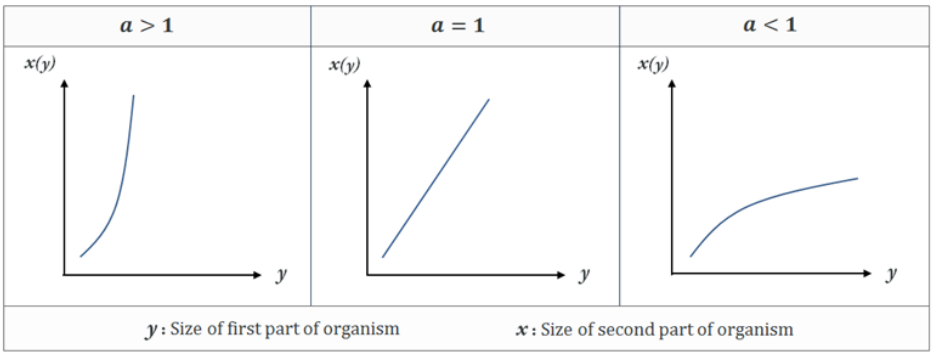

Figure 2: The allometric growth rate, $x(y) = ky^a$

In this paper, first the exponential growth rate, harvest exponential growth rate and allometric growth rate are introduced. Then, the solutions of these equations are investigated in the section of 3.

2 Preliminaries and models

2.1 The Exponential Growth Rate

Let t be as time and $x(t)$ as density of population. The exponential growth rate may be written as following form:

$$\begin{cases} x' = rx, \\ x(0) = x_0, \end{cases} \tag{2.1}$$

where r is a constant and x_0 is an initial value.
It is obvious that the solution of the above Initial Value Problem $(I.V.P)$ is given as follows:

$$x(t) = x_0 e^{rt}.$$

2.2 The Exponential Growth Rate; Having Constant Harvesting Factor

By considering constant harvesting factor the following model may be found. This model can be as

$$\begin{cases} x' = rx - h, \\ x(0) = x_0, \end{cases} \tag{2.2}$$

where r and h are positive constants and x_0 is an initial value. The solution of model (2) is

$$x(t) = (x_0 - \frac{h}{r})e^{rt} + \frac{h}{r}.$$

2.3 The Allometric Growth Rate

Two sizes x and y are allometrically related if their relative growth rates are proportional, or

$$\frac{x'}{x} = a\frac{y'}{y}, \quad a > 0. \tag{2.3}$$

Then, the solution of this equation is given as follows:

$$x(y) = x_0(\frac{y}{y_0})^a$$

where x_0 and y_0 are initial values (2).

3 Main results

In this section, we present a theorem by using picard iteration method. In fact, this method finds the solutions in the form of series for the models introduced in the previous section.

Theorem 3.1. *The following statments for exponential growth rate, harvest exponential growth rate and allometric growth rate are true:*

(*i*) *The exponential growth rate* (2.1) *has solution*

$$x(t) = x_0 \sum_{k=0}^{\infty} \frac{(rt)^k}{k!},$$

where r is a positive constant and x_0 is an initial value.

(ii) The harvest exponential growth rate (2.2) has solution

$$x(t) = \left(x_0 - \frac{h}{r}\right) \sum_{k=0}^{\infty} \frac{(rt)^k}{k!} + \frac{h}{r},$$

where r and h are positive constants and x_0 is an initial value.

(iii) The allometric growth rate (2.3) has solution

$$x(y) = x_0 \sum_{k=0}^{\infty} \frac{(aLn\,\frac{y}{y_0})^k}{k!},$$

where a is a positive constant and x_0 and y_0 are initial values.

Proof. (i) Consider the sequence of approximate solutions

$$x_{n+1}(t) = x_0 + \int_0^t r x_n(s)ds, \;\; x(0) = x_0.$$

Then,

$$x_1(t) = x_0 + \int_0^t r x_0 ds = x_0 + \left[r x_0 s\right]_0^t = x_0(1 + rt),$$

$$x_2(t) = x_0 + \int_0^t r x_1(s)ds = x_0 + r x_0 \int_0^t (1 + rs)ds = x_0 + r x_0 \left[s + \frac{r}{2}s^2\right]_0^t = x_0(1 + rt + \frac{r^2}{2!}t^2),$$

$$x_3(t) = x_0 + \int_0^t r x_2(s)ds = x_0 + \int_0^t r x_0(1 + rs + \frac{r^2}{2}s^2)ds =$$

$$x_0 + r x_0\left[s + \frac{r}{2}s^2 + \frac{r^2}{6}s^3\right]_0^t = x_0(1 + rt + \frac{r^2}{2!}t^2 + \frac{r^3}{3!}t^3).$$

By these expressions, it is easy to guess the n^{th} approximation

$$x_n(t) = x_0(1 + rt + \frac{r^2}{2!}t^2 + \ldots + \frac{r^{n-1}}{(n-1)!}t^{n-1} + \frac{r^n}{n!}t^n) = x_0 \sum_{k=0}^{n} \frac{(rt)^k}{k!}.$$

In this manner, we find out a sequence of approximate solutions for the $I.V.P.$ Thus

$$x(t) = \lim_{n\to\infty} x_n(t) = x_0 \sum_{k=0}^{\infty} \frac{(rt)^k}{k!} = x_0 e^{rt}.$$

(ii) Consider the iteration scheme:

$$x_{n+1}(t) = x_0 + \int_0^t (r x_n(s) - h)ds, \;\; x(0) = x_0.$$

Hence

$$x_1(t) = x_0 + \int_0^t (r x_0 - h)ds = x_0 + \left[(r x_0 - h)s\right]_0^t = x_0 + (x_0 - \frac{h}{r})rt.$$

Put $A = x_0 - \frac{h}{r}$. Then, we have

$x_1(t) = x_0 + Art$, $x_2(t) = x_0 + \int_0^t (rx_1(s) - h)ds = x_0 + \int_0^t [r(x_0 + Ars) - h]\, ds =$
$x_0 + \big[rx_0 s + A\frac{r^2}{2}s^2 - hs\big]_0^t = x_0 + Art + A\frac{r^2}{2!}t^2;$

$x_3(t) = x_0 + \int_0^t (rx_2(s) - h)ds = x_0 + \int_0^t [r(x_0 + Ars + A\frac{r^2}{2}s^2) - h]\, ds =$
$x_0 + Art + A\frac{r^2}{2!}t^2 + A\frac{r^3}{3!}t^3.$

It is easy to guess the n^{th} approximation

$x_n(t) = x_0 + Art + A\frac{r^2}{2!}t^2 + A\frac{r^3}{3!}t^3 + \ldots + A\frac{r^{n-1}}{(n-1)!}t^{n-1} + A\frac{r^n}{n!}t^n =$
$x_0 + A\sum_{k=1}^{n}\frac{(rt)^k}{k!} = \frac{h}{r} + A\sum_{k=0}^{n}\frac{(rt)^k}{k!}.$

Therefore

$$x(t) = \lim_{n\to\infty} x_n(t) = (x_0 - \frac{h}{r})\sum_{k=0}^{\infty}\frac{(rt)^k}{k!} + \frac{h}{r} = (x_0 - \frac{h}{r})e^{rt} + \frac{h}{r}.$$

(*iii*) Consider the allometric growth equation

$$\frac{x'}{x} = a\frac{y'}{y},\ a > 0.$$

It follows that $\frac{dx}{x} = a\frac{dy}{y}$ and we get $x' = a\frac{x}{y}$. Now by using iteration scheme for this equation, we have

$$\begin{aligned}
x_{n+1}(y) &= x_0 + a\int_{y_0}^{y}\frac{x_n(s)}{s}ds,\ \ x(y_0) = x_0,\\
x_1(y) &= x_0 + a\int_{y_0}^{y}\frac{x_0}{s}ds = x_0 + ax_0\big[ln\, s\big]_{y_0}^{y} = x_0(1 + a\, ln\,\frac{y}{y_0}),\\
x_2(y) &= x_0 + a\int_{y_0}^{y}\frac{x_1(s)}{s}ds = x_0 + ax_0\int_{y_0}^{y}\frac{1 + a\, ln\,\frac{s}{y_0}}{s}ds\\
&= x_0 + ax_0\, ln\,\frac{y}{y_0} + a^2x_0\left(\int_{y_0}^{y}\frac{ln\, s}{s}ds - \int_{y_0}^{y}\frac{ln\, y_0}{s}ds\right)\\
&= x_0 + ax_0\, ln\,\frac{y}{y_0} + a^2x_0\big[\frac{1}{2}(ln^2 y - ln^2 y_0) - ln\, y_0(ln\, y - ln\, y_0)\big]\\
&= x_0\left(1 + a\, ln\,\frac{y}{y_0} + \frac{a^2}{2!}ln^2\frac{y}{y_0}\right).
\end{aligned}$$

$$x_3(y) = x_0 + a\int_{y_0}^{y}\frac{x_2(s)}{s}ds = x_0 + ax_0\int_{y_0}^{y}\frac{1 + a\,ln\,\frac{s}{y_0} + \frac{a^2}{2}ln^2\frac{s}{y_0}}{s}ds$$
$$= x_0 + ax_0\,ln\,\frac{y}{y_0} + \frac{a^2x_0}{2}ln^2\frac{y}{y_0} + \frac{a^3x_0}{2}\int_{y_0}^{y}\frac{(ln\,s - ln\,y_0)^2}{s}ds$$
$$= x_0 + ax_0\,ln\,\frac{y}{y_0} + \frac{a^2x_0}{2}ln^2\frac{y}{y_0} + \frac{a^3x_0}{2}\Big[\int_{y_0}^{y}\frac{ln^2 s}{s}ds - 2ln\,y_0\int_{y_0}^{y}\frac{ln\,s}{s}ds + ln^2y_0\int_{y_0}^{y}\frac{1}{s}ds\Big]$$
$$= x_0 + ax_0\,ln\,\frac{y}{y_0} + \frac{a^2x_0}{2}ln^2\frac{y}{y_0} + \frac{a^3x_0}{2}\Big[\frac{1}{3}(ln^3y - ln^3y_0) - ln\,y_0(ln^2y - ln^2y_0) + ln^2y_0(ln\,y - ln\,y$$
$$= x_0(1 + a\,ln\frac{y}{y_0} + \frac{a^2}{2!}ln^2\frac{y}{y_0} + \frac{a^3}{3!}ln^3\frac{y}{y_0}).$$

And so, the following n^{th} approximation will be guessed

$$x_n(y) = x_0(1 + a\,ln\frac{y}{y_0} + \frac{a^2}{2!}ln^2\frac{y}{y_0} + \ldots + \frac{a^{n-1}}{(n-1)!}ln^{n-1}\frac{y}{y_0} + \frac{a^n}{n!}ln^n\frac{y}{y_0}) =$$
$$x_0\sum_{k=0}^{n}\frac{(a\,ln\frac{y}{y_0})^k}{k!}.$$

Therefore

$$x(y) = \lim_{n\to\infty}x_n(y) = x_0\sum_{k=0}^{\infty}\frac{(a\,ln\frac{y}{y_0})^k}{k!} = x_0e^{a\,ln\frac{y}{y_0}} = x_0(\frac{y}{y_0})^a.$$

□

4 Conclusion

In this research work, we used the picard iteration method to find the solution of equations related to three models of the growth rates. These obtained series are Maclaurin expansions for the classical solutions.

Acknowledgment

Authors would like to thanks from Neyshabur University for supporting this research.

References

[1] J. Gayon, *History of the Concept of Allometry*, Oxford University Press, (2000) 748-758.

[2] J.D. Logan, *A First Course in Differential Equations*, Springer-Verlag, NewYork, 2015 .

[3] J.D. Murray, *Mathematical Biology. An Introduction*, Volume I, Springer Verlag, New York, 2002.

[4] M.H. RahmaniDoust and M. Saraj, The logistic modeling population; having harvesting factor, *Yugoslav Journal of Operations Research*, **25**(1)(2015) 107-115.

Meshless method for solving a equation arisen form the spatial spread of an epidemic

Fatemeh Asadi-Mehregan*, Pouria Assari
Department of Mathematics, Faculty of Sciences, Bu-Ali Sina University, Hamedan, Iran

Abstract:

The model of the spread of an infection within a spatially distributed population under some epidemiological assumptions can be simulated by a nonlinear integral equation of mixed Volterra-Fredholm type. In this paper, we intend to propose a computational method for solving these types of biological problems. The presented scheme utilizes the shape functions of the local radial basis functions constructed on distributed data as a basis in the discrete collocation method. The algorithm of the new approach is computationally attractive and easy to implement on computers. Since the scheme does not require any mesh generations on the domain, it can be identified as a meshless method. The validity and efficiency of the new technique are demonstrated through one numerical example.

Keywords: Infectious contagion equation, Computational biology, Volterra-Fredholm integral equation, Meshless method **Mathematics Subject Classification (2010):** 13D45, 39B42

1 Introduction

Consider a population living in a habitat Ω (a closed subset of $\mathbb{R}^d$) and susceptible to some contagious disease. The main aim is to give a heuristic derivation of an equation for the evolution of an epidemic among the population on the basis of some simple assumptions (7). It should be noted that the infection is the only dynamical phenomenon which investigates in the current model. But to study this phenomenon

*Speaker: f.asadi@sci.basu.ac.ir

due to time dependence, as in other time-dependent models, it is assumed that contagious disease does not depend on factors associated with this parameter such as birth, migration, and other contamination factors. In addition, the contamination from the disease is assumed to affect the other sites in terms of sensitivity and vulnerability at one point. Therefore, the transmission and transmission of infectious diseases depends on the location and the time.

Let $S(t, \mathbf{x})$ and $I(t, \mathbf{x})$ denote the density of susceptibles and infectives, respectively, at time t and the position $\mathbf{x}$. Let $i(t, \tau, \mathbf{x})\mathrm{d}\tau$ be the density of infectives which were infected some time between $t - \tau$ and $t - \tau - \mathrm{d}\tau$ (7). Then

$$I(t, \mathbf{x}) = \int_0^\infty i(t, \tau, \mathbf{x})\mathrm{d}\tau. \tag{1.1}$$

The susceptible individuals are infected by the infectious influence and become infectious themselves after a period the length of which depends on their resistance to the disease as well as on the strength of the infectious influence. We suppose that an individual, once it has been infected, cannot become susceptible again (7).

Let the infectivity $B = B(t, \mathbf{x})$ be defined as the rate at which susceptibles become infective. The basic assumptions in this paper are as follows (7):

i: the disease induces permanent immunity, so the transition from I to S does not Occur,

ii: a nonnegative function $A(\tau, \mathbf{x}, \xi)$ is given such that

$$B(t, \mathbf{x}) = \int_0^\infty \int_\Omega i(t, \tau, \xi) A(\tau, \mathbf{x}, \xi)\mathrm{d}\xi\mathrm{d}\tau.$$

Thus, $A(\tau, \mathbf{x}, \xi)$ describes the infectivity at $\mathbf{x}$ due to one infective of 'age of illness' τ at ξ. Many characteristics of both the disease and the habitat are in fact incorporated in A.

The above definitions and assumptions lead to the following system of dynamical equations:

$$\begin{aligned} \frac{\partial S}{\partial t}(t, \mathbf{x}) &= -S(t, \mathbf{x})B(t, \mathbf{x}), \\ i(t, 0, \mathbf{x}) &= \frac{\partial S}{\partial t}(t, \mathbf{x}), \\ i(t, \tau, \mathbf{x}) &= i(t - \tau, 0, \mathbf{x}). \end{aligned}$$

It is easy to see that

$$\frac{\partial S}{\partial t}(t,\mathbf{x}) = S(t,\mathbf{x})\left\{\int_0^t\int_\Omega \frac{\partial S}{\partial t}(t-\tau,\xi)A(\tau,\mathbf{x},\xi)\mathrm{d}\xi\mathrm{d}\tau - h(t,\mathbf{x})\right\},$$

where

$$h(t,\mathbf{x}) = \int_0^\infty\int_\Omega i(0,\tau,\xi)A(t+\tau,\mathbf{x},\xi)\mathrm{d}\xi\mathrm{d}\tau.$$

How to spread and analyze the spread of an infectious disease can be examined using the following time-dependent integral equation (7):

$$u(t,\mathbf{x}) = \int_0^t\int_\Omega g(u(t-\tau,\xi))S_0(\xi)A(\tau,\mathbf{x},\xi)\mathrm{d}\xi\mathrm{d}\tau + f(t,\mathbf{x}), \tag{1.2}$$

where

$$u(t,\mathbf{x}) = -\ln\frac{S(t,\mathbf{x})}{S_0(\mathbf{x})}, \quad g(z) = 1-e^{-z}, \quad f(t,\mathbf{x}) = \int_0^t h(\tau,\mathbf{x})\mathrm{d}\tau.$$

In the literature, the nonlinear Volterra-Fredholm integral equation (1.2) is known as the equation of the epidemiological distribution of epidemics which was first examined by Deikmann in 1978 (7).

In the past few decades, radial basis functions (RBFs) as an effective meshless technique have been applied for interpolating a function over a set of scattered points. Since the classical RBFs are global functions, the resultant coefficient matrix with respect to them will be full and large when many points in the domain are considered for obtaining high-order accurate results (10). Although this coefficient matrix is non-singular, usually it is ill-conditioned, i.e. the condition number of this system is very large and so a small perturbation in the initial data may produce a large amount of perturbation in the solution (10). To overcome these difficulties, the advantages of RBFs with local supports can be utilized which called local radial basis functions (LRBFs) investigated in the manuscripts (8; 9). To construct the approximation function by LRBFs, the only geometrical data needed are used fallen within local influence domain. Therefore, LRBFs needs much less computational work than the globally supported RBFs and eventually, the interpolation matrix of LRBFs will be well-conditioned.

In the current study, we present a method for obtaining the numerical solution of nonlinear Volterra-Fredholm integral equation (1.2). The method is based on the discrete collocation method by combining the locally supported radial basis functions are used to approximate the mentioned integral equations. The scheme uses the composite Gauss-Legendre quadrature rule to compute its integrals. Furthermore,

the technique can be easily expanded to most classes of integral equations. It is seen that the presented method in the current paper in comparison with the method based on the globally supported RBFs for solving integral equations is well-conditioned and has much fewer volume computing.

2 Local radial basis functions

To approximate a function $u(\mathbf{x})$ at an arbitrary point $\mathbf{x} \in \Omega \subset \mathbb{R}^d$ using the global radial function $\Phi(\mathbf{x}) = \phi(\|\mathbf{x}\|)$ we can give the following linear combination (10):

$$u(\mathbf{x}) \approx \mathcal{G}_N u(\mathbf{x}) = \sum_{i=1}^{N} c_i \phi(\|\mathbf{x} - \mathbf{x}_i\|), \qquad \mathbf{x} \in \Omega. \tag{2.1}$$

To determine the values of the coefficients $\{c_1, ..., c_N\}$, one can evaluate the expansion (2.1) at all nodal points $X = \{\mathbf{x}_1, ..., \mathbf{x}_N\}$ by the interpolation equations.
Suppose $\{\Omega_i\}_{i=1}^{N}$ is an open bounded cover for Ω. Therefore, a function $u(\mathbf{x})$ on $\Omega_i,\ i = 1, ..., N$, cab be estimated as follows:

$$u(\mathbf{x}) \approx \mathcal{L}_i u(\mathbf{x}) = \sum_{j \in I_i} c_j^i \phi^i(\|\mathbf{x} - \mathbf{x}_j\|), \quad \mathbf{x} \in \Omega_i, \tag{2.2}$$

where I_i is the set of indexes corresponding to points fallen within the influence domain Ω_i (or cover) with the cardinal number $|I_i| = n_i$.
In the expansion (2.2), the coefficients $\{c_j^i\}_{j \in I_i}$ are determined by enforcing the interpolation conditions

$$\mathcal{L}_i u(\mathbf{x}_j) = u_j. \tag{2.3}$$

Therefore, we can rewrite the interpolation problem as the matrix form

$$\mathbf{B}^i \mathbf{C}^i = \mathbf{U}^i, \tag{2.4}$$

where

$$\mathbf{U}^i = [u_1, u_2, ..., u_{n_i}]^T, \qquad \mathbf{C}^i = [c_1^i, c_2^i, ..., c_{n_i}^i]^T, \tag{2.5}$$

and $\mathbf{B}^i$ is an $n_i \times n_i$ real symmetric coefficient matrix.
Therefore, we can represent the expansion (2.2) as (5; 6)

$$\mathcal{L}_i u(\mathbf{x}) = \sum_{j \in I_i} u_j \psi_j^i(\mathbf{x}), \tag{2.6}$$

where

$$\psi_j^i(\mathbf{x}) = \sum_{k\in I_i} [\mathbf{B}^{i^{-1}}]_{kj}\phi^i(\|\mathbf{x}-\mathbf{x}_k\|), \quad j \in I_i. \tag{2.7}$$

We explain the LRBF collocation method to approximate a function $u(\mathbf{x})$ at an arbitrary point $\mathbf{x} \in \mathbb{R}^d$ utilizing the RBF $\Phi(\mathbf{x}) = \phi(\|\mathbf{x}\|)$ by a linear combination as follows:

$$u(\mathbf{x}) \approx \sum_{i=1}^{N} u_i\psi_i^i(\mathbf{x}), \qquad \mathbf{x} \in \Omega, \tag{2.8}$$

where the functions $\psi_i^i(\mathbf{x})$ are called as the shape functions for the LRBF interpolation which satisfy the Kronecker delta condition (8).

3 Solving infectious contagion equation

We give the d-dimensional Volterra-Fredholm integral equations as follows:

$$u(t,x_1,...,x_d) = \int_0^t \int_\Omega g(u(t-\tau,\xi_1,...,\xi_d))S_0(\xi_1,...,\xi_d)A(\tau,x_1,...,x_d,\xi)\mathrm{d}\xi_1,...,\mathrm{d}\xi_d\mathrm{d}\tau + f(t,x_1,...,x_d), \tag{3.1}$$

where $(t,x_1,...,x_d) \in [0,1]\times\Omega = D$. In the collocation method, to determine the coefficients $\{\bar{c}_i\}$, we replace the unknown function $u(t,x_1,...,x_d)$ by the LRBF interpolation expansion and pick up the nodal points $(t_j,x_{1_j},...,x_{d_j})$, $j = 1,...,N$ in the integral equation (1.2) as follows:

$$\sum_{i=1}^{N}\bar{c}_i\psi_i^i(t_j,x_{1_j},...,x_{d_j}) = \int_0^{t_j}\int_\Omega g\left(\sum_{i=1}^{N}\bar{c}_i\psi_i^i(t_j-\tau,\xi_1,...,\xi_d)\right)\times S_0(\xi_1,...,\xi_d)A(\tau,x_{1_j},...,x_{d_j},\xi_1,...,\xi_d)\mathrm{d}\xi_1,...,\mathrm{d}\xi_d\mathrm{d}\tau + f(t_j,x_{1_j},...,x_{d_j}) \tag{3.2}$$

Since the support of the shape functions $\psi_i^i(t,x_1,...,x_d)$ is

$$D_i = [t_i-r_i,t_i+r_i]\times[x_{1_i}-r_i,x_{1_i}+r_i]\times...\times[x_{d_i}-r_i,x_{d_i}+r_i].$$

Now by applying the Kronecker delta condition, the system (3.2) converts to

$$\bar{c}_j = \int_{\alpha_i}^{t_j}\left(\int_{\alpha_{1_i}}^{\beta_{1_i}}...\int_{\alpha_{d_i}}^{\beta_{d_i}} g\left(\sum_{i=1}^{N}\bar{c}_i\psi_i^i(t_j-\tau,\xi_1,...,\xi_d)\right)S_0(\xi_1,...,\xi_d)A(\tau,x_{1_j},...,x_{d_j},\xi)\mathrm{d}\xi_1,...,\mathrm{d}\xi_d\right)\mathrm{d}\tau + f(t_j,x_{1_j}, \tag{3.3}$$

where $\alpha_i = \max\{0,t_i-r_i\}$, $\alpha_{p_i} = \max\{0,x_{p_i}-r_i\}$ and $\beta_{p_i} = \min\{1,x_{p_i}+r_i\}$ for every $p = 1,...,d$.

Using the m-point Gauss-Legendre quadrature rule relative to the coefficients $\{v_k\}$

and weights $\{w_k\}$ in the interval $[-1,1]$. Then the nonlinear system (3.3) gets replaced by

$$\bar{c}_j = \frac{(t_j-\alpha_i)(\beta_{1_i}-\alpha_{1_i})...(\beta_{d_i}-\alpha_{d_i})}{2^{d+1}} \sum_{k=1}^{m} w_k \sum_{k_1=1}^{m} ... \sum_{k_d=1}^{m} w_{k_1}...w_{k_d} \times$$
$$g\left(\sum_{i=1}^{N} \bar{c}_i \psi_i^i(t_j-\theta_{k,i},\theta_{k_1,i}...\theta_{k_d,i})\right) S_0(\theta_{k_1,i}...\theta_{k_d,i}) A(\theta_{k,i},x_j,\theta_{k,i}) + f(t_j,x_{1_j},...,x_{d_j}) \quad (3.4)$$

where $\theta_{k,i} = \frac{1}{2}[\alpha_i + t_j + (t_j-\alpha_i)v_k]$ and $\theta_{k_p,i} = \frac{1}{2}[\alpha_{p_i} + \beta_{p_i} + (\beta_{p_i}-\alpha_{p_i})v_k]$ for every $p = 1,...,d$.
Therefore solving equation (3.1) leads to find $\{\hat{c}_1,...,\hat{c}_N\}$ and the values of $u(t,x_1,...,x_d)$ at any point $(t,x_1,...,x_d) \in D$ can be approximated by

$$\hat{u}_N(t,x_1,...,x_d) = \sum_{i=1}^{N} \hat{c}_i \psi_i^i(t,x_1,...,x_d), \qquad (t,x_1,...,x_d) \in D. \quad (3.5)$$

Example 1. *In order to demonstrate the effectiveness of the proposed method, we solve the integral equation*

$$u(t,x) = \int_0^t \int_\Omega \frac{x(1-\xi^2)}{(1+t)(1+\tau^2)}(1-e^{(-u(\xi,\tau))})\mathrm{d}\xi\mathrm{d}\tau - \ln\left(1+\frac{xt}{1+t^2}\right) + \frac{xt^2}{8(1+t)(1+t^2)}, \quad (t,x) \in [0,1]\times$$

with $\Omega = [0,1]$ *and the exact solution* $u_{ex}(t,x) = -\ln\left(1+\frac{xt}{(1+t^2)}\right)$.
Table 1 reports $\|e\|_\infty, \|e\|_2$ *and the values of the ratio at different numbers of* N. *The obtained errors for different numbers of* N *are drawn in the logarithmic mode in Figure 1. In computations, we put* $c = 0.2 \times \sqrt{N}$ *for local Gaussian (LGA) and* $c = \frac{10}{\sqrt{N}}$ *for local inverse multiquadrics (LIMQ), respectively. We have written all routines in "Maple" software with the "Digits" 20 (Digits environment variable controls the number of digits in Maple) and a Laptop with 2.10 GHz of Core 2 CPU and 4 GB of RAM has been used to run these.To solve the final nonlinear system of algebraic equations the "Fsolve" command has been employed based on the use of oating-point arithmetic.*

References

[5] P. Assari, F. Asadi-Mehregan, *Local multiquadric scheme for solving two-dimensional weakly singular Hammerstein integral equations*, Int. J. Numer. Model. 32 (2019), pp. 1–23.

Table 1: Some numerical results for Example 1 using the proposed method

N	*LGA*				*LIMQ*			
	c	$\|e_N\|_2$	$\|e_N\|_\infty$	Ratio	c	$\|e_N\|_2$	$\|e_N\|_\infty$	Ratio
20	0.89	4.92×10^{-2}	8.29×10^{-2}	–	2.24	9.63×10^{-2}	1.65×10^{-1}	–
29	1.08	1.53×10^{-2}	2.51×10^{-2}	3.21	1.86	3.49×10^{-2}	5.98×10^{-2}	2.73
40	1.26	2.45×10^{-3}	4.12×10^{-3}	5.62	1.58	7.24×10^{-3}	1.22×10^{-2}	4.14
53	1.46	1.96×10^{-4}	3.37×10^{-4}	8.89	1.37	8.51×10^{-4}	1.48×10^{-3}	7.50
68	1.65	8.79×10^{-6}	1.48×10^{-5}	12.56	1.21	5.29×10^{-5}	9.17×10^{-5}	11.16
85	1.84	2.33×10^{-7}	3.87×10^{-7}	16.22	1.08	2.37×10^{-6}	4.21×10^{-6}	13.82

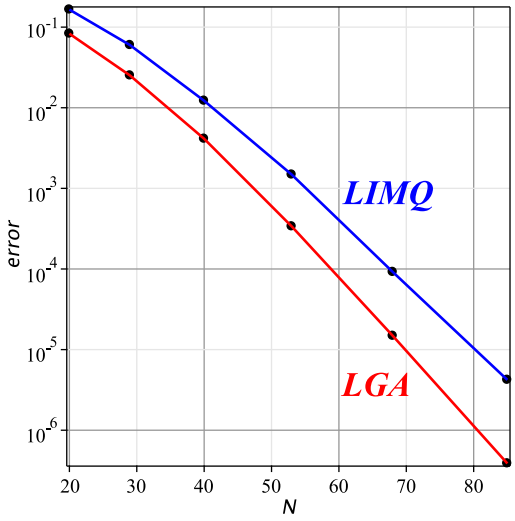

Figure 1: Distribution absolute error for Example 1

[6] P. Assari, F. Asadi-Mehregan, and M. Dehghan, *On the numerical solution of Fredholm integral equations utilizing the local radial basis function method*, Int. J. Comput. Math. (2018). DOI: 10.1080/00207160.2018.1500693

[7] O. Diekmann, *Thresholds and travelling waves for the geographical spread of infection*, J. Math Biology., 6 (1978), pp. 109–130.

[8] C. K. Lee, X. Liu, and S. C. Fan, *Local multiquadric approximation for solving boundary value problems*, Comput. Mech., 30 (2003), pp. 396–409.

[9] B. Sarler, R. Vertnik, *Meshfree explicit local radial basis function collocation method for diffusion problems*, Comput. Math. Appl.,51 (2006), pp. 1269–1282.

[10] H. Wendland, *Scattered Data Approximation*, Cambridge University Press, New York, (2005).

همایش ملی ریاضیات زیستی
اولین همایش ملی ریاضیات زیستی
۲۱ و ۲۲ اسفندماه ۱۳۹۷
دانشگاه نیشابور

Minimum number of fixed points in parallel dynamical systems

Ali Barzanouni*, Ghazaleh Malekbala and Leila Sharifan
Hakim Sabzevari University, Sabzevar, Iran

Abstract:

In this work, for a parallel discrete dynamical system over directed dependency graph associted to the maxterm MAX we find some criteria under which an arbitrary MAX – PDDS be a fixed point system. Also we will find a condition under which every point of a MAX – PDDS is either an eventually fixed point or an eventually $2-$*periodic* point.

Keywords: finite dynamical system, dependency graph, Boolean network.
Mathematics Subject Classification (2010): 37E15, 92B05.

1 Introduction

As an efficient formalism to describe the dynamics of biological systems, we can use the Boolean networks which are a spcial case of finite dynamical systems. Boolean networks were first introduced by Kauffman (20; 21) to model the gene regulatory networks. Finite dynamical systems, especially Boolean networks, use to model in various biology processes, such as gene regularity networks, signaling networks and Systems biology and etc. (18; 19)

A finite dynamical system is a function $f : X \to X$, where X is a finite set. The dynamics of f is generated by iteration of f. In this paper, we consider $f : \mathbb{F}_2^n \to \mathbb{F}_2^n = (f_1, \ldots, f_n)$, where $n \geqslant 1$ and each coordinate function $f_i : \mathbb{F}_2^n \to \mathbb{F}_2$ is a Boolean function of the n variables $x_1, \ldots, x_n$. Associated to a Boolean network ,f, one can construct a direced (undirected) graph which is called *dependency graph*

*Speaker: barzanouniali@gmail.com

representing dependencies of variables and Boolean functions in f. If variables in the system are updated in a synchronous manner then the system is named a *parallel* dynamical system (PDS), while if they are updated in an asynchronous manner, the system is named a *sequential* dynamical system (SDS). In this context, we assume that an entity (variable) influences another one but not vice versa, therefore we have a directed graph. Applications of finite dynamical systems (in particular Boolean networks) show that finding the relationship between the structure of the system and the resulting dynamics is very important. (12; 13; 14; 16; 15)

In this paper, corrosponding to a each direced graph $D = (V, E)$ on the vertex set $V = \{1, 2, \ldots, n\}$, we dertemine a finite dynamical system

$$f : \{0,1\}^n \to \{0,1\}^n$$

$$f(x_1, \ldots, x_n) = (y_1, \ldots, y_n)$$

such that each y_i is given by the local function f_i defined on the states of the influencing vertices and the vetrex i. Note that the directed graph D is the dependency graph of f. We assume that all entities are updated in a synchronous manner, so we have a parallel dynamical system. An $\mathrm{OR}-\mathrm{PDDS}$ (resp. $\mathrm{AND}-\mathrm{PDDS}$) is a parallel dynamical system over direced graph in which each Boolean function only uses disjunction (conjunction) operator on the variables. Also when each Boolean function f is a *maxterm* (resp. *minterm*), the system is called $\mathrm{MAX}-\mathrm{PDDS}$ ($\mathrm{MIN}-\mathrm{PDDS}$). Hear, by maxterm (resp. minterm) we mean $f(x_1, \ldots, x_n) = z_1 \vee \cdots \vee z_n$ (resp. $f(x_1, \ldots, x_n) = z_1 \wedge \cdots \wedge z_n$), where $z_i = x_i$ or $z_i = x_i'$.

In (12; 13) it have been proved that for a parallel discrete dynamical system over a simple graph corresponding to a maxterm OR (resp. minterm AND) only fixed or evetually fixed points exist while for a general $\mathrm{MAX}-\mathrm{PDS}$ (resp. $\mathrm{MIN}-\mathrm{PDS}$) either fixed points or $2-$*periodic* orbit can appear. Moreover in (13) the authors demonstrated that orbits with different periods can not coexist. In (12) the authors have shown that all orbits of an $\mathrm{OR}-\mathrm{PDDS}$ (rsep. $\mathrm{AND}-\mathrm{PDDS}$) are fixed points or eventually fixed points, as occure over simple dependency graph. Also they proved that in general case of maxterms (resp. minterms) corresponding to the $\mathrm{MAX}-\mathrm{PDDS}$ ($\mathrm{MIN}-\mathrm{PDDS}$) any period can appear unlike case $\mathrm{MAX}-\mathrm{PDS}$ ($\mathrm{MIN}-\mathrm{PDS}$). These results were a motivation that in (17) the orbit structure of parallel dynamical systems over some special directed graph classes have been studied.

In this paper, our principal aim is to find some criteria under which an arbitrary $\mathrm{MAX}-\mathrm{PDDS}$ be a fixed point system. Also we will find a condition under which

the orbit strucure of a MAX − PDDS has a similar manner to a general MAX − PDS. It means every point of a MAX − PDDS is either an eventually fixed point or an eventually $2-$*periodic* point.

2 Preliminaries

Let X be a non-empty finite set and $f : X \to X$ be a map. Then (X, f) is called a finite dynamical system. Often we simply say that f is dynamical system on X. A point $p \in X$ is called a fixed point if $f(p) = p$ and p is called a periodic point of period $t > 0$ when $f^t(p) = p$ and for each $0 < s < t$, $f^s(p) \neq p$. So, any fixed point is a point of period 1. We say that f is a fixed point system if all $p \in X$ is eventually a fixed point which means that for some $m \in \mathbb{N}$ and any $p \in X$, $f^m(p) = f^{m+1}(p)$.

A *path* from a vertex i to a vertex j in a directed graph $D = (V, E)$ is a sequence of vertices $i = i_0, i_1, \ldots, i_n = j$ that between any pair of vertices, there is an arc connecting them. An arc $i \to j$ in a directed graph D denoted by (i, j). We say that directed graph $D = (V, E)$ is a *strongly connected* if for all the pair of vertices $i, j \in V$, there exists a path from i to j and another one from j to i.

Let n be a positive integer. We are going to study dynamical systems on $X = \{0, 1\}^n$ that defined by Boolean functions.

Definition 1. A function

$$f : \{0, 1\}^n \longrightarrow \{0, 1\},$$

is a Boolean function when $f(x_1, \ldots, x_n)$ is obtained from $x_1, \ldots, x_n \in \{0, 1\}$ using the logical AND $(\wedge)$, the logical OR $(\vee)$, the logical NOT $(')$. A function f is called *maxterm* (resp. *minterm*) of n variables if

$$f(x_1, \ldots, x_n) = z_1 \vee \cdots \vee z_n$$

$$(\text{resp. } f(x_1, \ldots, x_n) = z_1 \wedge \cdots \wedge z_n),$$

where $z_i = x_i$ or $z_i = x_i'$.

We consider parallel dynamical systems associated to directed graphs. Let $D = (V, E)$ be a directed graph on the vertex set $V = \{1, \ldots, n\}$ and the arc set E. For each $i \in V$ and $Q \subseteq V$, we consider all the vertices that influence them in an updating of the system, thus we denote

$$I_D(i) = \{j \in V;\ (j, i) \in E\}$$

$$I_D(Q) = \cup_{i \in Q} I_D(i).$$

Let $f : \{0,1\}^n \longrightarrow \{0,1\}$ be a Boolean function. We define a dynamical system by means of f and D as

$$f_D : \{0,1\}^n \longrightarrow \{0,1\}^n,$$

$$f_D(x_1, \ldots, x_n) = (y_1, \ldots, y_n)$$

where each y_i is the updated state of entity i by applying a local function f_i over the states of the entiteties in $\{i\} \cup I_D(i)$.

3 Main results

In the following, we assume that f is a MAX − PDDS corresponding to a directed graph D and $W_f \subseteq V(D)$(resp. $W'_f \subseteq V(D)$) is the set of vertices in $V(D)$ such that the corresponding variables in MAX − PDDS appear in the usual (resp. complemented) form. Note that $W_f \cup W'_f = V(D)$ and $W_f \cap W'_f = \varnothing$.

Theorem 3.1. *(15, Theorem 1) Let* OR − PDDS *be a parallel dynamical system over a directed dependency graph $D = (V, E)$. Then all the orbits of this system are fixed point or evetually fixed point.*

Theorem 3.2. *(15, Theorem 3, theorem 4) Let* MAX − PDDS *be a general parallel dynamical system over a directed dependency graph $D = (V, E)$. Then periodic orbits of any period can appear.*

By the above result, for the general case of maxterms we can have coexistence of different periodic orbits depending on the sructure of the dependency graph. Motivated by this corollary, in the following we find some conditions under which an arbitrary MAX − PDDS be a fixed point system. We start with the crucial theorem for characterizing some MAX − PDDSs which are fixed point systems.

Theorem 3.3. *Let* MAX − PDDS *be a parallel dynamical system over a directed dependency graph $D = (V, E)$ and let $p = (a_1, \ldots, a_n)$ be a fixed point of f. Then every entity i whose state variable in MAX appears in complemented form is adjacent to an entity j whose state variable in MAX is in usual form and (j, i) is an arc. In the other words, for all $i \in W'_f$ there esixts a vertex $j \in W_f$ such that $(j, i) \in E$.*

Now we are ready to assert our main results.

Theorem 3.4. *Let f be a* MAX − PDDS *over a directed dependency graph $D = (V, E)$. Let for all entity i whose state variable in MAX appear in complemented form there exists an entity j whose state variabe in MAX is in usual form shuch*

that $(i,j),(j,i)$ are the arcs in D (in other words for all $i \in W'_f$ there exists an entity $j \in W_f$ such that $(i,j),(j,i) \in E$). (nemidonestam kodam tarze nevetiotan behtare???). Then f is a fixed point system.

Theorem 3.5. *Let f be a* MAX − PDDS *over a directed dependency graph $D = (V,E)$ and let $D|_{W_f}$ be a strongly connected such that for all entity i whose state variable in MAX appear in complemented form there exist entities j_1, j_2 whose state variabes in MAX are in usual form and $(i,j_1),(j_2,i) \in E$. (in other words for all $i \in W'_f$ there exist entities $j_1, j_2 \in W_f$ such that $(i,j_1),(j_2,i) \in E$) Then f is a fixed point system.*

Now for each $p = (a_1, a_2, \ldots, a_m, a_{m+1}, \ldots, a_n) \in \{0,1\}^n$, Without losing generality, suppose we arrang the entities in p where $1, \ldots, m$ are in complemented form and $m+1, \ldots, n$ are in usual form.

Theorem 3.6. *Let f be a* MAX − PDDS *over a directed dependency graph $D = (V,E)$ and let $D|_{W_f}$ be a strongly connected such that for all entity i whose state variable in MAX appear in complemented form there exists an entity j whose state variabes in MAX are in usual form and $(j,i) \in E$. (in other words for all $i \in W'_f$ there exists an entity $j \in W_f$ such that $(j,i) \in E$) Then $p = (a_1, a_2, \ldots, a_m, a_{m+1}, \ldots, a_n)$ is an evetually fixed point converge to $(1,1,\ldots,1)$ if for all $1 \leqslant j \leqslant m$ we have $a_j = 1$.*

At the last result, we detect a condition for a MAX − PDDS having either evetually fixed ponits or evetually $2-$*periodic* points.

Theorem 3.7. *Let f be a* MAX − PDDS *over a directed dependency graph $D = (V,E)$ and let $D|_{W'_f}$ contains(includes) no cycle. Then every point of f is either eventually fixed point or evetually $2-$periodic point.*

References

[11] Juan A. Aledo, S. Martinez, Jose C. Valverde. Parallel dynamical systems over directed dependency graphs. *Appl. Math. Comput.* 219 (2012), no. 3, 1114–1119.

[12] Aledo, J. A.; Martinez, S.; Pelayo, F. L.; Valverde, Jose C. Parallel discrete dynamical systems on maxterm and minterm Boolean functions. *Math. Comput. Modelling* 55 (2012), no. 3-4, 666–671.

[13] Aledo, Juan A.; Diaz, Luis G.; Martinez, Silvia; Valverde, Jose C. On the periods of parallel dynamical systems. *Complexity* 2017, Art. ID 7209762, 6 pp.

[14] Aledo, Juan A.; Diaz, Luis G.; Martinez, Silvia; Valverde, Jose C. Maximum number of periodic orbits in parallel dynamical systems. *Inform. Sci.* 468 (2018), 63–71.

[15] Aledo, Juan A.; Martinez, S.; Valverde, Jose C. Parallel dynamical systems over directed dependency graphs. *Appl. Math. Comput.* 219 (2012), no. 3, 1114–1119.

[16] Aledo, Juan A.; Martinez, S.; Valverde, Jose C. Parallel discrete dynamical systems on independent local functions. *J. Comput. Appl. Math.* 237 (2013), no. 1, 335–339.

[17] Juan A. Aledo, S. Martinez, Jose C. Valverde. Parallel dynamical systems over special digraph classes. *International Journal of Computer Mathematics*. vol. 90, no. 10, pp. 20392048, 2013.

[18] Wang RS, Saadatpour A, Albert R, Boolean modeling in systems biology: an overview of methodology and applications. *Phys Biol.* 2012 Oct; 9 (5).

[19] R. Robeva, B. Kirkwood, R. Davies. Boolean Biology: Introducing Boolean networks and finite dynamical systems models to biology and mathematics courses. *Math. Model. Nat. Phenom.* 6 (2011), No. 6, 3960

[20] S.A. Kauffman, Metabolic stability and epigenesis in randomly constructed genetic nets, J. Theoret. Biol. 22 (1969) 437–467.

[21] S.A. Kauffman, The Origins of Order: Self Organization and Selection in Evolution, Oxford University Press, 1993.

The next generation matrix and the stability analysis of a mathematical model of cancer virotherapy

Masume Behruzie* and Ehsan Anjidani
Department of Mathematics, University of Neyshabur, Neyshabur, Iran

Abstract:

In a mathematical model of cancer virotherapy, the next generation matrix, the basic reproduction rate and an immune response reproductive number are calculated. Moreover, a stability analysis of the equilibria of therapy failure and partial success is investigated.

Keywords: Cancer-viral therapy, next generation matrix, Basic reproduction rate, stability.
Mathematics Subject Classification (2010): 34D20, 92C50, 92D25.

1 Introduction

An autonomous model for tumors with virotherapy models was proposed by Dingli et al. (23) as follows:

$$\begin{cases} \frac{dy}{dt} = ry[1-(y+x)^{\epsilon}/K^{\epsilon}] - kyv, & y(t_v) = y_v, \\ \frac{dx}{dt} = kyv - \delta x, & x(t_v) = 0, \\ \frac{dv}{dt} = \alpha x - \omega v, & v(t_v) = v_0, \end{cases} \tag{1.1}$$

where, $y(t)$, $x(t)$, and $v(t)$ represent the population dynamics of uninfected tumor cells, virus-infected tumor cells, and free infectious virus particles, respectively. Uninfected tumor cells are produced at a generalized logistic growth rate

*Speaker: masume.behruzie1993@gmail.com

of $ry[1-(y+x)^{\epsilon}/K^{\epsilon}]$. These cells may come into contact with the virus and become infected at rate kyv. Virus-infected tumor cells naturally die at rate δx; the virus is replicated at rate x; and the virus is eventually extinct at rate ωv. The virus treatment is assumed to begin at time $t = t_v$.

In this paper, a mathematical model based on Dingli et al. (1.1) is developed. The virus-specific and tumor-specific cytotoxic T lymphocyte (CTL) response is included as follows:

$$\begin{cases} \frac{dT_i}{dt} = \beta V T_u - d_1 T_i - a_2 T_i I, \\ \frac{dV}{dt} = \pi T_i - d_2 V, \\ \frac{dI}{dt} = r_1 T_u I + r_2 T_i I - d_3 I, \\ \frac{dT_u}{dt} = a T_u[1 - b(T_u + T_i)] - \beta V T_u - a_1 T_u I, \end{cases} \tag{1.2}$$

with parameters for the strength of infection β, virus replication rate π, virus cytocixity d_1, and other constants, a and b. The variables $T_i(t)$, $V(t)$, $I(t)$, and $T_u(t)$ respectively represent the population dynamics of virus-infected tumor cells, the virus, CTLs, and uninfected tumor cells at time t. Specifically, uninfected tumor cells are infected through contact with a virus, and they become infected cells at rate βV. Infected tumor cells produce viral cells at rate π. The term $aT_u[1-b(T_u+T_i)]$ represents the logistic growth rate of uninfected tumor cells. Virus-infected tumor cells T_i and uninfected tumor cells T_u are removed by the CTLs at respective rates of a_2T_i and a_1T_u. The CTL population increases at a rate of $r_1T_uI + r_2T_iI$, and they are removed at rate d_3I. Tumor-specific and virus-specific CTL cells proliferate at the respective rates of r_1I and r_2I. Because viruses enhance presentation of tumor antigens, we assume that $r_2 = n \times r_1 (n \geqslant 1)$.

It is shown that, the solution for ODE Model (1.2) maintains positivity with non-negative initial conditions (22).

In this paper, the next generation matrix, the basic reproduction rate and an immune response reproductive number relating to model (1.2) are calculated. Then, a stability analysis of the equilibria of therapy failure and partial success is presented.

2 Main results

First, we introduce the next generatin matrix and the basic reproduction number of model (1.2) (see (25)). A therapy failure equilibrium E_0 always exists such that $E_0 = (0, 0, I_0, T_{u_0})$ and the equilibrium represents the state of the absence of viruses. To define the basic reproduction number and to verify local stability, denote the vec-

tors $\mathcal{F}$ and $\mathcal{V}$, the inflow and outflow from disease compartments T_i and V as follows:

$$\mathcal{F} = \begin{pmatrix} F_1 \\ F_2 \end{pmatrix} = \begin{pmatrix} \beta V T_u \\ \pi T_i \end{pmatrix}, \qquad \mathcal{V} = \begin{pmatrix} V_1 \\ V_2 \end{pmatrix} = \begin{pmatrix} (d_1 + a_2 I) T_i \\ d_2 V \end{pmatrix}.$$

Let $x = (x_1, x_2) = (T_i, V)$ and $y = (I, T_u)$ so that $F_i \equiv F_i(x, y)$ and $V_i \equiv V_i(x, y), i = 1, 2$. Five conditions are needed to verify local asymptotic stability of the model (1.2) and to define a basic reproduction number ((24)).

(1) $F_i(0, y) = 0$ and $V_i(0, y) = 0$ for $y \geqslant 0$.

(2) $F_i(x, y) \geqslant 0$ for all nonnegative x and y.

(3) $V_i(x, y) \leqslant 0$ if $x_i = 0$, $i = 1, 2$.

(4) $V_1(x, y) + V_2(x, y) \geqslant 0$ for all nonnegative x and y.

(5) The disease-free system $\dot{y} = h(0, y)$ has a unique equilibrium that is asymptotically stable.

It is straightforward to verify that all five conditions are satisfied. Now, we compute the 2×2 Jacobian matrices $\mathbb{F}$ and $\mathbb{V}$, as follows:

$$\mathbb{F} = \begin{pmatrix} 0 & \beta T_{u_0} \\ \pi & 0 \end{pmatrix}, \qquad \mathbb{V} = \begin{pmatrix} d_1 + a_2 I_0 & 0 \\ 0 & d_2 \end{pmatrix}.$$

The next generation matrix equals $\mathbb{K} = \mathbb{F}\mathbb{V}^{-1}$. Therefore, we obtain

$$\mathbb{K} = \begin{pmatrix} 0 & \frac{\beta T_{u_0}}{d_2} \\ \frac{\pi}{d_1 + a_2 I_0} & 0 \end{pmatrix}.$$

The basic reproduction number is the spectral radius of $\mathbb{K}$. A simple calculation shows that the spectral radius of $\mathbb{K}$ is

$$R_0 = \rho(\mathbb{K}) = \sqrt{\frac{\beta \pi T_{u_0}}{(d_1 + a_2 I_0) d_2}}.$$

Now assume that $r_2 > r_1$ and $a_1 r_2 > a_2 r_1$. Then, in the therapy failure equilibrium

E_0 we have

$$I_0 = \frac{a - abT_{u_0}}{a_1}, \qquad T_{u_0} = \frac{d_3}{r_1}.$$

Therefore, The basic reproduction rate, R_0, for ODE Model (1.2) becomes

$$R_0 = \sqrt{\frac{\beta\pi T_{u_0}}{(d_1 + a_2 I_0)d_2}} = \sqrt{\frac{a_1\beta\pi d_3}{(a_1 r_1 d_1 + a_2 a(r_1 - bd_3))d_2}}.$$

On therapy failure equilibrium E_0, it is proved that

Theorem 2.1. *(22) If $R_0 < 1$, then therapy failure equilibria $E_0 : (0, 0, I_0, T_{u_0})$ is locally asymptotically stable. Otherwise, E_0 is unstable.*

Theorem 2.2. *(22) If $R_0 < \frac{\beta\pi}{abd_2\beta\pi}$ and $d_1 + a_2 I_0 > abT_{u_0}$, then therapy failure equilibrium E_0 is globally asymptotically stable.*

Remark 1. *If β and π are small, then the possibility of satisfying the condition of Theorem 2.2 increases. Thus, the probability of virus therapy failure increases.*

Finally, to analyze the stability of a therapy partial success equilibrium, we calculate the immune response reproductive number R_1 in model (1.2). Putting $I = 0$ we obtain the equilibrium

$$E' = (T_i', V', 0, T_u') = (\frac{V' d_2}{\pi}, \frac{a\beta\pi - abd_1 d_2)}{\beta(\beta\pi + abd_2)}, 0, \frac{d_1 d_2}{\beta\pi}).$$

The vectors $\mathcal{F}$ and $\mathcal{V}$ are as follows:

$$\mathcal{F} = \begin{pmatrix} r_1 T_u I + r_2 T_i I \end{pmatrix}, \qquad \mathcal{V} = \begin{pmatrix} d_3 \end{pmatrix}.$$

We compute the 1×1 Jacobian matrices $\mathbb{F}$ and $\mathbb{V}$, as follows:

$$\mathbb{F} = \begin{pmatrix} r_1 T_u + r_2 T_i \end{pmatrix}, \qquad \mathbb{V} = \begin{pmatrix} d_3 \end{pmatrix}.$$

The next generation matrix equals $\mathbb{K} = \mathbb{F}\mathbb{V}^{-1} = \frac{r_1 T_u + r_2 T_i}{d_3}$ and hence

$$R_1 = \rho(\mathbb{K}) = \sqrt{\frac{r_1 T_u' + r_2 T_i'}{d_3}} = \sqrt{\frac{[r_1 d_1 d_2(abd_2 + \beta\pi + ar_2 d_2(\beta\pi - bd_1 d_2))]}{\beta\pi d_3(abd_2 + \beta\pi)}}.$$

Now, when $R_0 > 1$ and $R_1 > 1$, therapy partial success equilibrium E_1 exists such that

$$E_1 = (T_i^*, V^*, I^*, T_u^*) =$$

$$(\frac{\beta\pi a_1 d_3}{[(r_2-r_1)aa_2bd_2+(a_1r_2-a_2r_1)\beta\pi]}(1-\frac{1}{R_0}), \frac{\pi T_i^*}{d_2}, \frac{(d_3\beta\pi(abd_2+\beta\pi)(R_1-1))}{[aba_2d_2(r_2-r_1)+\beta\pi(a_1r_2-a_2r_1)d_2]}, \frac{a_2d_2I^*+a}{\beta\pi}$$

By calculating the eigenvalues of Jacobian matrix in equilibrium E_1, it is obtained a sufficient condition for that the endemic equilibrium $E_1 : (T_i^*, V^*, I^*, T_u^*)$ is locally asymptotically stable (22).

References

[22] K.S. Kim, S. Kim and I. Jung, *Dynamics of tumor virotherapy: A deterministic and stochastic model approach*, Stoch Anal Appl, 34 (2016), pp.483–495.

[23] D. Dingli, M. D. Cascino, K. Josic, S. J. Russell and Z. Bajzer, *Mathematical modeling of cancer radiovirotherapy*, Math. Biosci, 199(2006), pp.55–78.

[24] P. Van den Driessche, J. Watmough, *Further notes on the basic reproduction number*, in: F. Brauer, P. van den Driessche, J. Wu (Eds.), Mathematical Epidemiology, Springer, 2008, p. 159.

[25] Y. Yuan, L. J.S. Allen, *Stochastic models for virus and immune system dynamics*, Math. Biosci, 234(2011), pp.84–94.

The modelling of advection-dispersion by fractional differential equations

Nader Biranvand*, Esmaeil Babolian and Alireza Vahidi
Department of Mathematics, Yadegar-e-Imam Khomeini (RAH), Shahr-e-Rey Branch, Islamic Azad University, Tehran, Iran

Abstract:

In this article, we introduce a fractional differential equation model for advection-dispersions, that describe the Brownian motion of particles. In the following, wee concerns the existence of solutions to a fractional boundary-value problem. First for the eigenvalue problem associated with it, we prove that there is a sequence of positive and increasing real eigenvalues; a characterization of the first eigenvalue is also given. Then under different assumptions on the nonlinearity we show the existence of weak solutions of the problem. Our main tools are variational methods and critical point theorems.

Keywords: Weak solution, Fractional differential equation, Variational methods
Mathematics Subject Classification (2010): 34B37, 58E05, 58E30, 26A33.

1 Introduction

As a generalization of differentiation and integration to arbitrary non-integer order, fractional calculus, is a significant tool for solving complex problems from various fields such as engineering, science, viscoelasticity, diffusion and pure and applied mathematics. In the past few years, theory of fractional differential equation has been investigated extensively, see the monographs of Kilbas et al (34) and the papers (26; 28; 29; 30; 31; 32) and the reference therein.

*Speaker: nabiranvand@gmail.com

Inspired by the results in (32; 33), we consider the existence of weak solution to the fractional boundary-value problem

$$-\frac{d}{dt}\big(p_i(t){}_0D_t^{-\beta}+q_i(t){}_tD_T^{-\beta}\big)u_i'(t)-r_i(t)u_i(t)=\lambda F_{u_i}(t,u_1(t),...,u_n(t)),\quad \text{a.e. } t\in[0,T],$$
$$u_i(0)=0,\quad u_i(T)=0. \tag{1.1}$$

for $1\leqslant i\leqslant n$, where $n\geqslant 1$ is an integer, $p_i,\ q_i,\ r_i\in L^\infty([0,T])$ with $P_i^-:=ess\inf_{[0,T]}p_i(t)>0$ for $1\leqslant i\leqslant n$, $0\leqslant r_i(t)\leqslant 1$ for every $t\in[0,T]$ and $1\leqslant i\leqslant n$, $\lambda\in\mathbb{R}$ is a positive parameter, $F:[0,T]\times\mathbb{R}^n\longrightarrow\mathbb{R}$ is a function such that $F(.,x_1,...,x_n)$ is measurable in $[0,T]$ for all $(x_1,...,x_n)\in\mathbb{R}^n$, $F(t,.,...,.)$ is C^1 in $\mathbb{R}^n$ for every $t\in[0,T]$, F_{u_i} denotes partial derivative of F with respect to u_i for $1\leqslant i\leqslant n$, $0<\beta<1$ and ${}_0D_t^{-\beta}$, ${}_tD_T^{-\beta}$ are the left and right fractional integrals of order β.

2 Preliminaries

Definition 2. *(Left and Right Riemann-Liouville fractional integral) Let u be a function defined an $[a,b]$ the left(right) Riemann-Liouville fractional integral of order $\alpha>0$ for function u is defined by*

$${}_aI_t^\alpha u(t)=\frac{1}{\Gamma(\alpha)}\int_a^t\frac{u(s)}{(t-s)^{1-\alpha}}ds,\quad t\in[a,b],\qquad {}_tI_b^\alpha u(t)=\frac{1}{\Gamma(\alpha)}\int_t^b\frac{u(s)}{(s-t)^{\alpha-1}}ds,\quad t\in[a,b],$$

is called the Riemann-Liouville fractional integral of order α, where $\alpha>0$ and $\Gamma(\alpha)$ denotes the gamma function.

Definition 3. *(Left and Right Riemann-Liouville fractional derivative) Let u be a function defined an $[a,b]$ the left(right) Riemann-Liouville fractional derivative of order $\alpha>0$ for function u denoted by ${}_aD_t^\alpha u(t)$ and ${}_tD_b^\alpha u(t)$ respectively, are defined by*

$${}_aD_t^\alpha u(t)=\frac{d^n}{dt^n}\ {}_aI_t^\alpha u(t),\qquad {}_aD_t^\alpha u(t)=(-1)^n\frac{d^n}{dt^n}\ {}_tI_b^{n-\alpha}u(t),$$

where $t\in[a,b]$ and $n-1\leqslant\alpha<n$ and $n\in\mathbb{N}$.

Now we announce some properties of the Riemann-Liouville fractional integral and derivative operators.

Theorem 2.1.

$${}_aI_t^\alpha({}_aI_t^\beta u(t))={}_aI_t^{\alpha+\beta}u(t)\quad\text{and}\quad {}_tI_b^\alpha({}_tI_b^\beta u(t))={}_tI_b^{\alpha+\beta}u(t),\quad \forall\alpha,\beta>0$$

in any point $t \in [a,b]$ *for continuous function* u *and for almost every point in* $[a,b]$ *if the function* $u \in L^1[a,b]$.

Theorem 2.2. *Let* $u \in L^1[a,b]$ *and* $\alpha > 0$,

$$ {}_aD_t^{\alpha}({}_aI_t^{\beta}u(t)) = u(t), \quad a.e.\ t \in [a,b] \quad \text{and} \quad {}_tD_b^{\alpha}({}_tI_b^{\beta}u(t)) = u(t), \quad a.e.\ t \in [a,b] $$

Now to apply critical point theory for the existence of solutions for problem (1.1), we shall state some basic notation and results (33), which will be used in the proof of our main results.

Throughout this paper, we denote $\alpha = 1 - \frac{\beta}{2}$, and assume that the following condition is satisfied.

(H1) $F(t,x)$ is measurable in t for every $x \in \mathbb{R}^N$ and continuously differentiable in x for a.e $t \in [0,T]$, and there exist $a \in C(\mathbb{R}^+, \mathbb{R}^+)$, $b \in L^1(0,T;\mathbb{R}^+)$ such that,

$$ |F(t,x)| \leqslant a(|x|)b(t), \quad \sum_{i=1}^{n} |F_{x_i}(t,x_1,...,x_n)| \leqslant a(|x|)b(t) \tag{2.1} $$

for all $x \in \mathbb{R}^N$ and $t \in [0,T]$.

Let the fractional derivative space $E^{\alpha,i}$ is defined by the completion of $C_0^{\infty}((0,T),\mathbb{R}^N)$ with respect to the norm

$$ \|u_i\| = \Big(\int_0^T (p_i(t) + q_i(t)) \, |{}_0D_t^{\alpha}u_i(t)|^2 + |u_i(t)|^2 dt \Big)^{1/2}, $$

where ${}_0D_t^{\alpha}$ and ${}_tD_T^{\alpha}$ are the α-order left and right Riemann-Liouville fractional derivative respectively. If $u_i \in E^{\alpha,i}$, then ${}_0D_t^{\alpha}u_i(t)$ exists a.e. in $[0,T]$. The sets $E^{\alpha,i}$ are reflexive and separable Hilbert spaces. And we set

$$ X := E^{\alpha,1} \times ... \times E^{\alpha,n} $$

with respect to the equivalent norm

$$ \|u\|_{\alpha} = \|(u_1,...,u_n)\|_{\alpha} = \left(- \sum_{i=1}^{m} \int_0^T (p_i(t) + q_i(t)) \, ({}_0D_t^{\alpha}u_i(t), {}_tD_T u_i(t)) \, dt \right)^{\frac{1}{2}}. $$

Lemma 2.3 ((33)). *For all $u = (u_1, ..., u_n) \in X$, we have*

$$\sum_{i=1}^{n} \|u_i\|_{L^2}^2 \leqslant \frac{T^\alpha}{\Gamma(\alpha+1)} \sum_{i=1}^{n} \|{}_0D_t^\alpha u_i\|_{L^2}^2, \tag{2.2}$$

$$\sum_{i=1}^{n} \|u_i\|_\infty \leqslant \frac{T^{\alpha-\frac{1}{2}}}{\Gamma(\alpha)(2\alpha-1)^{1/2}} \sum_{i=1}^{n} \|{}_0D_t^\alpha u_i\|_{L^2}. \tag{2.3}$$

Similar to the proof of (32, Proposition 4.1), we have the following property.

Definition 4. A weak solution of (1.1) is a function $u \in X$ such that

$$-\sum_{i=1}^{n} \int_0^T p_i(t)\big({}_0D_t^\alpha u_i(t), {}_tD_T^\alpha v_i(t)\big) + q_i(t)\big({}_tD_T^\alpha u_i(t), {}_0D_t^\alpha v_i(t)\big)$$
$$+ r_i(t)\big(u_i(t), v_i(t)\big) + \lambda\big(F_{u_i}(t, u_1(t), ..., u_n(t)), v_i(t)\big)dt = 0$$

for every $v \in X$.

We consider the functionals $\Phi : X \to \mathbb{R}$ and $\Psi : X \to \mathbb{R}$ defined by

$$\Phi(u) = -\sum_{i=1}^{n} \int_0^T (p_i(t) + q_i(t))\big({}_0D_t^\alpha u_i(t), {}_tD_T^\alpha u_i(t)\big) + \frac{r_i(t)}{2}|u_i(t)|^2 dt. \tag{2.4}$$

and

$$\Psi(u) = \int_0^T F(t, u_1(t), ..., u_n(t))dt. \tag{2.5}$$

Then Φ and Ψ is continuously differentiable under assumption (H1), and

$$\begin{aligned}\langle \Phi'(u), v\rangle = &-\sum_{i=1}^{n} \int_0^T p_i(t)\big({}_0D_t^\alpha u_i(t),\ {}_tD_T^\alpha v_i(t)\big) + q_i(t)\big({}_tD_T^\alpha u_i(t),\ {}_0D_t^\alpha v_i(t)\big)dt \\ &-\sum_{i=1}^{n} \int_0^T r_i(t)\big(u_i(t), v_i(t)\big)dt\end{aligned} \tag{2.6}$$

and

$$(\Psi'(u), v) = \sum_{i=1}^{n} \int_0^T \big(F_{u_i}(t, u_1(t), ..., u_n(t)),\ v_i(t)\big)dt. \tag{2.7}$$

for $u, v \in X$. Hence a critical point of $I_\lambda := \Phi - \lambda\Psi$ is a weak solution of (1.1).

For our proofs, we need the following results in critical point theory.

Definition 5. *Let E be a real Banach space and $\varphi \in C^1(E, \mathbb{R})$. We say that φ satisfies the (PS) condition if any sequence $\{u_m\} \subset E$ for which $\varphi(u_m)$ is bounded and $\varphi'(u_m) \to 0$, as $m \to \infty$, posses a convergent subsequence.*

Theorem 2.4 (Mountain Pass theorem). *Let E be a real Banach space and $\varphi \in C^1(E, \mathbb{R})$ satisfying (PS). Suppose $\varphi(0) = 0$ and*

(C1) there are constants $\rho, \alpha > 0$ such that $\varphi|_{\partial B_\rho} \geqslant \alpha$, where $B_\rho = \{x \in E : \|x\| < \rho\}$,

(C2) there is an $e \in E \backslash \overline{B}_\rho$ such that $\varphi(e) \leqslant 0$.

Then φ possesses a critical value $c \geqslant \alpha$. Moreover c can be characterized as

$$c = \inf_{g \in \Gamma} \max_{u \in g([0,1])} \varphi(u),$$

where $\Gamma = \{g \in C([0,1], E) | g(0) = 0, g(1) = e\}$.

3 Main results

In (35), Risken introduced an advection-dispersion equation to describe the Brownian motion of particles

$$\frac{\partial C(x,t)}{\partial t} = \left[-v \frac{\partial}{\partial x} + D \frac{\partial^2}{\partial x^2} \right] C(x,t)$$

where $C(x,t)$ is a concentration field of space variable x at time t, $D > 0$ is the diffusion coefficient and $v > 0$ is the drift coefficient. According to (27), an anomalous dispersion process should be described by the following advection-dispersion equation containing the left and the right fractional differential operators

$$\frac{\partial C(x,t)}{\partial t} = -v \frac{\partial C(x,t)}{\partial x} + Dj \frac{\partial^\gamma C(x,t)}{\partial x^\gamma} + D(1-j) \frac{\partial^\gamma C(x,t)}{\partial (-x)^\gamma} \tag{3.1}$$

where C is the expected concentration field of space variable x at time t, v is a constant mean velocity, x is the distance in the direction of the mean velocity, D is a constant dispersion coefficient, $0 \leqslant j \leqslant 1$ describes the skewness of the transport process, and γ is the order of left and right fractional differential operators (see (27, Appendix) for details about left and right fractional differential operators). Especially, if $\gamma = 2$, the dispersion operator reduces to the classical advection-dispersion operator and (3.1) becomes the classical advection-dispersion equation. On the other hand, if $j = \frac{1}{2}$, (3.1) describes symmetric transitions. Define an equivalent Riesz potential symmetric operator

$$2\nabla^\gamma \equiv D_+^\gamma + D_-^\gamma,$$

which gives the mass balance equation for the symmetric fractional advection dispersion

$$\frac{\partial C(x,t)}{\partial t} = -v\nabla C(x,t) + D\nabla^{\gamma} C(x,t),$$

that this modeled by equation (1.1). In the following, we give a Lemma and a theorem to investigate of the solutions of the problem (1.1).

Now, we give the following lemma for established our main result.

Lemma 3.1. *Suppose the*

(H2) there are constants $\mu > 2$ and $R > 0$ such that, for $|x| = |(x_1, ..., x_n)| \geqslant R$,

$$0 < \mu F(t,x) \leqslant \sum_{i=1}^{n} (x,\ F_{x_i}(t, x_1, ..., x_n)). \tag{3.2}$$

Then I_λ satisfies the (PS) condition.

Theorem 3.2. *If* (H2) *holds and*

(H3) $F(t,x) = o(|x|^2)$ as $x \to 0$

Then (1.1) *has at least one nontrivial weak solution.*

Proof. The proof relies on the Mountain Pass theorem. It is clear that $\varphi \in C^1(E^\alpha, R)$, $\varphi(0) = 0$, and φ satisfies the (PS) condition from Lemma 3.1. From (H3), for an $\varepsilon_1 > 0$ there exists a constant $\delta > 0$, such that

$$F(t,x) \leqslant \varepsilon_1 |x|^2, \quad t \in [0,T],\ |x| < \delta.$$

Let $u \in X$ with $\|u\|_\alpha \leqslant \frac{(\tilde{p}+\tilde{q})\Gamma(\alpha+1)|\cos(\pi\alpha)|^{\frac{1}{2}}\delta}{T^\alpha}$, then by (2.3) and (7) $\|u\|_\infty \leqslant \frac{\delta}{T(2\alpha-1)^{\frac{1}{2}}} \leqslant \delta$. Thus we have

$$\begin{aligned} I_\lambda(u) &= -\sum_{i=1}^{n} \int_0^T (p_i(t) + q_i(t)) \big({}_0D_t^\alpha u_i(t),\ {}_tD_T^\alpha u_i(t)\big) - \frac{r_i(t)}{2}|u_i(t)|^2 dt - \lambda \int_0^T F(t, u_1(t), ..., u_n(t)) dt \\ &\geqslant (1 - \frac{\tilde{r}^2}{2} - \lambda\epsilon_1) \frac{T^{2\alpha}}{(\tilde{p}+\tilde{q})\Gamma^2(\alpha+1)|\cos(\pi\alpha)|} \|u\|_\alpha^2. \end{aligned}$$

If we choose $\rho = \frac{(\tilde{p}+\tilde{q})\Gamma(\alpha+1)|\cos(\pi\alpha)|^{\frac{1}{2}}\delta}{T^\alpha}$ and $\gamma = (1 - \frac{\tilde{r}^2}{2} - \lambda\epsilon_1)\frac{T^{2\alpha}}{(\tilde{p}+\tilde{q})\Gamma^2(\alpha+1)|\cos(\pi\alpha)|}\rho^2$, then $\varphi|_{\partial B_\rho} \geqslant \gamma$.

Let $w = (w_1, ..., w_n) \in X$, and choose $r > 0$. Thus

$$I_\lambda(rw) = \left[\sum_{i=1}^{n}\int_0^T -r^2(p_i(t)+q_i(t))\big({}_0D_t^\alpha w_i(t), {}_tD_T^\alpha w_i(t)\big) - \frac{r^2 r_i(t)}{2}|w_i(t)|^2 dt\right] - \lambda F(t, rw_1(t), ..., rw_n($$
$$\leqslant r^2\|w\|_\alpha^2 - \frac{r^2}{2}\|w\|_{L^2}^2 - a_1\lambda r^\mu \|w_1\|_{L^\mu}^\mu + a_2 T,$$

which implies that $I_\lambda(rw_) \to -\infty$ as $r \to \infty$.

The above discussions show that I_λ has at least one nontrivial critical point, thus (1.1) has at least one nontrivial weak solution. □

References

[26] R. P. Agarwal, M. Benchohra, S.Hamani; *A survey on existence results for boundary value problems of nonlinear fractional differential equations and inclusions*, Acta Appl. Math. 109 (2010), 973-1033.

[27] D. Benson, S. Wheatcraft, M. Meerschaert, *Application of a fractional advection dispersion equation,* Water Resour. Res. **36** (2000) 1403-1412.

[28] N. Biranvand, A. Salari, *Energy estimate for impulsive fractional advection dispersion equation in anomalous diffusions,*J. Nonlinear Funct. Anal. 2018 (2018) 1-17.

[29] S. Heidarkhani, M. Ferrara, A. Salari, *Infinitely many periodic solutions for a class of perturbed second-order differential equations with impulses,* Acta Appl. Math. **139** (2015) 81–94.

[30] S. Heidarkhani, A. Salari, *Nontrivial solutions for impulsive fractional differential systems through variational methods,* Comput. Math. Appl. (2016), http://dx.doi.org/10.1016/j.camwa.2016.04.016.

[31] W. Jiang; *The existence of solutions for boundary value problems of fractional differential equations at resonance*, Nonlinear Anal. 74 (2011) 1987-1994.

[32] F. Jiao, Y. Zhou; *Existence of solutions for a class of fractional boundary value problem via critical point theory*, Comput. Math. Appl., 62 (2011) 1181-1199.

[33] F. Jiao, Y. Zhou; *Existence results for fractional boundary value problem via critical point theory*, J. Bifur. Chaos. App. Sci. Engrg. 22 (2012) 1250086.

[34] A. A. Kilbas, H. M. Srivastava, J. J. Trujillo; *Theory and Applications of Fractional Differential Equations*, in: North-Holland Mathematics Studies, vol. 204, Elsevier Science B.V., Amsterdam, 2006.

[35] H. Risken, *The Fokker-Planck Equation,* Springer, Berlin, 1988.

On a New Biological Fractional-order Lotka-Voltra Predator-Prey Model and Its Dynamical Behaviors

Nader Biranvand *, Esmaeil Babolian and Alireza Vahidi
Department of Mathematics, Yadegar-e-Imam Khomeini (RAH), Shahr-e-Rey Branch, Islamic Azad University, Tehran, Iran

Abstract:

In this paper, we study the dynamical behaviors of new fractional-order Lotka-Volterra predator-prey model and its discretized counterpart. It is shown that the discretized model exhibits much richer dynamical behavior than its corresponding fractional-order form.

Keywords: Fractional Calculus, Predator-prey, Lotka-Volterra, Discretization
Mathematics Subject Classification (2010): 62N01, 962F10.

1 Introduction

Fractional calculus is one of the branches of mathematics which is the concept of convolution integral.

From the recent decades onwards, fractional order differentials are widely used in many research areas owing to its application in modelling and investigating complicated phenomena, such as neural network systems, viscoelastic systems, Kinetic equations, dynamical and non-linear systems, financial systems, and so forth. This powerful mathematical approach provides researchers with the opportunity to derive further and precise information about complex natural systems showing a non-linear behavior of themselves compared to the ordinary calculus (36; 37; 38; 39; 40).

In 2014, a prey-predator Lotka-Volterra equation with logistic behavior for two species was investigated (41). Also, dynamical behaviors of prey-predator Lotka-Volterra with discretization was probed (38).

*Speaker: Nabiranvand@gmail.com

In this study, a new fractional model considering negative feedback on two species is proposed as following and the biological interpretation of it is also presented.

$$\frac{dN(T)}{dT} = N(T)\left(a - bN(T) - cP(T)\right), \tag{1.1}$$

$$\frac{dP(T)}{dT} = P(T)\left(-f + ceN(T)\right) - kP^2(T),$$

2 prellinimaries

In this section, some basic definition employed in the paper are presented.

Definition 6 (Fractional Caputo derivative)**.** *Let $f \in C^n[a,b]$ and $n-1 < \alpha < n$, then the Caputo derivative is defined as follows:*

$$\prescript{C}{a}{D}_t^{\alpha} f(t) = \frac{1}{\Gamma(\alpha - n)} \int_a^t \frac{D^n f(\tau)}{(t-\tau)^{\alpha - n + 1}} d\tau. \tag{2.1}$$

Definition 7 (Riemann-Liouville fractional integral)**.** *Let $\alpha \in R_+$. The operator D_a^{-n}, defined on $L_1[a,b]$ by*

$$D_t^{-\alpha} f(t) = \frac{1}{\Gamma(\alpha)} \int_a^t (t-\tau)^{\alpha-1} f(\tau) d\tau. \tag{2.2}$$

for $a < t < b$, is called the Riemann-Liouville fractional integral operator of order α.

2.1 Fractional continuous Lotka-Volterra with negative feedback on two species

To investigate species interaction, quite a few models have been proposed so far. Although each model has its own application and could be used for special purposes, they are not always capable of predicting species connection and behavior well enough. One reason why such matters come up could be referred to both the system complexity and simplification of the model. Considering this, in this section, a new fractional model with negative feedback on both prey and predator is proposed as equation (1.1).

In this model, we have

1. N and P are population density of prey and predator respectively.
2. a and f are rate of growth for prey and predator respectively.
3. b and k are rate of death, causing by interaction between two different species.
4. Preys would be injured when they are faced with predators, giving rise to an inclination of their population. Regarding that, a coefficient like c is donated to the death rate of preys due to their interaction with predators. However, all preys faced with predators are not always haunted, and some of them would be able to escape and remain alive. Thus, a coefficient like e is considered for preys that couldn't escape when they interact with predators, so multiplying of these two parameters (ce) represents feeding rate of cooperation attack which increases the predators' population density.

By considering the following parameters, the system (1.1) will be nondimensionalized as follows.

$$T = \frac{1}{a}t, \qquad N(T) = \frac{a}{b}X(t), \qquad P(T) = \frac{a}{c}Y(t),$$

and

$$\begin{aligned} \frac{dX}{dt} &= X(t)\left(1 - X(t) - Y(t)\right), \\ \frac{dY}{dt} &= Y(t)\left(-\beta - hY(t) + \varepsilon X(t)\right), \end{aligned} \tag{2.3}$$

where $\beta = \frac{f}{a}, \varepsilon = \frac{ce}{b}$ and $h = \frac{k}{c}$.

Since system (2.3) investigates the species behavior locally, in the next step by fractionalizing the system, we wish to extend the model. The Eq. (2.2) indeed look at the system from an extensive spectrum compared to the Eq. (2.3) because

the whole information of the system regarding species interaction and behavior are saved with a weight function $(t) = t^{(\alpha-1)}/\Gamma(\alpha)$ over time. Thus,

$$\begin{aligned} D^{\alpha}X(t) &= X(t)\left(1 - X(t) - Y(t)\right), \\ D^{\alpha}Y(t) &= Y(t)\left(-\beta - hY(t) + \varepsilon X(t)\right), \end{aligned} \tag{2.4}$$

where $\alpha \in (0, 1]$ and $t > 0$.

2.2 Discretization of fractional Lotka-Volterra Prey-predator model

In this section, we focus on the discretization of fractional Lotka- Volterra Prey-predator model with negative feedback, Eq. (2.4). This equation can be rewritten as follows by considering uniform discretization with time step s.

$$\begin{aligned} D^{\alpha}X(t) &= X\left([\tfrac{t}{s}]s\right)\left[\left(1 - X\left([\tfrac{t}{s}]s\right)\right) - Y\left([\tfrac{t}{s}]s\right)\right], \\ D^{\alpha}Y(t) &= Y\left([\tfrac{t}{s}]s\right)\left[-\beta - hY\left([\tfrac{t}{s}]s\right) + \varepsilon X\left([\tfrac{t}{s}]s\right)\right]. \end{aligned} \tag{2.5}$$

Assume that $X(0) = 0, Y(0) = 0$, and $t \in [0, s)$, so $t/s \in [0, 1)$. Thus, we have

$$\begin{aligned} D^{\alpha}X_1 &= X_0\left[1 - X_0 - Y_0\right], \\ D^{\alpha}Y_1 &= Y_0\left[-\beta - hY_0 + \varepsilon X_0\right]. \end{aligned} \tag{2.6}$$

So, with the help of Riemann-Liouville integral, the Eq. (2.6) is rewritten as follows:

$$\begin{aligned} X_1(t) &= X_0 + \frac{t^{\alpha}}{\alpha\Gamma(\alpha)}\left(X_0\left[1 - X_0 - Y_0\right]\right), \\ Y_1(t) &= Y_0 + \frac{t^{\alpha}}{\alpha\Gamma(\alpha)}\left(Y_0\left[-\beta - hY_0 + \varepsilon X_0\right]\right). \end{aligned} \tag{2.7}$$

As a result, after n step, Eq. (2.8) will be obtained.

$$\begin{aligned} X_{n+1}(t) &= X_n(ns) + \frac{(t-ns)^{\alpha}}{\alpha\Gamma(\alpha)}\left(X_n(ns)\left[1 - X_n(ns) - Y_n(ns)\right]\right), \\ Y_{n+1}(t) &= Y_n(ns) + \frac{(t-ns)^{\alpha}}{\alpha\Gamma(\alpha)}\left(Y_n(ns)\left[-\beta - hY_n(ns) + \varepsilon X_n(ns)\right]\right). \end{aligned} \tag{2.8}$$

Also, let $t \in [ns, (n+1)s]$ when $t \longrightarrow (n+1)s$, so we have

$$X_{n+1} = X_n + \frac{s^\alpha}{\alpha\Gamma(\alpha)} \left(X_n \left[1 - X_n - Y_n\right]\right), \tag{2.9}$$
$$Y_{n+1} = Y_n + \frac{s^\alpha}{\alpha\Gamma(\alpha)} \left(Y_n \left[-\beta - hY_n + \varepsilon X_n\right]\right).$$

2.3 Investigation of dynamical behavior of discrete and continuous fractional Lotka-Volterra prey-predator model

In this section, the dynamical behavior of fractional Lotka-Volterra Prey-predator model, associated with four parameters $\beta, \alpha, \varepsilon$ and h, is investigated.
Consider non-linear fractional system (2.2). With y_i as initial point $(i = 1, 2, \ldots, n)$.

$${}_0D_t^{\alpha_i} x_i(t) = f_i\left(x_1(t), x_2(t), \ldots, x_n(t), t\right), \qquad x_i(t) = y_i, \qquad i = 1, 2, \ldots, n. \tag{2.10}$$

By rewriting the above equation, we will have (38)

$$D^\alpha x = f(x). \tag{2.11}$$

for $i = 1, 2, \ldots, n, 0 < \alpha_i < 1, \alpha = [\alpha_1, \alpha_2, \cdots, \alpha_n]^T$ and $x \in R^n$. $E^* = (x_1^*, x_2^*, \cdots, x_n^*)$ is fixed point if and only if

$$f(x) = 0. \tag{2.12}$$

Also, Jacobian of the system (2.2) is

$$J = \begin{pmatrix} \frac{\partial f_1}{\partial x_1} & \frac{\partial f_1}{\partial x_2} & \cdots & \frac{\partial f_1}{\partial x_n} \\ \frac{\partial f_2}{\partial x_1} & \frac{\partial f_2}{\partial x_2} & \cdots & \frac{\partial f_2}{\partial x_n} \\ \vdots & \vdots & \cdots & \vdots \\ \frac{\partial f_n}{\partial x_1} & \frac{\partial f_n}{\partial x_2} & \cdots & \frac{\partial f_n}{\partial x_n} \end{pmatrix}. \tag{2.13}$$

Theorem 2.1 ((38)). *: When the following condition of the Jacobian matrix (2.13) at the fixed point (x^*, y^*) is held, the fixed point will be stable.*

$$\det(J) > 0, \quad trce(J) < 0.$$

Lemma 2.2 ((38)). *Assume that λ_1 and λ_2 are eigenvalues of matrix Jacobian (2.13) in fixed point (x^*, y^*), then*

(i) A fixed point (x^*, y^*) is named a sink if $|\lambda_1| < 1$ and $|\lambda_2| < 1$, so the sink is locally asymptotically stable.

(ii) *A fixed point* (x^*, y^*) *is named a source if* $|\lambda_1| > 1$ *and* $|\lambda_2| > 1$*, so the source is locally stable.*

(iii) *A fixed point* (x^*, y^*) *is named a saddle if* $|\lambda_1| < 1$ *and* $|\lambda_2| > 1$ *or* $|\lambda_1| > 1$ *and* $|\lambda_2| < 1$*.*

(iv) *A fixed point* (x^*, y^*) *is named a non-hyperbolic if either* $|\lambda_1| = 1$ *or* $|\lambda_2| = 1$*.*

2.4 Stability of the continuous model

Assume that $E^* = (x^*, y^*)$ is the fixed point of Eq. (2.3). Based on Jacobean matrix we have

$$J(x^*, y^*) = \begin{pmatrix} 1 - 2x^* - y^* & -x^* \\ \varepsilon y^* & -\beta - 2hy^* + \varepsilon x^* \end{pmatrix}. \tag{2.14}$$

Also, it can be shown that the following points are the fixed points of system (2.3).

$$E_1 = (0, 0), \quad E_2 = (1, 0), \quad E_3 = (\frac{h+\beta}{h+\varepsilon}, \frac{\varepsilon-\beta}{h+\varepsilon}).$$

Proposition 2.3. *The fixed points of system (2.4),* E_1, E_2*, and* E_3*, have the following properties:*

(i) E_1 *is an unstable point.*

(ii) *The sufficient and coefficient situation for the stability of point* E_2 *is* $\varepsilon < \beta$*. Otherwise,* E_2 *will be a non-hyperbolic point.*

(iii) E_3 *is a stable point when* $\beta < \varepsilon$ *and* $h \leqslant \beta$*.*

3 Main Results

In this section, we prove our main proposition and present our conclusions.

Proposition 3.1. E_1, E_2*, and* E_3 *in system (2.9) have the following properties:*

(i) E_1 *is a saddle point.*

(ii) E_2 *is a sink point.*

(iii) *Under the following condition* E_3 *is a stable point*

$$\beta > \varepsilon, \quad s > (2\alpha\Gamma(\alpha))^{\frac{1}{\alpha}}, \quad h > \frac{\varepsilon}{6(\beta-\varepsilon)-1}.$$

Interaction among species is of great importance to control the creatures from being virtually extinct. Considering this, scholars have proposed various models to study such sophisticated phenomena. However, the models sometimes fail to probe the system enough well due to the complexity of the system. In this conducted research, we extend a prey-predator model on two species with a negative feedback on both preys and predators and then, in order to look at the system more realistically, with the help of fractional calculus, both preys and predators are given different memories as well. The stability and dynamical analysis of the suggested model is obtained and its discretized counterpart is also calculated. Finally, according to biological interpretation, it is numerically shown that the stability of the model by donating memory to the system in both continuous and discretization state is increased.

References

[36] Magin, R.L., *Fractional calculus in bioengineering* , Begell House Publishers Redding, 2006.

[37] Dalir, M. and M. Bashour, *Applications of fractional calculus.* Applied Mathematical Sciences, 21 (2010), pp. 1021–1032.

[38] Elsadany, A. and A. Matouk, *Dynamical behaviors of fractional-order Lotka-Volterra predatorprey model and its discretization.* Journal of Applied Mathematics and Computing, 49 (2015), pp. 269–283.

[39] Kotalczyk, G. and F. Kruis, *Fractional Monte Carlo time steps for the simulation of coagulation for parallelized flowsheet simulations.* Chemical Engineering Research and Design, 136 (2018), pp. 71–82.

[40] Poursaeidesfahani, A., et al., *Computation of thermodynamic properties in the continuous fractional component Monte Carlo Gibbs ensemble.* Molecular Simulation, 43 (2017), pp. 189–195.

[41] Rahmani Doust, M. and S. GHolizade, *The Lotka-Volterra Predator-Prey Equations.* Caspian Journal of Mathematical Sciences (CJMS), 2 (2014), pp. 221–225.

[42] Vaidyanathan, S.,*Lotka-Volterra population biology models with negative feedback and their ecological monitoring.* Int J PharmTech Res, 5 (2015), pp. 974–981.

همایش ملی ریاضیات زیستی

اولین همایش ملی ریاضیات زیستی

۲۱ و ۲۲ اسفندماه ۱۳۹۷

دانشگاه نیشابور

Analysis of a disease model with two susceptible groups

Atena Ghasemabadi*

Esfarayen University of Technology, Esfarayen, North Khorasan, Iran

Abstract:

The present paper considers a disease model with two calsses of susceptible individuls. The first group is common susceptible of disease and the second group is awareness susceptible of disease. The free- disease and endemic equilibria was obtained. The reproduction number denotes by R_0. The free- disease equilibrium is locally and globally stable. By using Poincare-Bendixon theorm, the endemic equilibrium was obtained.

Keywords: difference scheme; Asymptotic stability; Epidemic models.
Mathematics Subject Classification (2010): 62N01, 962F10.

1 Introduction

Mathematical models are increasingly used to understand the dynamics of infectious diseases. They represent the mechanisms and temporal dynamics of infectious disease epidemics and are increasingly used in the field of infectious diseases to better understand natural history, make predictions about the future, and evaluate potential interventions [1-3]. As modeling studies have proliferated and grown more complex, it has become more difficult for clinicians and policy makers to understand their inner workings [1, 3]. Interpretation of these models conclusions without an understanding of their underlying assumptions and mechanics can be misleading [4].

In this paper, we suppose that the population is divided into three classes; the susceptible individuals S_1, the infected individuals I, i.e. disease users, and the

*Speaker: ghasemabadi.math@gmail.com

aware susceptible individuals S_2, i.e. the suceptible individuals who have information about the harms and dangers of disease. We assume that due to media outreach programs, (in T.V., newspapers, social networks,...), about the harms and dangers of disease, susceptibles from S_1 are transferred to S_2. In this model, we consider two routes for information dissemination:
(i) information dissemination via direct contact between individuals given by f_1(e.g., mass-action or some form of nonlinear incidence), and,
(ii) population-wide dissemination of disease related information given by f_2. Contact between individuals is best characterised by frequency dependent contact (i.e., mass-action). The natural choice for f_1 is given by,

$$f_1 = S_1(\frac{I}{N})$$

The rate of population-wide transmission of information is asumed to depend on the disease prevalence. However the effect of this, will be limited and will saturate for high prevalence with little further impact on individuals behaviour. Thus we consider a MichaelisMenton function as f_2,

$$f_2 = \frac{I}{K + I}$$

where K is a positive constant. As a result of either of these two types of information dissemination, susceptible individuals move to the aware susceptible individuals. However, information that covers the same topic repeatedly will loose its value over time. We consider d as the rate of decay of information and awareness. In this model β is the contact rate of susceptibles with infectious individuals. The constants ν, μ and A, represent the recovery rate, the natural death rate and the rate of immigration or suceptibles, respectively. The dynamics of model is governed by the following system of nonlinear ordinary differential equations:

$$\begin{cases} \frac{dS_1}{dt} = A - \alpha_s S_1(\frac{I}{N}) - \alpha_l S_1(\frac{I}{I+K}) + dS_2 - \mu S_1 + \nu I - \beta S_1(\frac{I}{N}) \\ \frac{dS_2}{dt} = \alpha_s S_1(\frac{I}{N}) - dS_2 + \alpha_l S_1(\frac{I}{I+K}) - \mu S_2 \\ \frac{dI}{dt} = \beta S_1(\frac{I}{N}) - \nu I - \mu I \end{cases} \tag{1.1}$$

The total population, $N = S_1 + S_2 + I$, satisfies $\frac{dN}{dt} = A - \mu N$, hence it can be assumed to be of constant size, i.e., $N = \frac{A}{\mu}$. We introduce the fractions, $s_1 = \frac{S_1}{N}, s_2 = \frac{S_2}{N}, i = \frac{I}{N}$, and $k = \frac{K}{N}$, which satisfies $s_1 + s_2 + i = 1$. Using this relations,

finally we consider the following two dimensional system:

$$\begin{cases} \dfrac{ds_1}{dt} = \mu - \alpha_s s_1 u - \alpha_l s_1(\frac{i}{i+k}) + d(1 - s_1 - i) - \mu s_1 + \nu i - \beta s_1 u \\ \dfrac{di}{dt} = \beta s_1 i - \nu i - \mu i \end{cases} \tag{1.2}$$

1.1 Stability of the disease free equilibrium

System (1.2), has the disease free equilibrium $P_0 = (1, 0)$. The Jacobian of the system, is given by,

$$J(s_1, i) = \begin{pmatrix} -\alpha_s i - \alpha_l(\frac{i}{i+k}) - d - \mu - \beta i & -\alpha_s s_1 - \alpha_l s_1(\frac{k}{(k+i)^2}) - d + \nu - \beta s_1 \\ \beta i & \beta s_1 - \nu - \mu \end{pmatrix}$$

and,

$$J(1, 0) = \begin{pmatrix} -d - \mu & -\alpha_s - \frac{\alpha_l}{k} - d + \nu - \beta \\ 0 & \beta - \nu - \mu \end{pmatrix}$$

The eigenvalues of this matrix are $\lambda_1 = -d - \mu$ and $\lambda_2 = \beta - \nu - \mu$, the first eigenvalue is negative and the second eigenvalue is negative, if $\beta < \nu + \mu$. We introduce $R_0 = \frac{\beta}{\nu+\mu}$ as the basic reproduction number, and obtain the following result on the local stability of the disease-free equilibrium.

Theorem 1.1. *The disease-free equilibrium P_0 is asymptotically stable when $R_0 < 1$ and unstable when $R_0 > 1$.*

Furthere more we can prove the global stability of the disease-free equilibrium point.

Lemma 1.2. *The disease-free equilibrium point, P_0, is globally asymptotically stable if $R_0 < 1$.*

Proof. We consider $V(t) = i(t)$ as a Lyapunov function. Then the derivative of V along the solutions of the system, has the following form,

$$\frac{dV}{dt} = \frac{di}{dt} \leqslant (\mu + \nu)(R_0 - 1)i$$

Therefore, when $R_0 < 1$, $\dfrac{dV}{dt} \leqslant 0$, and, $\dfrac{dV}{dt} = 0$ if and only if $i = 0$. Hence P_0 is global asymptotic stable.

1.2 Endemic equilibrium

Let $i^* \neq 0$, the second equation of the system imply:

$$s_1^* = \frac{\nu + \mu}{\beta} = \frac{1}{R_0} \tag{1.3}$$

Now, substituting this value in the first equation of (1.2), and setting equal to zero, we obtain,

$$\mu - \alpha_s(\frac{\nu+\mu}{\beta})u^* - \alpha_l(\frac{\nu+\mu}{\beta})(\frac{u^*}{i^*+k}) + d(1-(\frac{\nu+\mu}{\beta})-i) - \mu(\frac{\nu+\mu}{\beta}) + \nu u^* - \beta(\frac{\nu+\mu}{\beta})i^* = 0$$

Which reduces to,

$$Ai^{*2} + Bi^* + C = 0 \tag{1.4}$$

With the following coefficients:

$A = (\nu+\mu)(-\alpha_s - \beta) + \beta(\nu - d) = (\nu+\mu)(-\alpha_s - R_0(\mu+d)),$
$B = k((\nu+\mu)(-\alpha_s - \beta) + \beta(\nu - d)) + (\mu+d)(\beta - \nu - \mu) - \alpha_l(\nu+\mu)$
$= k(-\alpha_s(\nu+\mu) - \beta(\mu+d)) + (\mu+d)(\nu+\mu)(R_0 - 1) - \alpha_l(\nu+\mu),$
$C = k(\mu+\nu)(\beta - \nu - \mu) = k(\mu+\nu)^2(R_0 - 1)$

Since at an endemic equilibrium $s_1^* < 1$, the endemic equilibrium exists only when, $R_0 > 1$, and C is a positive real number. On the other hand, since i^* is a positive real number, we consider the case $\Delta \geqslant 0$. Solving the equation (1.4), yield:

$$i_{1,2} = \frac{-B}{2A} \pm \frac{\sqrt{\Delta}}{2A} \tag{1.5}$$

We consider two curves $y_1 = Ai^2 + Bi$ and $y_2 = -C$, the intersection points of this curves are the endemic values of i^*. We consider the following different cases for the calculation of i^*:

1) $B > 0$.

In this case, $y_1'' = 2A < 0$, hence the positive point $\frac{-B}{2A}$ is a relative maximum for y_1, and $y_1(\frac{-B}{2A}) = -\frac{B^2}{4A} > 0$. Therefore, there is only one endemic value for i^*. Furtheremore $|\frac{B}{2A}| < |\frac{\sqrt{\Delta}}{2A}|$, implies that $i_1^* = \frac{-B}{2A} - \frac{\sqrt{\Delta}}{2A}$ is positive, therefore in this case, $P^* = (s_1^*, s_2^*, i^*) = (\frac{\nu+\mu}{\beta}, 1 - (\frac{\nu+\mu}{\beta}) - \frac{(-B-\sqrt{\Delta})}{2A}, \frac{-B-\sqrt{\Delta}}{2A})$ is the only endemic equilibrium point.

2) $B < 0$.

In this case, $y_1(\frac{-B}{2A}) = -\frac{B^2}{4A} > 0$ and $y_1'' = 2A < 0$. Therefore the negative point $\frac{-B}{2A}$, is a relative maximum point for y_1, and there is a positive value for i^*. Since $|\frac{B}{2A}| < |\frac{\sqrt{\Delta}}{2A}|$, the root $i_1^* = \frac{-B}{2A} - \frac{\sqrt{\Delta}}{2A}$, is the positive value of i^*. So in this case, $P^* = (s_1^*, s_2^*, i^*) = (\frac{\nu+\mu}{\beta}, 1 - (\frac{\nu+\mu}{\beta}) - \frac{(-B-\sqrt{\Delta})}{2A}, \frac{-B-\sqrt{\Delta}}{2A})$ is the endemic equilibrium point.

3) $B = 0$.
When $B = 0$, then, $P^* = (s_1^*, s_2^*, i^*) = (\frac{\nu+\mu}{\beta}, 1 - (\frac{\nu+\mu}{\beta}) - \sqrt{\frac{-C}{A}}, \sqrt{\frac{-C}{A}})$ is the endemic equilibrium point of the system.

Now we investigate the local stability of the endemic equilibrium. The characteristic equation of the Jacobian matrix of the endemic euilibrium has the following form,

$$\lambda^2 - \lambda p + q = 0$$

Where $p = TraceJ(P^*) = -\alpha_s i^* - \alpha_l(\frac{i^*}{i^*+k}) - d - \mu - \beta i^* < 0$ and
$q = DetJ(P^*) = \beta i^*(\alpha_s(\frac{\nu+\mu}{\beta}) + \alpha_l(\frac{\nu+\mu}{\beta})(\frac{k}{(k+i^*)^2}) + d + \mu) > 0$, which shows the local stability of the endemic equilibrium point. Now if $\Delta = p^2 - 4q \geqslant 0$, the endemic equilibrium is a stable node and if $\Delta \leqslant 0$, the endemic equilibrium is a stable focus.

For the study of global stability of the endemic equilibrium point, we use the Poincare-Bendixon theorem. It is easy to verify that the triangle T in the $s_1 i$ phase plan given by $T = \{(s_1, i) : s_1 \geqslant 0, i \geqslant 0, s_1 + i \leqslant 1\}$, is positively invariant. We use the dulac function $B(s_1, i) = \frac{1}{i}$, for which, $div(Bf, Bg) = -\alpha_s - \alpha_l(\frac{1}{i+k}) - \frac{d}{i} - \frac{\mu}{i} - \beta < 0$. Therefore, there are no periodic solutions for $i > 0$.
The above discusions imply the following theorem.

Theorem 1.3. *If $R_0 > 1$, system (1.2), has a unique and globallly asymptotic stable equilibrium point P^*.*

References

[43] F. Topsze, *Topology and Measure*, Lecture Notes in Mathematics, Vol. 133, Springer, Berlin, 1970.

[44] Arino J, McCluskey CC, Van den Driessche P. *Global results for an epidemic model with vaccination that exhibits backward bifurcation.* SIAM Journal on Applied Mathematics.2003;64(1):260-276.

[45] Buonomo B, Lacitignola D. *Global stability for a four dimensional epidemic model. Note di Matematica.* 2011;30(2):83-96.

[46] Buonomo B, Lacitignola D. *On the use of the geometric approach to global stability for three dimensional ODE systems: a bilinear case.* Journal of Mathematical Analysis and Applications. 2008;348(1):255-266.

[47] Buonomo B, dOnofrio A, Lacitignola D. *Global stability of an SIR epidemic model with information dependent vaccination.* Mathematical Biosciences. 2008;216(1):9-16.

[48] Castillo-Chavez C, Song B. *Dynamical models of tuberculosis and their applications.* Math Biosci Eng. 2004;2:361-404.

[49] Feng X, Teng Z, Wang K, Zhang F. *Backward bifurcation and global stability in an epidemic model with treatment and vaccination. Discrete and Continuous Dynamical Systems-Series B.* 2014;19(4):999-1025.

[50] Gumel AB, McCluskey CC, Watmough J. *An SVEIR model for assessing potential impact of an imperfect anti-SARS vaccine.* Math Biosci Eng. 2006;3:485-512.

Modelling a disease with a nonlinear incidence function

Atena Ghasemabadi*
Esfarayen University of Technology, Esfarayen,North Khorasan, Iran

Abstract:

The present paper considers a disease model with nonlinear incidence function. It studies its boundedness. Since the real world is Boundedness of solutions is important for well-defined model. We obtain free- disease and endemic equilibria both $m = 0$ and $m > 0$. We define the reproduction number by R_0. The model has at least one and at most three positive equilibrium (endemic equilibria) provided $R_0 > 1$. We show that free- disease equilibrium $(0, 0, 0)$ is unstable. The disease free equilibrium $(K, 0, 0)$ is globally asymptotically stable provided $R_0 < 1$.

Keywords: difference scheme; Asymptotic stability; Epidemic models.
Mathematics Subject Classification (2010): 62N01, 962F10.

1 Introduction

In recent years, realistic mathematical models of infectious diseases has been considered. Mathematical models play a key role in the control and spread and of infectious disease. One of the most important factors in modelling of communicable diseases is the incidence function. In the classical communicable models, the incidence rate is assumed to be by SI, where is a positive parameter and it is the probability of transmission per contact. non-linear incidence rates But the nonlinear incidence rates is closer to real world. There are many models using variety of different nonlinear incidence functions to study the disease transmission. In this paper, the incidence function $\beta(I) = \mu e^{-mI}$ is the contact and transmission term, it measures the transmission spread of the virus from the infected to the susceptible

*Speaker: ghasemabadi.math@gmail.com

individual. The transmission rate is a constant provided $m = 0$. Naturally the alertness to the disease of each susceptible individual of the population is important. Here we use the parameter $m > 0$ to reflect the impact of alertness individual.

We consider the following compartments in the population: $S(n)$, the number of susceptible individuals, $E(t)$, the number of exposed individuals but not infectious individuals, and $I(t)$, the number of infected individuals who are infectious. By assuming that the total population obey logistic growth, their model takes the following form:

$$\begin{aligned} S_{n+1} &= \frac{(1+b\phi_1)S_n}{1+\frac{b}{K}\phi_1 S_n + \mu\phi_1 I_n e^{-mI_n}}, \\ E_{n+1} &= \frac{E_n + \mu\phi_2 S_{n+1} I_n e^{-mI_n}}{1+(c+d)\phi_2}, \\ I_{n+1} &= \frac{I_n + c\phi_3 E_{n+1}}{1+\gamma\phi_3}, \end{aligned} \tag{1.1}$$

For any solution (S_n, E_n, I_n) of the system (1.1), the total population $N_n = S_n + E_n + I_n$. In this system total population is not constant, in the following theorem, we prove its boundedness. In this model total population is not constant, we prove its boundedness.

Theorem 1.1. *For any solution (S_n, E_n, I_n) of the system (1.1), the total population, $N_n = S_n + E_n + I_n$, satisfies*

$$\limsup_{n\to\infty} N_n \leqslant \frac{bK}{l},$$

where $l = \min\{b, d, \gamma\}$.

Proof. From system (1.1), we have

$$S_{n+1} = \frac{(1+b\phi_1)S_n}{1+\frac{b}{K}\phi_1 S_n + \mu\phi_1 I_n e^{-mI_n}} \leqslant \frac{(1+b\phi_1)S_n}{1+\frac{b}{K}\phi_1 S_n}.$$

Let $S_n = \frac{1}{z_n}$, then we have

$$z_{n+1} \geqslant \frac{z_n}{1+b\phi_1} + \frac{b\phi_1}{K(1+b\phi_1)}.$$

Hence,

$$z_n \geqslant \frac{1}{(1+b\phi_1)^n} z_0 + \left[1 - \frac{1}{(1+b\phi_1)^n}\right]\frac{1}{K}.$$

As a consequence, we have

$$\limsup_{n\to\infty} S_n \leqslant K.$$

Let $\phi_i(h) = h$ for $i = 1, 2, 3$ and $N_n = S_n + E_n + I_n$. Then we have

$$\begin{aligned}\frac{N_{n+1} - N_n}{h} &= \left(b - \frac{b}{K}S_{n+1}\right) S_n - dE_{n+1} - \gamma I_{n+1} \\ &\leqslant \left(b - \frac{b}{K}S_{n+1}\right) K - dE_{n+1} - \gamma I_{n+1},\end{aligned}$$

for all large n. Now we consider $l = \min\{b, d, \gamma\}$. Therefore

$$\frac{N_{n+1} - N_n}{h} \leqslant bK - lN_{n+1},$$

and we have

$$N_{n+1} \leqslant \frac{1}{1+lh}N_n + \frac{bhK}{1+lh}.$$

Consequently

$$N_n \leqslant \frac{1}{(1+lh)^n}N_0 + \left[1 - \frac{1}{(1+lh)^n}\right]\frac{bK}{l}.$$

From the above discussion, we note that if $N_n \leqslant \frac{bK}{l}$, then

$$N_{n+1} \leqslant \frac{bK}{l(1+lh)} + \frac{bhK}{1+lh} = \frac{bK}{l}.$$

This completes the proof. □

We can conclude that the region

$$D = \left\{(S, E, I) \in R^3 \middle| \quad 0 \leqslant S + E + I \leqslant \frac{bK}{l}, \quad l = \min\{b, d, \gamma\}\right\},$$

is positively-invariant. Now we study equilibrium points of (1.1). We consider the system

$$\begin{aligned}S &= \frac{(1+b\phi_1)S}{1 + \frac{b}{K}\phi_1 S + \mu\phi_1 I e^{-mI}}, \\ E &= \frac{E + \mu\phi_2 SIe^{-mI}}{1 + (c+d)\phi_2}, \\ I &= \frac{I + c\phi_3 E}{1 + \gamma\phi_3}.\end{aligned} \tag{1.2}$$

Clearly $G_0 = (0, 0, 0)$ and $G_1 = (K, 0, 0)$ are equilibrium points of (1.1). Further-

emore system (1.1) has endemic equilibrium points which we determine it in the following cases.

- $m = 0$. In this case (1.2) takes the following form:

$$\begin{aligned} S &= \frac{(1+b\phi_1)S}{1+\frac{b}{K}\phi_1 S+\mu\phi_1 I}, \\ E &= \frac{E+\mu\phi_2 SI}{1+(c+d)\phi_2}, \\ I &= \frac{I+c\phi_3 E}{1+\gamma\phi_3}. \end{aligned}$$

  We define the reproduction number by $R_0 = \frac{\mu cK}{\gamma(c+d)}$. From the above system, system (1.1) has a unique endemic equilibrium $G_2 = (S_0^*, E_0^*, I_0^*)$ provided $R_0 > 1$, as follows:

$$\begin{aligned} S_0^* &= \frac{\gamma(c+d)}{\mu c} = \frac{K}{R_0}, \\ E_0^* &= \frac{b\gamma^2(c+d)}{\mu^2 c^2 K}(R_0-1), \\ I_0^* &= \frac{b\gamma(c+d)}{\mu^2 cK}(R_0-1). \end{aligned}$$

- $m > 0$. We slove system (1.2) and we obtain

$$\begin{aligned} S^* &= K(1-\frac{\mu}{b}I^* e^{-mI^*}) := g(I^*), \\ E^* &= \frac{\gamma}{c}I^*, \\ S^* &= \frac{\gamma(c+d)}{c\mu}e^{mI^*} := h(I^*). \end{aligned}$$

  Clearly, if $R_0 > 1$, then $g(0) > h(0)$. Note that $\lim_{I^*\to\infty} g(I^*) = K$ and $\lim_{I^*\to\infty} h(I^*) = \infty$. Hence if $R_0 > 1$, the two curves $S = g(I)$ and $S = h(I)$ have at least one positive intersection which gives at least one endemic equilibrium. Now we develop conditions to decide the tangency of the two curves in order to determine the number of positive equilibria. If the two curves $S = g(I)$ and $S = h(I)$ are tangent at some positive points, we must

have $S = g(I) = h(I)$ and $g'(I) = h'(I)$. Or equivalently,

$$\begin{aligned} K\left(1 - \frac{\mu}{b} I^* e^{-mI^*}\right) &= \frac{\gamma(c+d)}{\mu c} e^{mI^*}, \\ -\frac{K\mu}{b}(1 - mI^*)e^{-mI^*} &= \frac{\gamma(c+d)m}{\mu c} e^{mI^*}. \end{aligned}$$

By eliminating exponential terms in the above system we see that, if the two curves are tangent, then I coordinate must satisfy the following quadratic equation

$$R_0 m(mI^* - 1) = (2mI^* - 1)^2 \frac{\mu}{b}. \tag{1.3}$$

Hence, if the tangency occurs at some points, its I coordinate must satisfy $mI^* > 1$.

Let

$$\delta := \frac{\mu}{b}, \quad m_0 := \frac{8\mu}{bR_0} = \frac{8\delta}{R_0}.$$

By a straightforward calculation we see that (1.3) has two distinct positive roots satisfying $mI > 1$ if and only if $R_0 > 1$ and $m > m_0$. for $m > 0$, by solving (1.3) in terms of I, we have

$$I^* = \frac{mR_0 + 4\delta \pm \sqrt{mR_0(mR_0 - 8\delta)}}{8m\delta}. \tag{1.4}$$

Theorem 1.2. *If $R_0 > 1$, then the model (1.1) has at least one and at most three positive equilibrium (endemic equilibria). Furthermore,*
1) if $0 < m < m_0$, the model (1.1) has a unique endemic equilibrium;
2) if $m > m_0$, the model has three endemic equilibrium.

2 Stability

In this section we investigate stability of equilibrium points $G_0 = (0, 0, 0)$ and $G_1 = (K, 0, 0)$.

Theorem 2.1. *The equilibrium point $G_0 = (0, 0, 0)$ is unstable*

Proof. The Jacobian evaluated at this point is given by the following matrix:

$$J(0,0,0) = \begin{bmatrix} 1+b\phi_1 & 0 & 0 \\ 0 & \frac{1}{1+(c+d)\phi_2} & 0 \\ 0 & \frac{c\phi_3}{1+\gamma\phi_3} & \frac{1}{1+\gamma\phi_3} \end{bmatrix}$$

The eigenvalues of $J(0,0,0)$ are $1+b\phi_1$, $\frac{1}{1+(c+d)\phi_2}$ and $\frac{1}{1+\gamma\phi_3}$. Since $1+b\phi_1 > 1$, $(0,0,0)$ is unstable. □

At the point $(K,0,0)$ we have the following Jacobian matrix:

$$J(K,0,0) = \begin{bmatrix} 1-\frac{b\phi_1}{1+b\phi_1} & 0 & -\frac{\mu K\phi_1}{1+b\phi_1} \\ 0 & \frac{1}{1+(c+d)\phi_2} & \frac{\mu K\phi_2}{1+(c+d)\phi_2} \\ 0 & \frac{c\phi_3}{1+\gamma\phi_3} & \frac{1}{1+\gamma\phi_3}. \end{bmatrix}$$

It is clear that $1-\frac{b\phi_1}{1+b\phi_1} < 1$. Consider the following submatrix

$$B = \begin{bmatrix} \frac{1}{1+(c+d)\phi_2} & \frac{\mu K\phi_2}{1+(c+d)\phi_2} \\ \frac{c\phi_3}{1+\gamma\phi_3} & \frac{1}{1+\gamma\phi_3}. \end{bmatrix}$$

We show that $\det B < 1$ and $trB < 1+\det B$ which implies that eigenvalues of B lies inside unit circle. It is easy to see that $\det B < 1$. We show that $trB < 1+\det B$. This is equivalent to

$$\begin{aligned} & [1+(c+d)\phi_2 + 1+\gamma\phi_3](1+\gamma\phi_3)[1+(c+d)\phi_2] \\ < \; & [1+(c+d)\phi_2]^2(1+\gamma\phi_3)^2 + [1+(c+d)\phi_2](1+\gamma\phi_3)(1-\mu cK\phi_2\phi_3) \end{aligned}$$

which is equivalent to

$$2+(c+d)\phi_2+\gamma\phi_3 < [1+(c+d)\phi_2](1+\gamma\phi_3) + (1-\mu cK\phi_2\phi_3)$$

and this is true if and only if

$$\gamma(c+d)\phi_2\phi_3 - \mu cK\phi_2\phi_3 > 0$$

which is the same as $R_0 < 1$. Hence we have the following theorem.

Theorem 2.2. *The disease free equilibrium* $(K,0,0)$ *is locally asymptotically stable*

if $R_0 < 1$, and unstable if $R_0 > 1$. Now we prove global stability of $(K, 0, 0)$ when $m = 0$. Let $m = 0$, if $R_0 < 1$, then the disease free equilibrium $(K, 0, 0)$ is globally asymptotically stable.

References

[51] Cui, J. Sun, Y. and Zhu, H. "*The impact of media on the control of infectious diseases*", Journal of Dynamics and Differential Equations, 20 (2008) 31-53.

[52] Garba, S.M. Gumel, A.B. and Lubuma, J.M.-S. "*Dynamically-consistent non-standard finite difference method for an epidemic model*", Mathematical and Computer Modelling 53 (2011) 131-150.

[53] Jodar, L., Villanueva, R. J., Arenas, A. J. and Gonzalez, G. "*Nonstandard numerical methods for a mathematical model for influenza disease*", Mathematics and Computers in Simulation 79 (2008) 622-633.

[54] Gonzalez-Parra, G., Arenas, A. J. and Chen-Charpentier, B. M. "*Combination of nonstandard schemes and Richardson's extrapolation to improve the numerical solution of population models*", Mathematical and Computer Modelling 52 (2010) 1030-1036.

[55] Mickens, R. E. "*Advances in the applications of nonstandard finite difference schemes*", World Scientific Publishing Co. Pte. Ltd, 2005.

[56] Mickens, R. E. "*Discrete models of differential equations: The roles of dynamic consistency and positivity*", in: Allen, Linda J S. Aulbach, B. Elaydi, S and Sacker, R. "*Difference Equations and Discrete Dynamical Systems*", Proceeding of the 9th International Conference.

[57] Elaydi, S. "*An Introduction to difference equations*", Third Edition, Springer-verlag, 2004.

[58] Kuznetsov, Y. A. "*Elements of applied bifurcation theory*", Second Edition, Springer-verlag, 1998.

[59] Murray, J. D. "*Mathematical biology*", Springer-Verlag, Berlin, 1998.

[60] Roeger, L. I. W., Mickens, R. E. "*Exact finite-difference schemes for first order differential equations having three fixed points*", J. Difference Equations and applications, 13 (2007) 1179-1185.

[61] Wen, G. L., Xu, D. and Han, X., "*On creation of Hopf bifurcations in discrete-time nonlinear systems*", Chaos, 12 (2002) 350-355.

Backward bifurcations in epidemiological models

Azizeh Jabbari*[1],Hossein Kheiri[2], Mohsen Jafari[2] and Fatemeh Iranzad [2]
[1]Marand Faculty of Engineering, University of Tabriz, Tabriz, Iran
[2] Faculty of Mathematical Sciences, University of Tabriz, Tabriz, Iran

Abstract:

This paper is about the phenomenological study of bifurcations in epidemiological models, in particular, in backward bifurcation. We consider models that exhibit such bifurcation and also consider the factors that cause them. The phenomenon of backward bifurcation in disease transmission models, where a stable endemic equilibrium co-exists with a stable disease-free equilibrium when the associated reproduction number is less than unity, has been observed in a number of disease transmission models. The epidemiological consequence of backward bifurcation is that the classical requirement of the reproduction number being less than unity becomes only a necessary, but not sufficient, for disease elimination (hence, the presence of this phenomenon in the transmission dynamics of a disease makes its effective control in the community difficult).

Keywords: Backward bifurcation, Equilibrium, Reproduction number, Stability
Mathematics Subject Classification (2010): 62N01, 962F10.

1 Introduction

In compartmental models for the transmission of communicable diseases there is usually a basic reproductive number $\mathcal{R}_0$, representing the mean number of secondary infections caused by a single infective introduced into a susceptible population. When $\mathcal{R}_0$ is less than unity, a small influx of infected individuals will not generate large outbreaks, and the disease dies out in time (in this case, the corresponding disease-free equilibrium (DFE) is asymptotically-stable). On the other hand, the disease

*Speaker: jabari@tabrizu.ac.ir

will persist if $\mathcal{R}_0$ exceeds unity, where a stable endemic equilibrium exists. This phenomenon, where the disease-free equilibrium loses its stability and a stable endemic equilibrium appears as $\mathcal{R}_0$ increases through one, is known as forward bifurcation. Some of the main characteristics of forward bifurcation are the absence of positive (endemic) equilibria near the DFE when $\mathcal{R}_0 < 1$ (in this setting, the DFE is often the only equilibrium when $\mathcal{R}_0 < 1$) and a low level of endemicity when $\mathcal{R}_0 < 1$ is slightly above unity (62). The forward bifurcation phenomenon, first noted by Kermack and McKendrick, has been observed in numerous disease transmission models. For models that exhibit forward bifurcation, the requirement $\mathcal{R}_0 < 1$ is necessary and sufficient for disease elimination. Other models for disease transmission undergo another type of bifurcation, known as backward bifurcation, where a stable endemic equilibrium co-exists with a stable DFE when $\mathcal{R}_0 < 1$. The epidemiological implication of backward bifurcation is that the requirement $\mathcal{R}_0 < 1$, while necessary, is not sufficient for effective disease control. In a backward bifurcation setting, once $\mathcal{R}_0$ crosses unity, the disease can invade to a relatively high endemic level. In this case, decreasing $\mathcal{R}_0$ to its former level will not necessarily make the disease disappear (62). The common causes of backward bifurcation in disease transmission models are the use of an imperfect vaccine and exogenous re-infection in the transmission dynamics of mycobacterium tuberculosis (TB).

The aim of this study is to provide a short review of some of the common mechanisms (biological, epidemiological, social etc.) that cause the phenomenon of backward bifurcation in disease transmission models. To achieve this aim, a number of deterministic models for the spread of some emerging and re-emerging diseases will be considered. The paper contains a summary of some established results and some new results.

2 Bifurcation Theory

Real-life systems arising in the natural and engineering sciences typically involve parameters which appear in their governing system of equations. As these parameters are varied, changes may occur in the qualitative structures of the solutions of the system of equations (modelling the real-life phenomenon) for certain parameter values. These changes are called bifurcations. The parameter values where bifurcations occur are called bifurcation values (or bifurcation points). A formal definition of bifurcation at a point is given below.

Definition 8. *Let*

$$\dot{x} = f(x, \mu), \quad x \in \mathbb{R}^n, \quad \mu \in \mathbb{R}, \tag{2.1}$$

be a one-parameter family of one-dimensional ODEs. An equilibrium solution of (2.1) *given by* $(x, \mu) = (0, 0)$ *is said to undergo bifurcation at* $\mu = 0$ *if the flow for* μ *near zero and* x *near zero is not qualitatively the same as the flow near* $x = 0$ *at* $\mu = 0$.

There are numerous types of bifurcations, including saddle-node, forward (transcritical), pitchfork, Hopf, and backward bifurcation. Two of these bifurcations (forward and backward) are relevant to the paper, and are briefly discussed below.

2.1 Forward bifurcation

The dynamics of disease transmission models is often characterized by the reproduction number ($\mathcal{R}_0$), a threshold quantity which measures the average number of new cases generated by a typical infected individual when introduced into a completely susceptible population. Typically, when $\mathcal{R}_0$ is less than unity, a small stream of infected individuals will not generate large outbreaks (and the disease dies out in time). In such a case, the disease-free equilibrium (DFE) of the model is asymptotically-stable. On the other hand, the disease persists in the population if $\mathcal{R}_0$ exceeds unity (where, in this case, an asymptotically-stable endemic equilibrium point (EEP) exists). This phenomenon, where the DFE and an EEP of a model exchange their stability at $\mathcal{R}_0 = 1$, is known as forward bifurcation.

2.2 Backward bifurcation

In general, for models that exhibit forward bifurcation, the requirement $\mathcal{R}_0 < 1$ is necessary and sufficient for effective community-wide control (or elimination) of the disease being modelled. However, it has been observed in some other modelling studies, that although $\mathcal{R}_0 < 1$ is necessary for effective disease control (or elimination), the condition may not be sufficient. This is owing to a dynamic phenomenon known as backward bifurcation, where two stable attractors (typically the DFE and an asymptotically-stable EEP) of the model co-exist when $\mathcal{R}_0 < 1$. The public health implication of backward bifurcation is that disease control (or elimination), when $\mathcal{R}_0 < 1$, is dependent on the initial sizes of the sub-populations of the model. Thus, the presence of backward bifurcation in the transmission dynamics of a disease in a population makes its effective community-wide control difficult. The following the-

orem will be used to explore the possibility of the presence of backward bifurcation in the models to be considered in next section of this paper.

Theorem 2.1. *Consider the following general system of ordinary differential equations with a parameter* ϕ

$$\frac{dx}{dt} = f(x,\phi), \quad f : \mathbb{R}^n \times \mathbb{R} \to \mathbb{R}^n, \quad \text{and} \quad f \in \mathbb{C}^2(\mathbb{R}^n \times \mathbb{R}), \tag{2.2}$$

where 0 *is an equilibrium point of the system (that is,* $f(0,\phi) \equiv 0$ *for all* ϕ*) and assume*

1. $A = D_x f(0,0) = (\frac{\partial f_i}{\partial x_j}(0,0))$ *is the linearization matrix of the system (2.2) around the equilibrium* 0 *with* ϕ *evaluated at* 0*. Zero is a simple eigenvalue of* A *and other eigenvalues of* A *have negative real parts;*

2. *Matrix* A *has a right eigenvector* w *and a left eigenvector* v *(each corresponding to the zero eigenvalue).*

Let f_k *be the* k*-th component of* f *and*

$$\begin{aligned} a &= \sum_{k,i,j=1}^{n} v_k w_i w_j \frac{\partial^2 f_k}{\partial x_i \partial x_j}(0,0) \\ b &= \sum_{k,i=1}^{n} v_k w_i \frac{\partial^2 f_k}{\partial x_i \partial \phi}(0,0). \end{aligned}$$

Then the local dynamics of the system around the equilibrium point 0 *is totally determined by the signs of* a *and* b*. Particularly, if* $a > 0$ *and* $b > 0$*, then a backward bifurcation occurs at* $\phi = 0$*.*

3 Common sources of backward bifurcation

3.1 Exogenous re-infection

Consider the following model for the transmission dynamics of TB

$$\begin{aligned} \frac{dS}{dt} &= \Lambda - \lambda S - \mu S, \\ \frac{dE}{dt} &= (1-p)\lambda S + rI - \zeta\lambda E - \sigma E - \mu E, \\ \frac{dI}{dt} &= p\lambda S + \sigma E + \zeta\lambda E - rI - dI - \mu I, \end{aligned} \tag{3.1}$$

where

$$\lambda = \frac{\beta I}{N}. \tag{3.2}$$

The model (3.1) has a disease-free equilibrium (DFE) given by

$$\varepsilon_0^{wt} = (\frac{\Lambda}{\mu}, 0, 0).$$

Furthermore, the associated reproduction number of the model is given by

$$\mathcal{R}_0 = \frac{\beta[p\mu + \sigma]}{\mu(\mu + d + r) + \sigma(\mu + d)}, \tag{3.3}$$

Let β^* be the bifurcation parameter (obtained by setting $\mathcal{R}_0 = 1$ and solving for β). Consider the associated invariant region for the model

$$\mathcal{D} = \left\{ (S, E, I) \in \mathbb{R}^3_+ : N \leqslant \frac{\Lambda}{\mu} \right\}.$$

The following result can be established using center manifold theory

Theorem 3.1. *The model (3.1) undergoes backward bifurcation if $\mathcal{R}_0 < 1$ and $\mu + d > \beta^*$.*

3.1.1 Non-existence of backward bifurcation

In this case ($\zeta = 0$), no endemic equilibrium exists whenever $\mathcal{R}_0 \leqslant 1$. It then follows that, owing to the absence of multiple endemic equilibria for system (3.1) with $\zeta = 0$ and $\mathcal{R}_0 \leqslant 1$, a backward bifurcation would not occur for system (3.1) with $\zeta = 0$ and $\mathcal{R}_0 \leqslant 1$.

The absence of multiple endemic equilibria suggests that the disease-free equilibrium of model (3.1) is globally asymptotically stable when $\mathcal{R}_0 \leqslant 1$. Then, we have the following result:

Theorem 3.2. *Consider the model (3.1) with $\zeta = 0$. The disease-free equilibrium is globally asymptotically stable in $\mathcal{D}$ whenever $\mathcal{R}_0 \leqslant 1$.*

3.2 Models with imperfect vaccine

Consider the SVIRS vaccination model with waning vaccine-induced (ω_ν) and natural (ω_r) immunity (63; 64):

$$\begin{aligned}
\frac{dS}{dt} &= \Pi(1-\phi) + \omega_\nu V + \omega_r R - \lambda S - \mu S,\\
\frac{dV}{dt} &= \Pi\phi - (1-\psi)\lambda V - (\omega_\nu + \mu)V,\\
\frac{dI}{dt} &= \lambda S + (1-\psi)\lambda V - (\sigma_u + \mu)I,\\
\frac{dR}{dt}&\sigma_u I - (\omega_r + \mu)R,
\end{aligned} \tag{3.4}$$

where

$$\lambda = \frac{\beta I}{N}. \tag{3.5}$$

Define:

$$\mathcal{R}_\nu = \mathcal{R}_0\left(1 - \frac{\mu\phi\psi}{\omega_\nu + \mu}\right), \qquad \text{with} \qquad \mathcal{R}_0 = \frac{\beta}{\sigma_u + \mu}.$$

Following (63; 64), the vaccine failure duration (V_F) and a critical vaccine failure duration (V_F^C) are defined, respectively, by

$$V_F = \frac{1-\psi}{\omega_\nu + \mu}, \qquad V_F^C = \frac{\sigma_u + \mu + \omega_r}{(\mu + \omega_r)(\sigma_u + \mu)(\mathcal{R}_0 - 1)}.$$

The following results were established in (63).

Theorem 3.3. *The vaccination model* (3.4) *exhibits backward bifurcation at* $\mathcal{R}_\nu = 1$ *whenever*

$$\frac{\sigma_u\omega_r}{(\mu + \omega_r)(\sigma_u + \mu)} > \mathcal{R}_0\left(1 - \frac{\mu\phi\psi}{(\omega_\nu + \mu)}\left(1 + \frac{\mu(1-\psi)}{(\omega_\nu + \mu)}\right)\right).$$

Theorem 3.4. *The vaccination model* (3.4) *does not undergo backward bifurcation at* $\mathcal{R}_\nu = 1$ *if any of the following conditions hold:*

(i) *The vaccine offers perfect protection against break-through infection (i.e.,* $\psi = 1$*)*

(ii) *Vaccine-derived immunity wanes faster than natural immunity (i.e.,* $\omega_\nu \geqslant \omega_r$ *)*

(iii) *Vaccine failure duration does not exceed a certain critical value (i.e.,* $V_F \leqslant V_F^C$ *).*

The imperfect nature of the vaccine is a well-known reason for the presence of backward bifurcation in vaccination models (Case (i) of Theorem 3.4 shows that if this imperfection is removed, then the phenomenon of backward bifurcation will not occur). Cases (ii) and (iii) of Theorem 3.4 are new additional sources of eliminating backward bifurcation in SIRS models that incorporate an imperfect vaccine. It follows from Case (iii) that the backward bifurcation will disappear if infection offers permanent immunity against e-infection ($\omega_r = 0$).

In summary, the SVIRS model (3.4) will not undergo backward bifurcation if any of the scenarios in Theorem 3.4 hold.

4 Conclusions

This paper identifies some epidemiological mechanisms that can induce the phenomenon of backward bifurcation in standard KermackMcKendrick type disease transmission models (that use standard incidence rate for the infection rate). It is shown that backward bifurcation, which has significant consequences on the persistence or elimination of the disease when the associated reproduction number of the model is less than unity, could arise due to mechanisms such as:

(1) Exogenous re-infection (of latently-infected individuals) in models for the spread of mycobacterium tuberculosis. Reinfection, in general, causes backward bifurcation (see, for instance, for the role of re-infection in the backward bifurcation phenomenon observed in Chlamydia transmission dynamics);

(2) Vaccination. The main sources of backward bifurcation in vaccination models are:

- **(i)** The vaccine offers perfect protection against break-through infection (i.e., $\psi = 1$)
- **(ii)** Vaccine-derived immunity wanes faster than natural immunity (i.e., $\omega_\nu \geqslant \omega_r$)
- **(iii)** Vaccine failure duration does not exceed a certain critical value (i.e., $V_F \leqslant V_F^C$).

References

[62] J. Dushoff, H. Wenzhang, C. Castillo-Chavez, *Backwards bifurcations and catastrophe in simple models of fatal diseases*, Journal of Mathematical Biology, 36 (1998), pp. 227–248.

[63] E.H. Elbasha, C.N. Podder, A.B. Gumel, *Analyzing the dynamics of an SIRS vaccination model with waning natural and vaccine-induced immunity*, Nonlinear Analysis: Real World Applications, 12 (2011), pp. 2692–2705.

[64] A.B. Gumel, *Causes of backward bifurcations in some epidemiological models*, Journal of Mathematical Analysis and Applications, 395 (2012), pp. 355–365.

همایش ملی ریاضیات زیستی
اولین همایش ملی ریاضیات زیستی
۲۱ و ۲۲ اسفندماه ۱۳۹۷
دانشگاه نیشابور

Application of the optimal q-homotopy analysis method for solving a model for HIV infection of $CD4^+$T-cells

Fatemeh Kazemi *[1],Maryam Alipour [2]
[1]Department of Mathematics, University of Sistan and Baluchestan, Zahedan Iran
[2]Department of Mathematics, Faculty of Mathematics, University of Sistan and Baluchestan, Zahedan Iran

Abstract:

The aim of this paper is to find the approximate solution of a model for HIV infection of $CD4^+$ T-cells by q-homotopy analysis method (q-HAM). q-HAM is a flexible method that is used to solve a variety of differntial equations. The results obtained show that this method has a lot of efficiency.

Keywords: q-homotopy analysis method, HIV infection model, Analytical solution
Mathematics Subject Classification (2010): 62N01, 962F10.

1 Introduction

Over the years, several nonlinear mathematical models have been proposed to describe infection by the human immune deficiency virus (HIV) and its association whit the immune system. In (65), an HIV infection model was introduced that was used extensively. Wang et al. (66) examined an HIV model for the stability of the uninfected equilibrium point based on the Lyapunov theory. In (67) an HIV optimal control problem was proposed to reduce maintains the drug strength low and maximizes the number of T-cell and immune response cells. In (68), HIV-infection of T- cells was examined by means of homotopy decomposition technique and system

*Speaker: fatemekazemi7222@gmail.com

of fractional differential equations. Recently, Alipour et al. (69) Bernstein operational matrices have been studied for approximate the response of the HIV fractional model. In (70), a model for the infection of the human immune system by HIV was presented. This model of virus spread has three variables: the population sizes of uninfected cells, infected cells, and free virus particles. Perelson et al. (71) extended the model described in(70) and developed a new model by considering four variables:

1. cells that are uninfected,
2. cells that are latently infected,
3. cells that are actively infected,
4. free virus particles.

Their model is described by a system of four ordinary differential equations. It was noted that the model can replicate many of the symptoms of AIDS observed clinically. Culshaw and Ruan(72) reduced the model described in(71) to a system of three ordinary differential equations by assuming that all the infected cells are capable of producing the virus.

In this paper, the q-homotopy analysis method (q-HAM) is introduced and developed for analytical approximation the model for HIV infection of $CD4^+$ T-cells of Culshaw and Ruan described above. The model is (72)

$$\begin{aligned} \frac{dT}{dt} &= s - \mu_T T + rT(1 - \frac{T+I}{T_{max}}) - k_1 VT, \\ \frac{dI}{dt} &= k_1' VT - \mu_I I, \\ \frac{dV}{dt} &= N\mu_b I - k_1 VT - \mu_V V, \end{aligned} \tag{1.1}$$

where $T(t)$, $I(t)$, and $V(t)$ represent the concentration of healthy $CD4^+$ T-cells at timet, infected $CD4^+$ T-cells, and free HIV at timet, respectively.

2 The optimal q-homotopy analysis method

Consider the following differential equations,

$$N[u(t)] = 0, \tag{2.1}$$

where N is a non-linear operator, t denotes independent variable, and $u(t)$ is an unknown function, respectively (73). Let us constructed the so-called zero-order

Table 1: List of variables and parameters (modified from(72)).

Parameters and variables	Meaning
Dependent variables	
T	Uninfected $CD4^+$ T-cell concentration
I	Infected $CD4^+$ T-cell concentration
V	Concentration of HIV RNA
Parameters and constants	
μ_T	Natural death rate of $CD4^+$T-cell concentration
μ_I	Blanket death rate of infected $CD4^+$ T-cells
μ_b	Lytic death rate for infected cells
μ_V	Death rate of free virus
k_1	Rate $CD4^+$ T-cells become infected with virus
k_1'	Rate infected cells become active
r	Growth rate of $CD4^+$T-cell concentration
N	Number of virion produced by infected $CD4^+$-cells
T_{max}	Maximal concentration of $CD4^+$ T-cells
s	Source term for uninfected $CD4^+$ T-cells
Derived quantities	
T_0	$CD4^+$ T-cell concentration for HIV-negative persons

deformation equation

$$(1-nq)L[\phi(t;q)-u_0(t)] = F(n)qN[\phi(t;q)], \tag{2.2}$$

where $q \in [0, \frac{1}{n}]$, is an embedding parameter, n is a non-zero auxiliary parameter, $F(n)$ is a non-zero auxiliary function, $n \geqslant 1$, L is an auxiliary linear operator with the property $L(c_1) = 0$ where c_1 is an integral constant, $u_0(t)$ is an initial guess of $u(t)$ and $\phi(t;q)$ is an unknown function. It is important to note that, one has great freedom to choose auxiliary objects such as q and L in HAM. Obviously, when $q = 0$ and $q = \frac{1}{n}$,

$$\phi(t;0) = u_0(t), and \phi(t;1) = u(t) \tag{2.3}$$

respectively. Thus, as q increases from 0 to 1, the solutions $\phi(t;q)$ varies from the initial guess $u_0(t)$ to the solution $u(t)$. Expanding $\phi(t;q)$ in Taylor series with respect to q, we have

$$\phi(t;q) = u_0(t) + \sum_{m=1}^{+\infty} u_m(t)q^m, \tag{2.4}$$

where

$$u_m(t) = \frac{1}{m!}\frac{\partial^m \phi(t;q)}{\partial q^m}|_{q=0}, \tag{2.5}$$

Assume that $F(n)$, $u_0(t)$, L are so properly chosen such that the series converges at $q = \frac{1}{n}$ and we have

$$u(t) = \phi(t; \frac{1}{n}) = u_0(t) + \sum_{m=1}^{+\infty} u_m(t)(\frac{1}{n})^m, \tag{2.6}$$

Defining the vector $u_r(t) = \{u_0(t), u_1(t), u_2(t), ..., u_r(t)\}$. Differentiating Equation (2) m times with respect to q and then setting $q = 0$ and finally dividing them by $m!$ we have the so-called m^{th} order deformation equation:

$$L[u_m(t) - k_m u_{m-1}(t)] = F(n)R_m(\vec{u_{m-1}}), \tag{2.7}$$

Where and

$$R_m(\vec{v_{m-1}}) = \frac{1}{(m-1)!}\frac{\partial^{m-1}N[\phi(t;q)]}{\partial q^{m-1}}|_{q=0}, \tag{2.8}$$

and

$$k_m = \begin{cases} 0, & m \leqslant 1, \\ n, & \text{otherwise} \end{cases} \tag{2.9}$$

3 Example

In this section, to illustrate the capability of the q-HAM, the variables and parameters, described in Table1, are considered as follows (72):
$T_0 = 1000$, $I_0 = 0$, $V_0 = 0.001$, $r = 0.03$, $\mu_T = 0.02$, $\mu_I = 0.26$, $\mu_b = 0.24$,
$\mu_V = 2.4$, $k_1 = 2.4*10^{-5}$, $k_1' = 2*10^{-5}$, $N = 500$, $s = 10$, $T_{max} = 1500$.
By using Mathematica software, five-term approximations for T_t, I_t, and V_t, were

calculated, and they are presented below.

$$\begin{aligned}
\varphi_T(t) &= T_0 + \sum_{i=1}^{5} T^{(0,i)}(\frac{1}{n})^i = 1000. - 0.000024t + \frac{(0.000024t)}{n^5} + 0.000029248t^2 \\
&+ \frac{(0.000116992t^2)}{n^5} + ... \\
\varphi_I(t) &= I_0 + \sum_{i=1}^{5} I^{(0,i)}(\frac{1}{n})^i = 0. + 0.00002t - \frac{(0.00002t)}{n^5} - 0.00002684t^2 \\
&- \frac{(0.00010736t^2)}{n^5} + ... \\
\varphi_V(t) &= V_0 + \sum_{i=1}^{5} V^{(0,i)}(\frac{1}{n})^i = 0.001 - 0.002424t + \frac{(0.002424t)}{n^5} + 0.00413789t^2 \\
&+ \frac{(0.0165516t^2)}{n^5} + ... \quad ,
\end{aligned} \tag{3.1}$$

to find the optimal values of n, an error analysis is performed. We substitute Eqs 3.1 into 1.1 and obtain the residual function $ER_i(T, I, V)$, $i = 1, 2, 3$ as follows:

$$\begin{aligned}
ER_1(T, I, V; n) &= \frac{\varphi_T(t)}{dt} - s + \mu_T\varphi_T(t) - r\varphi_T(t)(1 - \frac{\varphi_T(t) + \varphi_I(t)}{T_{max}}) - k_1\varphi_V(t)\varphi_T(t), \\
ER_2(T, I, V; n) &= \frac{dI}{dt} = k_1'\varphi_V(t)\varphi_T(t) - \mu_I\varphi_I(t), \\
ER_3(T, I, V; n) &= \frac{dV}{dt} = N\mu_b\varphi_I(t) - k_1\varphi_V(t)\varphi_T(t) - \mu_V\varphi_V(t),
\end{aligned} \tag{3.2}$$

and we define the square residual error for the fifxth-order approximation to be:

$$\begin{aligned}
RT_1 &= \int_0^1 (ER_1(T, I, V; n))^2 dt, \\
RT_2 &= \int_0^1 (ER_2(T, I, V; n))^2 dt, \\
RT_3 &= \int_0^1 (ER_3(T, I, V; n))^2 dt,
\end{aligned} \tag{3.3}$$

value of n, for which RT_1, RT_2, and RT_3 are minimum can be obtained. Thus, we have

$\frac{DRT_1}{Dn} = 0, \qquad \frac{DRT_2}{Dn} = 0, \qquad \frac{DRT_3}{Dn} = 0,$

then, in table [2], the minimum values of RT_1, RT_2, and RT_3 have been given for optimal values of n.

Table 2: The minimum values of RT_1, RT_2, and RT_3.

n	Minimum value
2.55956	$-3.83099 * 10^{-23}$
5.23314	$1.44776 * 10^{-15}$
5.15428	$5.78318 * 10^{-15}$

4 Conclusion

In this paper, the Q-homotopy analysis method has been successfully developed and applied for solving a model for HIV infection of $CD4^+$ T-cells. The results obtained show that the q-HAM is an accurate and effective technique for obtaining the approximate solution of HIV infection of $CD4^+$ T-cells.

References

[65] F. Li, J. Wang, *Analysis of an HIV infection model with logistic target-cell growth and cell-to-cell transmission*, Chaos Soliton Fract, 81 (2015), pA. 136-145.

[66] Y. Wang, J. Liu, L. Liu, *Viral dynamics of an HIV model with latent infection incorporating antiretroviral therapy*, Adv Differ Equ, 225 (2016), 1-15.

[67] D. Rocha, C. J. Silva, D. F. M. Torres, *Stability and optimal control of a delayed HIV model*, Math Methods Appl Sci, 4207 (2016), doi. 10.1002/mma.

[68] A. Atangana, E. Alabaraoye, *Solving a system of fractional partial differential equations arising in the model of HIV infection of CD4 + cells and attractor one-dimensional Keller-Segel equations*, Adv Differ Equ, 94 (2013), 1-14.

[69] M. Alipour, S. Arshad, D. Baleanu, *Numerical and bifurcations analysis for mul-ti-order fractional model of HIV infection of CD4 + T-cells*, UPB Sci Bull, 78 (2016), A.(4). 243-58.

[70] A .S. Perelson, *Modelling the interaction of the immune system with HIV*, C.Castillo-Chavez(Ed.)& Mathematical and Statistical Approaches to AIDS Epidemiology, Springer, Berlin, 350 (1989), p.

[71] A. S. Perelson, D. E. Kirschner, R. DeBoer, *Dynamics of HIV infection of CD4+ T-cells*, Mathematical Biosciences, 114 (1993) 81.

[72] R. V. Culshaw, S. Ruan, *Adelay-differential equation model of HIV infection of CD4+ T-cells*, Mathematical Biosciences, 165 (2000) 27-39.

[73] S. J. Liao, *Introduction to the homotopy analysis method*, Beyond perturbation, CRC Press, Boca Raton, Chapman Hall, (2003).

Estimating Gompertz Survival and Hazard Functions

Bahareh Khatib Astaneh*[1]
[1]Department of Mathematics, University of Neyshabur

Abstract:

In the situations in which the lifetimes of the experimental units are related to some covariates, the Gompertz model may be considered to fit the real data. In this paper, it is assumed that the lifetimes are related to a fixed covariate and the unknown parameters of the model of interest are estimated via maximum likelihood approach. The survival function as well as the hazard function of the model are estimated and the results are applied on a real data set.

Keywords: Fixed covariate model, Lifetime, Maximum likelihood estimation, Q-Q plot
Mathematics Subject Classification (2010): 62N01, 962F10.

1 Introduction

The Gompertz model plays an important role in modeling human mortality and fitting actuarial tables. This model was introduced by Gompertz (75). Recently, it has found more application in fields such as biology and demography. The hazard function of the non-negative continuous random variable T which has Gompertz model, is

$$h(t) = \lambda e^{\gamma t}, t > 0, \lambda > 0, \gamma > 0, \tag{1.1}$$

where λ and γ are scale and shape parameters, respectively.
The Gompertz model has been studied with fixed as well as time-dependent covariates. Fixed covariates are measured at the start of study and stay constant over the

*Speaker: khatib_b@neyshabur.ac.ir

study duration, for example, gender or race. Time-dependent covariates vary over time such as age and blood pressure. Following (77), (79) and (80) the history of a time-dependent covariate process up to time may be incorporated into the model to assess the effect of the covariate on the relative risk of the event over time. (81) proposed a parametric family of survival regression models for left, right and interval-censored data with both fixed and time-dependent covariates. It is noted that when $\gamma \to 0$, the Gompertz distribution will tend to an exponential distribution.

Now suppose that in (1.1), we have

$$\lambda = e^{\beta_0+\beta_1 y},$$

where y is a fixed covariate, so the hazard function of T is expressed as

$$h(t) = e^{\beta_0+\beta_1 y+\gamma t}. \tag{1.2}$$

Using (1.2), The survival function of the model is

$$S(t) = \exp\{\frac{e^{\beta_0+\beta_1 y}}{\gamma}\big(1 - e^{\gamma t}\big)\}, t > 0, \gamma > 0, \tag{1.3}$$

and the probability density function is

$$f(t) = e^{\beta_0+\beta_1 y+\gamma t} \exp\{\frac{e^{\beta_0+\beta_1 y}}{\gamma}\big(1 - e^{\gamma t}\big)\}, t > 0, \gamma > 0. \tag{1.4}$$

The properties of the Gompertz distribution are presented in (76). (74) obtained maximum likelihood estimate (MLE) of the parameters of Gompertz distribution. (82) proposed unweighted and weighted least squares estimates for parameters of the Gompertz distribution under the complete data and first failure-censored data. In this paper, we study the Gompertz model with fixed covariate.

The rest of this paper is organized as follows. In Section 2, the maximum likelihood estimation of the model parameters is studied. In Section 3, a real data set is used to illustrate the results of the paper. Kolmogorov-Smirnov fitness of good test is applied to test the data come from Gompertz model. Using this data set, the parameters is estimated and the behaviors of survival function and hazard function are considered in this section. Finally, some conclusions are stated in Section 4.

2 Maximum likelihood estimation

Let $(\mathbf{T}, \mathbf{Y}) = (T_1, Y_1, T_2, Y_2, \ldots, T_n, Y_2)$ be the vector of observations such that T_i is the lifetimes of n independent Gompertz experimental units and y_i is a fixed covariate corresponding to the ith unit. For a data set with a fixed covariate yi where $i = 1, 2, \cdots, n$, the hazard function for ith subject can be expressed as

$$h(t_i) = e^{\beta_0 + \beta_1 y_i + \gamma t_i}, \tag{2.1}$$

where $\boldsymbol{\theta} = (\beta_0, \beta_1, \gamma)$ is a vector of parameters, which may be estimated by various methods such as maximum likelihood estimation. The likelihood function of θ is given by

$$\begin{aligned} L(\boldsymbol{\theta}) &= \prod_{i=1}^{n} f(t_i, y_i; \boldsymbol{\theta}) \\ &= \prod_{i=1}^{n} f(t_i \mid y_i; \boldsymbol{\theta}) f(y_i), \end{aligned}$$

where $f(y_i)$ does not depend on $\boldsymbol{\theta}$; therefore, to infer about $\boldsymbol{\theta}$ it may be omitted. In other word, the likelihood function may be considered as follows

$$L_1(\boldsymbol{\theta}) = \prod_{i=1}^{n} f(t_i, y_i; \boldsymbol{\theta}).$$

So, the maximum likelihood estimator (MLE) of $\boldsymbol{\theta}$ can be derived by maximizing $L_1(\boldsymbol{\theta})$, which is the solution of the following equation

$$\frac{\partial}{\partial \boldsymbol{\theta}} \log L_1(\boldsymbol{\theta}) = 0. \tag{2.2}$$

Using (2.2), the MLEs of β_0, β_1 and γ may be derived by solving the following equations

$$\begin{aligned} &n + \frac{1}{\gamma} \sum_{i=1}^{n} e^{\beta_0 + \beta_1 y_i} \left(1 - e^{\gamma t_i}\right) = 0, \\ &\sum_{i=1}^{n} y_i + \frac{1}{\gamma} \sum_{i=1}^{n} y_i e^{\beta_0 + \beta_1 y_i} \left(1 - e^{\gamma t_i}\right) = 0, \\ &\sum_{i=1}^{n} t_i - \frac{1}{\gamma^2} \sum_{i=1}^{n} e^{\beta_0 + \beta_1 y_i} \left(1 - e^{\gamma t_i}\right) - \frac{1}{\gamma} \sum_{i=1}^{n} t_i e^{\beta_0 + \beta_1 y_i + \gamma t_i} = 0. \end{aligned}$$

After finding the MLEs of the model parameters, according to the invariance property of such estimator, the MLEs of hazard function and survival function will be derived using (1.2) and (1.3), respectively.

3 Application to a real data set

The data set utilized in this study has been collected in the dermatology clinic of Ghaem Hospital in Mashhad from January 2013 to February 2015. The data set was collected from patients, with plantar warts, who had referred to the dermatology clinic. This type of warts is one of the most common wart types. The age of patient (year) and time elapsed before treatment (month) are two features gathered in this data set, which are presented in Table 1. The second feature is considered as response variable in this model and the first one is assumed to be a fixed covariate.

Table 1. The wart treatment data set.

Age	Time	Age	Time	Age	Time	Age	Time	Age	Time	Age	Time
35	12	17	5.25	35	9.25	17	5.25	35	7.25	17	5.75
29	7	23	11.75	29	7.25	23	9.5	29	11.75	23	10.25
50	8	27	8.75	50	8.75	27	10	50	9.5	27	10.5
32	11.75	15	4.25	32	12	15	4	32	12	15	5.5
67	9.25	18	5.75	67	12	18	4.5	67	10	18	4
41	8	22	5.5	41	10.5	22	5	41	7.75	22	4.5
36	11	16	8.5	36	11	16	10.25	36	10.5	16	11
59	3.5	28	4.75	63	2.75	28	4	67	3.75	28	5
20	4.5	40	9.75	20	5	40	8.75	20	4	40	11.5
34	11.25	30	2.5	34	12	30	0.5	34	11.25	30	0.25
21	10.75	34	12	21	10.5	34	10.75	21	10.75	34	12
15	6	20	0.5	15	8	20	3.75	15	10.5	20	3.5
15	2	35	12	15	3.5	35	8.5	15	2	35	8.25
15	3.75	24	9.5	15	1.5	24	9.5	15	2	24	10.75
17	11	19	8.75	17	11.5	19	8	17	9.25	19	8

In order to test the times elapsed before treatment come from Gompertz distribution, Kolmogorov-Smirnov test has been done; the observed test statistic is 0.1037 with the corresponding p-value to be 0.2928. Based on these observations, there is no reason to reject the null hypothesis that the data come from Gompertz distribution. The Q-Q plot is also presented in the Figure 1.

Using the data set of Table 1, the maximum likelihood estimator of $\boldsymbol{\theta}$ is as follows

$$\hat{\beta}_0 = -3.4906, \quad \hat{\beta}_1 = -0.0208, \quad \hat{\gamma} = 0.3342.$$

The behaviors of $S(t)$ and $h(t)$ with various fixed covariate are plotted in Figure 2, for $y = 20, 35$ and 55.

From Figure 2 it is deduced that the survival function is decreasing with respect to time to treatment, whereas the hazard function is increasing.

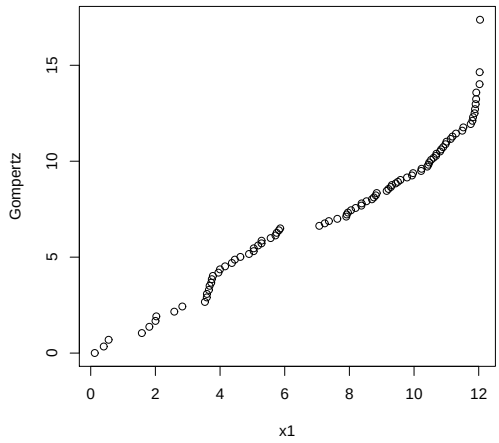

Figure 1: Q-Q plot of Gompertz distribution for the time to treatment.

4 Concluding Remark

In this paper a Gompertz model with fixed covariate was considered. The problem of estimating the unknown parameters was investigated and parameters of this model were estimated by maximum likelihood method. The proposed estimators was derived numerically for a given data set. In order to study the behaviors of survival function and hazard function, $S(t)$ and $h(t)$ graphs versus time to treatment were plotted.

References

[74] Garg, M.L., Rao, B.R. and Redmond, C.K. (1970), Maximum likelihood estimation of the parameters of the gompertz survival function, *J. R. Stat. Soc. Ser. C. Appl. Stat.*, **19**, 152–159.

[75] Gompertz, B. *On the nature of the function expressive of the law of human mortality and on the new mode of determining the value of life contingencies*, Philosophical Transactions of Royal Society A 115: 513580, 1825.

[76] Johnson, N.L., Kotz, S. and Balakrishnan, N. (1995), *Continuous Univariate Distributions*, Volume 2, New York, Wiley Press.

[77] Kalbfleisch, J.D. and Prentice, R.L. (2002), *The Statistical Analysis of Failure Time Data*, New York, Wiley Press.

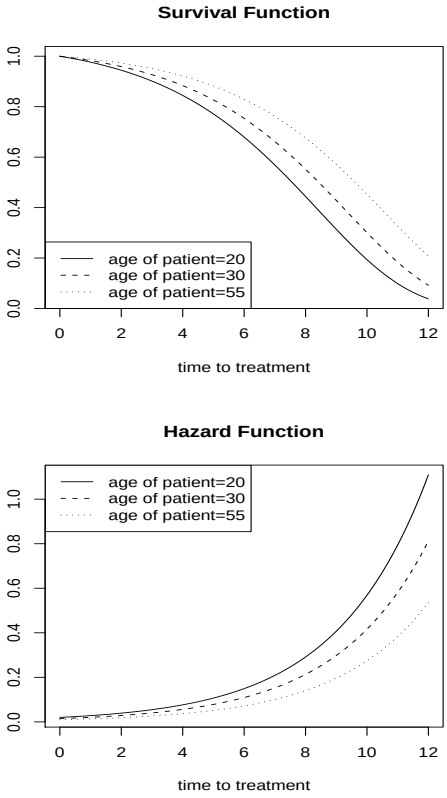

Figure 2: survival function and hazard function of Gompertz distribution for the time to treatment.

[78] Khozeimeh, F. , Alizadehsani,R., Roshanzamir,M., Khosravi,A., Layegh,P. and Nahavandi,S. (2017), *An expert system for selecting wart treatment method*, Computers in Biology and Medicine, **81**, 167-175.

[79] Lachin, J.M. (2000), *Biostatistical Methods: The Assessment of Relative Risk*, New York: Wiley Press, 2000.

[80] Sparling, Y.H. (2002), *Parametric Survival Models for Interval- Censored Data with Time-Dependent Covariates*, Ph.D. Thesis, George Washington University. USA.

[81] Sparling, Y.H., Younes, N., Lachin, J.M. and Bautista, O.M. (2006), Parametric survival models for interval-censored data with time-dependent covariates. *Biostat.*, **7**(4), 599–614.

[82] Wu, J.W., Hung, W.L. and Tsai, C.H. (2004), Estimation of Parameters of the gompertz distribution using the least squares method, *Appl. Math. Comput.*, **158**(1), 133–147.

Role of fractional derivative order in a model for the spread of HIV/AIDS epidemic

Hossein Kheiri*[1],Mohsen Jafari[1] , Azizeh Jabbari[2] and Fatemeh Iranzad1
[1]Faculty of Mathematical Sciences, University of Tabriz, Tabriz, Iran
[2]Marand Faculty of Engineering, University of Tabriz, Tabriz, Iran

Abstract:

In this paper, we present a fractional model for transmission dynamics of HIV/AIDS with screening, and investigate the efficacy of the fractional derivative order α $(0.6 \leqslant \alpha < 1)$ on the spread of HIV/AIDS epidemic using the Adams type predictor-corrector method. The numerical results show that the derivative order α can play the role of precautions against infection transmission, treatment of infection and delay in accepting HIV testing.

Keywords: Fractional calculus, HIV/AIDS epidemic, Numerical simulation
Mathematics Subject Classification (2010): 62N01, 962F10.

1 Introduction

In human societies, evolution and control of epidemics are not possible without regard to any memory effect (83). When a disease develops in a community, the experience or knowledge of people about the spread of disease in the past affects their response. (83; 84). Saeedian et al. (83) have included memory effects in a susceptible-infected-recovered (SIR) epidemic model and investigated role of memory effects in the disease spreading using fractional derivatives. They have mentioned that the reduction of the memory kernel depends on the fractional derivative order α $(0 < \alpha \leqslant 1)$, and as α limits to 1, the memory effect is reduced. Sun et al. (85) have presented a comparison of integer-order derivative, constant-order

*Speaker: h-kheiri@tabrizu.ac.ir

fractional derivative and two types of variable-order fractional derivatives in characterizing the memory effect of systems. They have pointed out that the memory effect characterized by fractional derivative decreases when α limits to 1. Rihan (86) has provided a class of fractional-order differential models of biological systems with memory, such as dynamics of tumor-immune system and dynamics of HIV infection of CD4+ T cells. He has mentioned that the fractional derivative order α play the role of time delay in ordinary differential models. In (87), the authors present a fractional-order model for the dengue epidemic and show that the fractional model simulates the first recorded epidemic in the coast of west Africa, in 2009, better than the integer model. The authors of (88) show that numerical results of a fractional order epidemic model agree very well with real data of influenza A (H1N1) at the population level. Therefore, due to the memory effects of fractional derivatives, the fractional calculus and their applications have been widely used in the fields of science, engineering, and many more (89; 90).

In this paper, we consider an HIV/AIDS epidemic fractional order model with screening that has been given by Zahra et al. (91). The model is the generalization, to fractional order, of the model proposed by Al-Sheikh et al. (92). The authors in (91) have discussed the local stability of the equilibria of the model by using the fractional Routh-Hurwitz stability conditions. We investigate the efficacy of the fractional derivative order α $(0.6 \leqslant \alpha < 1)$ on the spread of HIV/AIDS epidemic in the model using the Adams type predictor-corrector method. We show numerically that the derivative order α can play the role of precautions against infection transmission, treatment of infection and delay in accepting HIV testing.

2 Description of the model

The model is given by

$$\begin{aligned}
{}_0^cD_t^\alpha S &= \Lambda - (\beta_1 S I_1 + \beta_2 S I_2) - \mu S,\\
{}_0^cD_t^\alpha I_1 &= (\beta_1 S I_1 + \beta_2 S I_2) - (\theta + \delta_1 + \mu) I_1,\\
{}_0^cD_t^\alpha I_2 &= \theta I_1 - (\delta_2 + \mu) I_2,\\
{}_0^cD_t^\alpha A &= \delta_1 I_1 + \delta_2 I_2 - (\mu + d) A,
\end{aligned} \tag{2.1}$$

where ${}_0^cD_t^\alpha$ represents the left Caputo fractional derivative of order α and for a function f is difined as

$$ {}_a^cD_t^\alpha f(t) = \frac{1}{\Gamma(n-\alpha)} \int_a^t (t-\tau)^{n-1-\alpha} f^{(n)}(\tau) d\tau, \tag{2.2} $$

$0 < \alpha \leqslant 1$, S represents the susceptible population, I_1 represents the infectives that do not know they are infected, I_2 is the infectives that know they are infected (by way of medical screening or otherwise), and A is the people diagnosed with AIDS. Description of the model parameters is as follows:

- Λ : constant recruitment rate of susceptible population;
- β_1 : the per capita contact rate for susceptible individuals with unaware infectives;
- β_2 : the per capita contact rate for susceptible individuals with aware infectives ($\beta_2 \leqslant \beta_1$);
- θ : the rate of unaware infectives to become aware infectives by screening;
- δ_1 : the rate by which unaware infectives develops AIDS;
- δ_2 : the rate by which aware infectives develops AIDS ($\delta_2 \leqslant \delta_1$);
- μ : the natural mortality rate unrelated to AIDS;
- d : the AIDS related death rate.

System (2.1) has a disease-free equilibrium point $E_0(\frac{\Lambda}{\mu}, 0, 0, 0)$, and there is a unique positive endemic equilibrium $E^*(S^*, X^*, Y^*, A^*)$ if $R_0 > 1$, where R_0, the basic reproduction number, can be calculated by the next generation matrix technique of (93) as:

$$ R_0 = \frac{\Lambda[\beta_1(\delta_2+\mu) + \beta_2\theta]}{(\mu+u_1+u_2)(\delta_2+\mu)(\theta+\delta_1+\mu)} $$

and $S^* = \frac{\Lambda}{R_0(\mu+u_1+u_2)}$, $I_1^* = \frac{\Lambda(R_0-1)}{R_0(\theta+\delta_1+\mu)}$, $I_2^* = \frac{\theta}{\delta_2+\mu} I_1^*$ and $A^* = \frac{\delta_1 {I_1}^* + \delta_2 {I_2}^*}{\mu+d}$.

The disease-free equilibrium E_0 is locally asymptotically stable if $R_0 \leqslant 1$. When $R_0 > 1$, the E_0 is unstable and the unique endemic equilibrium E^* under the fractional Routh-Hurwitz stability conditions in (94) is locally asymptotically stable (see (91)).

Table 1: Parameter values used in numerical simulations

Parameter	Value	Reference
Λ	800	-
β_1	0.000090	(91)
β_2	0.000027	(91)
θ	0.02	(92)
δ_1	0.10	(92)
δ_2	0.08	(92)
μ	0.02	(92)
d	1	(92)

3 Numerical simulation

In this section, we examine role of the order of fractional derivative α $(0.6 \leqslant \alpha \leqslant 1)$ on the spread of HIV/AIDS epidemic in the model. The numerical simulations are carried out using the Adams type predictor-corrector method and applying the values of parameters given in Table 1, the initial conditions $S(0) = 30000$, $I_1(0) = 700$, $I_2(0) = 500$, $A(0) = 200$, $R(0) = E(0) = 0$ and for different values of derivative order α.

Fig. **??** shows the effect of the fractional derivative order α on the spread of HIV/AIDS epidemic for$\alpha = 0.6,\ 0.7,\ 0.8,\ 0.9$ and 1. We observe that when the derivative order α is reduced from 1, the memory effect of the system increases, and therefore the infection grows slowly and the number of HIV-infected population and AIDS people increases for a long time.

On the other hand, the experience of individuals about the past of disease makes susceptible individuals take precautions, such as vaccination and the use of condoms, against infection transmission (83; 84). As a result, infection among the population grows slowly. Also, unaware HIV-infected population in some communities refuse to perform HIV testing for unpleasant reasons and fear of identification (95). This causes delays in identifying people living with HIV, increasing the number of unaware HIV-infected people , rapid progression of AIDS, and increasing the number of people with AIDS. In addition, the experience or knowledge about disease helps the aware HIV-infected people and AIDS people to use the antiretroviral therapy to delay the onset of AIDS and death due to AIDS. This shows that the number of aware HIV-infected population and AIDS people increases for a long time. Therefore, numerical results in Fig. **??** show that the derivative order α $(0.6 \leqslant \alpha < 1)$ can play the role of precautions against infection transmission, treatment of infection and delay in accepting HIV testing.

4 Conclution

A fractional model for transmission dynamics of HIV/AIDS with screening has been presented. We have investigated the effect of the fractional derivative order α ($0.6 \leqslant \alpha < 1$) on the spread of HIV/AIDS epidemic using the Adams type predictor-corrector method. The numerical results have shown that the derivative order α can play the role of precautions against infection transmission, treatment of infection and delay in accepting HIV testing.

References

[83] M. Saeedian, M. Khalighi, N. Azimi-Tafreshi, G. R. Jafari, M. Ausloos, Memory effects on epidemic evolution: The susceptible-infected-recovered epidemic model, Phys. Rev. E 95 (2) (2017) 022409.

[84] Vitanov NK, Ausloos MR, Knowledge epidemics and population dynamics models for describing idea diffusion, in Models of Science Dynamics: Encounters Between Complexity Theory and Information Sciences, Scharnhorst A, Boerner K, van den Besselaar P, Eds. Springer Verlag, Berlin Heidelberg, Ch. 3, pp. 69-125, 2012.

[85] H. G. Sun, W. Chen, H. Wei and Y. Q. chen, A comparative study of constant-order and variable-order fractional models in characterizing memory property of systems, Eur. Phys. J. Special Topics 193 (1) (2011) 185-192.

[86] F. A. Rihan, Numerical modeling of fractional-order biological systems, Abstr. Appl. Anal. 2013 (2013) Article ID 816803, 11 pages.

[87] S. Pooseh, H. S. Rodrigues, D. F. M. Torres. Fractional derivatives in Dengue epidemics. AIP Conf. Proc. 1389 (2011), no. 1, 739742. arXiv:1108.1683

[88] G. Gonzalez-Parra, A.J. Arenas, B.M. Chen-Charpentier, A fractional order epidemic model for the simulation of outbreaks of influenza A(H1N1). Math. Meth. Appl. Sci. 37 (15)(2014) 2218-2226.

[89] I. Petras, Fractional-Order Nonlinear Systems: Modeling, Analysis and Simulation, Springer, 2011.

[90] I. Podlubny, Fractional Differential Equations, Mathematics in Science and Engineering, Academic Press, San Diego, Calif, USA, 1999.

[91] W. K. Zahra, M. M. Hika and T. A. Bahnasy, Stability analysis of an HIV/AIDS epidemic fractional order model with screening and time delay, American Association for Science and Technology, 2 (3) (2015) 41-49.

[92] S. Al-Sheikh, F. Musali and M. Alsolami, Stability Analysis of an HIV/AIDS Epidemic Model with Screening, International Mathematical Forum, 6 (66) (2011) 3251-3273.

[93] P. van den Driessche and J. Watmough, Reproduction numbers and subthreshhold endemic equilibria for compartmental models of disease transmission, Math. Biosci. 180 (2002) 29-48.

[94] E. Ahmed, A. M. A. El-Sayed, and H. A. A. El-Saka, On some routhhurwitz conditions for fractional order differential equations and their applications in lorenz, rssler, chua and chen systems, Physics Letters A 358 (2006) 1-4.

[95] Meiberg, A.E., Bos, A.E.R., Onya, H.E., Schaalma, H.P.: Fear of stigmatization as barrier to voluntary HIV counselling and testing in South Africa. East African journal of public health **5** (2), 49-54 (2008)

Persistent homology for protein folding analysis

Ameneh Babaee*[2], Hanieh Mirebrahimi[1]
[1]Department of pure mathematics, Ferdowsi university of Mashhad, Mashhad, Iran
[2]Department of biophysics, Tarbiat Modares university of Tehran, Tehran, Iran

Abstract:

Persistent homology is a concept in topological data analysis used to reduce the dimensionality and complexity of the data sets, and also to determine topological features and delete noises. In this talk, unfolding process is simulated with the constant velocity pulling algorithm of SMD. Then, we apply the persistent homology to reveal the topological features of intermediate configurations. Furthermore, we construct a quantitative model based on the accumulation bar length A_1 to predict the energy and stability of protein configurations, which establishes a solid topology-function relationship of proteins with the constant velocity pulling algorithm of SMD.

Keywords: persistent homology, protein folding, topological data analysis.
Mathematics Subject Classification (2010): 62N01, 962F10.

1 Persistent homology

Homology groups are used to classify the topological spaces.

We can simplify homology group to the number of its generators denoted by β_i, called ith Betti number, counting the connected components for $i = 0$, cycles for $i = 1$, holes for $i = 2$, voids for $i = 3$ and ... in a simplicial complex.

Consider a set of points in the euclidean space (see Figure 1). Start with a distance α, and connect pairs of points that are no further apart than α.

Then, we fill in complete simplexes, that is if we find three points connected by edges that form a triangle, we fill in the triangle with a 2-dimensional face. Any 4 points that are all pairwise connected get filled in a 3-simplex and ....

*Speaker: am.babaee@mail.um.ac.ir

The resulting simplicial complex is called the Rips complex complex. We then apply homology to this complex which reveals the presence of the holes.

How can we choose the best distance α?

If α is too small, we might see multiple connected components and small holes that are all the fact of simply. On the other hand, if α is too large, then any two points get connected, and we get a complete simplicial complex, which has trivial homology.

This choice of α reveals holes, but it is important that which holes in different values of α are persistent. Therefore, we consider all distances α.

Note that each hole appears at some particular value of α, namely α_1 and disappears at another α, namely α_2. We can represent the persistence or age of this hole as a pair (α_1, α_2). See Figure 1.

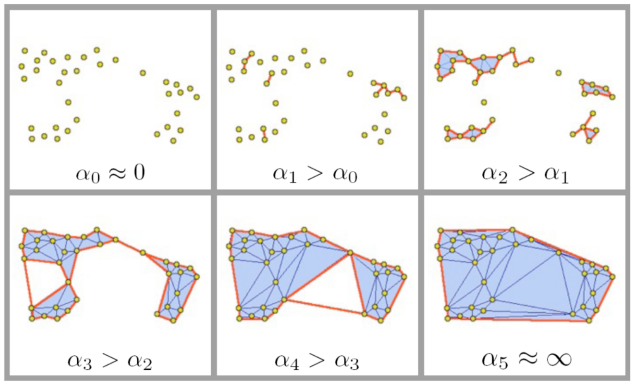

Figure 1: When distance α increases, the complex converges to be completed.

We can also visualize the pair (α_1, α_2) as an interval or bar from α_1 to α_2. This bar is a visual representation of the persistence of the hole. A collection of such bars is called a barcode, and barcodes are essential objects of study in persistent homology. See Figure 2.

2 Protein folding

Protein folding is the process by which a protein structure assumes its functional shape or conformation. This process produces characteristic and functional 3-dimensional topological structures from un-folded polypeptides or disordered coils. The folding funnel hypothesis associates each folded protein structure with a global minimum of the Gibbs free energy.

Protein folding and unfolding involve massive changes in its local and global topology. Protein topological evolution can be tracked by the trajectory of protein topological invariants.

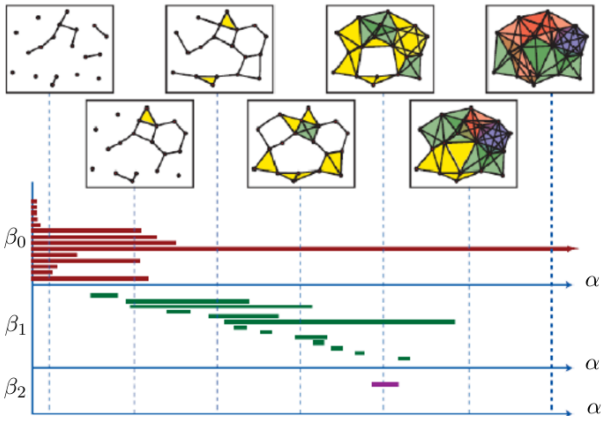

Figure 2: Horizontal axis shows the distance and vertical axis shows the number of holes, called Betti number.

In this talk, the unfolding process is simulated with the constant velocity pulling algorithm of SMD. Intermediate configurations are extracted from the trajectory. Then, we employ the persistent homology to reveal the topological features of intermediate configurations. Furthermore, we construct a quantitative model based on the accumulation bar length A_1 to predict the energy and stability of protein configurations, which establishes a solid topology-function relationship of proteins.

The SMD is carried out through one of three ways: high temperature, constant force pulling, and constant velocity pulling.

In this talk, the molecular dynamical simulation tool NAMD is employed to generate the partially folded and unfolded protein conformations. Two processes are involved, the relaxation of the structure and unfolding with constant velocity pulling.

As proteins used in our simulation are relatively small with about 80 residues. The spring constant is set as 7 kcal/mol A^2, with 1 kcal/mol A^2 / equaling 69.74 pN A. The constant velocity is 0.005 A per time step. As many as 30000 simulation steps for protein 1I2T and 40000 for 2GI9 are employed for their pulling processes. We extract 31 conformations from the simulation results at an equal time interval. The total energies (kcal/mol) are computed for all configurations. For each pair of configurations, their relative values of total energies determine their relative stability. A few representative conformations of unfolding 1I2T are depicted in Fig. 19. Obviously, topological connectivities, that is 2-dimensional complexes and 3-dimensional complexes, reduce dramatically from conformation Figure 3a to conformation Figure 3g.

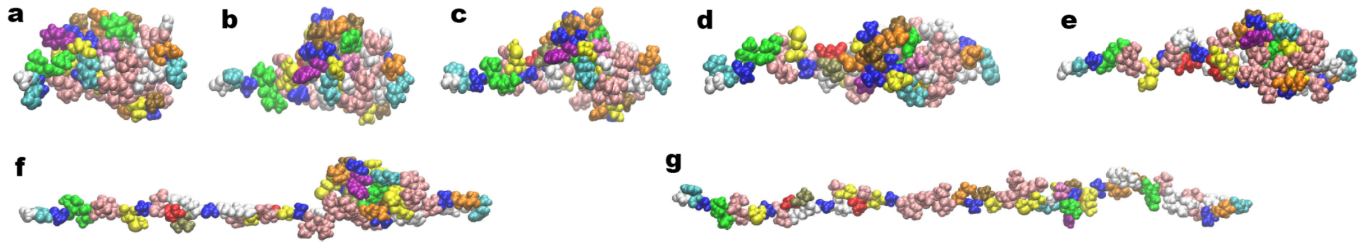

Figure 3: The unfolding configurations of protein 1I2T obtained from the steered molecular dynamics with the constant velocity pulling algorithm. Charts a, b, c, d, e, f and g are the corresponding configuration frames 1, 3, 5, 7, 10, 20, and 30. Amino acid residues are labeled with different colors. From a to g, protein topological connectivity decreases, while protein total energy increases (98).

3 Data analysis for protein folding

The steered molecular dynamics (SMD) is used to generate the protein folding process. Basically, by pulling one end of the protein, the coiled structure is stretched into a straight-line like shape. It is found that during the unfolding process, the hydrogen bonds that support the basic protein configuration are continuously broken. Consequently, the number of high order complexes that may be formed during the filtration decreases because of protein unfolding.

To validate our hypothesis, we employ the coarse- grained model in our persistent homology analysis although the all-atom model is used in our SMD calculations.

We compute topological invariants via the distance based filtration for all 31 configurations of protein 1I2T. We found that as the protein unfolded, their related β_1 value decreases. See Figure 4.

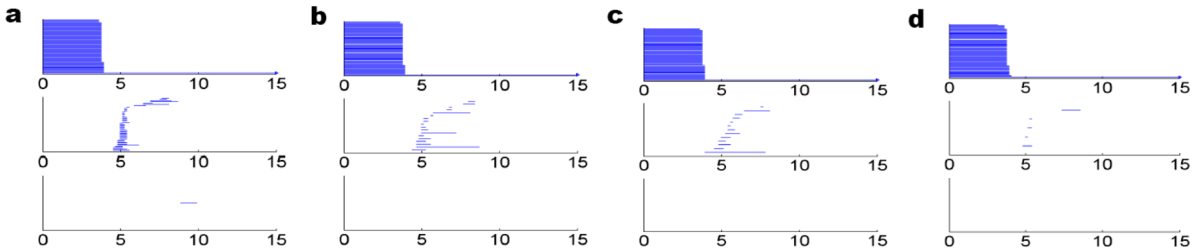

Figure 4: Topological fingerprints of four configurations of protein 1I2T generated by using the distance based filtration. Charts a, b, c, and d are for frame 1, 10, 20 and 30, respec- tively (see Figure **??**a, 3e, 3f and 3g for their geometric shapes.). It can be seen that as the protein unfolds, the β_0 bars are continuously decreasing, which corresponds to the reduction of topological connectivity among protein atoms (98).

Additionally, as a protein unfolds, its stability decrease. State differently, protein becomes more and more unstable during its unfolding process, and its total energy

becomes higher during the SMD simulation. As discussed above, the first Betti number decreases as protein unfolds. Therefore, there is a strong anti-correlation between protein total energy and its first Betti number during the protein unfolding process. However, using the least square fitting, we found that this linear relation is not highly accurate with a correlation coefficient about 0.89 for 31 configurations of 1I2T. A more robust quantitative model is to correlate protein total energy with the negative accumulation bar length of $\beta_1(A_1^- = -A_1)$. Indeed, a striking linear relation between the total energy and A_1 can be found. We demonstrate our results in the left chart of Figure 5. Using a linear regression algorithm, a correlation coefficient about 0.947 can be obtained for 31 configurations of protein 1I2T. To further validate the relation between the negative accumulation bar length and total energy, the correlation matrix based filtration process is employed. We choose the exponential kernel with optimized parameter $\kappa = 2$ and $\eta = 7A$. The results are illustrated in the right chart of Figure 5. A linear correlation is found with the CC value of 0.944.

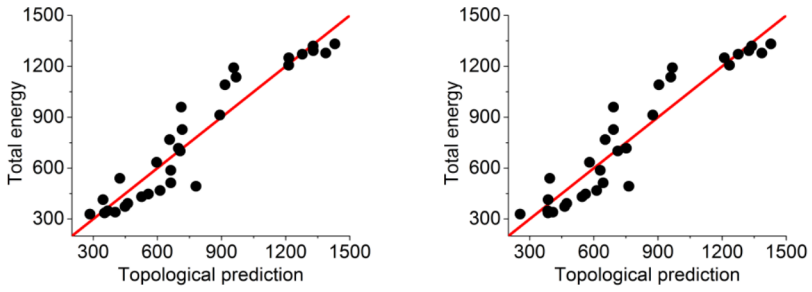

Figure 5: Comparison between the total energies and the persistent homology prediction for 31 configurations of protein 1I2T. The unfolding configurations are generated by using the SMD. The negative accumulation bar length of $\beta_1(A_1^-)$ is used in the persistent homology prediction with both distance based filtration (left chart) and correlation matrix based filtration (right chart). Their correlation coefficients are 0.947 and 0.944, respectively. Clearly, there is a linear correlation between the negative accumulation bar length of $\beta_1(A_1^-)$ and total energy (98).

To further validate our persistent homology based quantitative model for the stability analysis of protein folding, we consider protein 2GI9. The same procedure described above is utilized to create 31 configurations. We use both distance based filtration and correlation matrix based filtration to compute A_1^- for all the extracted intermediate structures. Our results are depicted in Figure 6. Again the linear correlation between the energy prediction using negative accumulation bar length of the first Betti number and total energy is confirmed. The CC values are as high as 0.972 and 0.971, for distance based filtration and correlation matrix based filtration,

respectively.

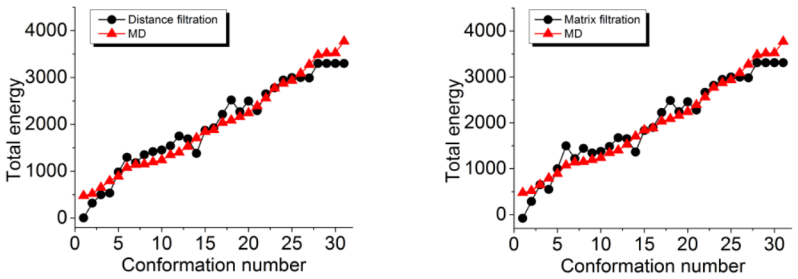

Figure 6: Comparison between the total energy and the persistent homology prediction for 31 configurations of protein 2GI9 (98).

References

[96] M. Kerber and H. Schreiber, Barcodes of Towers and a Streaming Algorithm for Persistent Homology, *Discrete Comput Geom* (2018), 1–28.

[97] J.J. Rotman, Introduction to algebraic topology, Springer, New York, 1988.

[98] K. Xia and G. Wei, Persistent homology analysis of protein structure, flexibility, and folding. Int. J. Numer. Meth. Biomed. Engng., 30 (2014), 814-844.

[99] A. Zomorodian, Topology for Computing, Cambridge University Press, Cambridge, 2005.

Persistent homology for prediction of protein folding

H. Mirebrahimi*[1], A. Babaee[2]
[1]Department of pure mathematics, Ferdowsi university of Mashhad, Mashhad, Iran
[2]Department of biophysics, Tarbiat Modares university of Tehran, Tehran, Iran

Abstract:

Topological data analysis in an approach to use topological techniques for analysis of datasets. Persistent homology is one of the main tools of topological data analysis used for reducing the dimension and complexity of the data sets, and also to distinguish topological features and delete noises. Site directed mutagenesis is widely used to understand the structure and function of biomolecules. Computational prediction of protein mutation impacts offers a fast, economical and potentially accurate alternative to laboratory mutagenesis.

In this talk, topology based mutation predictor (T-MP) is introduced to dramatically reduce the geometric complexity and number of degrees of freedom of proteins, while element specific persistent homology is proposed to retain essential biological information. The present approach is found to outperform other existing methods in globular protein mutation impact predictions.

Keywords: persistent homology, protein folding, topological data analysis.
Mathematics Subject Classification (2010): 62N01, 962F10.

1 Persistent homology

Persistent homology is an algebraical tool to investigate topological features. In topology, a group structure was defined called homology group for simplicial complexes, denoted by H_i indexed by $i = 0, 1, 2, \ldots$ related to the dimension of holes. We can simplify homology to the number of its generators denoted by β_i, called ith

*Speaker: a.asgharzadeh@umz.ac.ir

Betti number, counting the connected components for $i = 0$, cycles for $i = 1$, holes for $i = 2$, voids for $i = 3$ and ... in a simplicial complex. By a simplicial complex, we mean a set of points called vertices, a subset of pair of vertices called edges, a subset of triple of vertices that are pairly joined by edges, called triangles, and ....

Consider a set of points in the euclidean space (see Figure 1). Start with a distance α, and connect pairs of points that are no further apart than α. Then, we fill in complete simplexes, that is if we find three points connected by edges that form a triangle, we fill in the triangle with a 2-dimensional face. Any 4 points that are all pairwise connected get filled in a 3-simplex and .... The resulting simplicial complex is called the Rips complex or the Vietoris-Rips complex. We then apply homology to this complex which reveals the presence of the holes.

Note that each hole appears at some particular value of α, namely α_1 and disappears at another α, namely α_2. We can represent the persistence or age of this hole as a pair (α_1, α_2). See Figure 1.

A collection of such bars is called a barcode, and barcodes are essential objects of study in persistent homology. See Figure 1.

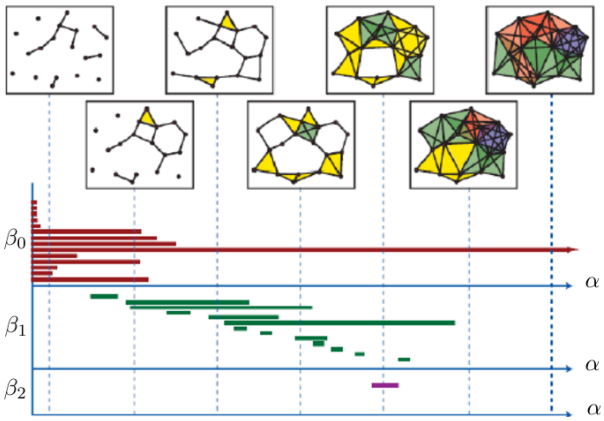

Figure 1: Horizontal axis shows the distance and vertical axis shows the number of holes, called Betti number.

The small holes, having short persistence, are not important in our data analysis and represented by short bars in the barcodes, but larger holes, having long persistence, can be considered as significant feature of the data, and they are represented by a long bar in the barcode. Therefore, the brief interpretation of the barcodes can be stated as: short bars represent noise, and long bars represent features.

A key property of barcodes is that they are stable under perturbations of the data. In other words, if you move a point a little bit, the barcode only changes a little bit. This stability of barcodes is caused by topological invariance of the homology groups, and it is important in applications in dynamical cases. For more

details and applications see (101).

Standard algorithms exist to compute barcodes such as streaming algorithm. Streaming algorithms are algorithms for processing data streams in which the input is presented as a sequence of items and can be examined in only a few passes.

The worst case runtime of these algorithms is cubed in the number of simplices, although the complication is really worst case. In addition, improving data structures by topological simplification can speed up the computation significantly.

2 Protein stability upon mutation

Mutagenesis, as a basic biological process that changes the genetic information of organisms, serves as a primary source for many kinds of cancer and heritable diseases, as well as a driving force for natural evolution. In laboratories, site directed mutagenesis analysis is a vital experimental procedure for exploring protein functional changes. Nonetheless, site directed mutagenesis analysis is both time-consuming and expensive. Computational prediction of protein mutation impacts is an important alternative to experimental mutagenesis analysis for the systematical exploration of protein structural instabilities, functions, disease connections, and organism evolution pathways. A major advantage of these approaches is that they provide an economical, fast, and potentially accurate alternative to site directed mutagenesis experiments.

The last class of approaches is knowledge based methods that invoke modern machine learning techniques to uncover hidden relationships between protein stability and protein structure as well as sequence. A major advantage of knowledge based mutation predictors is their ability to handle increasingly large and diverse mutation data sets.

A common challenge for all existing mutation impact prediction models is in achieving accurate and reliable predictions of membrane protein stability changes upon mutation.

A key feature of all existing structure based mutation impact predictors is that they either fully or partially rely on direct geometric descriptions which rest in excessively high dimensional spaces resulting in large number of degrees of freedom. In practice, the geometry can easily be over simplified. Mathematically, topology, in contrast to geometry, concerns the connectivity of different components in a space, and offers the ultimate level of abstraction of data. However, conventional topology incurs too much reduction of geometric information to be practically useful in biomolecular analysis. Persistent homology, a new branch of algebraic topology, re-

tains partial geometric information in topological description, and thus bridges the gap between geometry and topology. It has been applied to biomolecular characterization, identification and analysis. However, conventional persistent homology makes no distinction of different atoms in a biomolecule, which results in a heavy loss of biological information and limits its performance in protein classification. In the present work, we introduce element specific persistent homology (ESPH), interactive persistent homology and binned barcode representation to retain essential biological information in the topological simplification of biological complexity. We further integrate ESPH and machine learning to analyze and predict protein mutation impacts. The essential idea of our topological mutation predictor (T-MP) is to use ESPH to transform the biomolecular data in the high-dimensional space with full biological complexity to a space of fewer dimensions and simplified biological complexity, and to use machine learning to deal with massive and diverse data sets. A distinct feature of the present T-MP is that the prediction results can be analyzed and interpreted in physical terms to shed light on the molecular mechanism of protein folding energy changes upon mutation. Additionally, the mathematical model for different types of mutations can be adaptively optimized according to the performance analysis of ESPH features.

3 Persistent homology characterization of protein

Unlike physics based models which describe protein folding in terms of covalent bonds, hydrogen bonds, electrostatic and van der Waals interactions, the natural language of persistent homology is topological invariants, i.e., the intrinsic features of the underlying topological space.

When persistent homology is used to analyze three dimensional (3D) protein structures, one-dimensional (1D) persistent homology barcodes are obtained as topological fingerprints (TFs).

As an illustration, we consider the persistent homology analysis of a wild type protein (PDB:1ey0) and its mutant. The mutation (G88W) occurred at residue 88 from Gly to Typ is shown at Figure 2 a and b. In this case, a small residue (Gly) is replaced by a large one (Typ). We carry out persistent homology analysis of a set of heavy atoms within 6A from the mutation site. Persistent homology barcodes of the wild type and the mutant are respectively given in Figure 2 c and d.

The above topological representation of proteins does not contain sufficient biological information, such as bond length distribution of a given type of atoms, hydrogen bonds, hydrophobic and hydrophilic effects, to offer an accurate model for

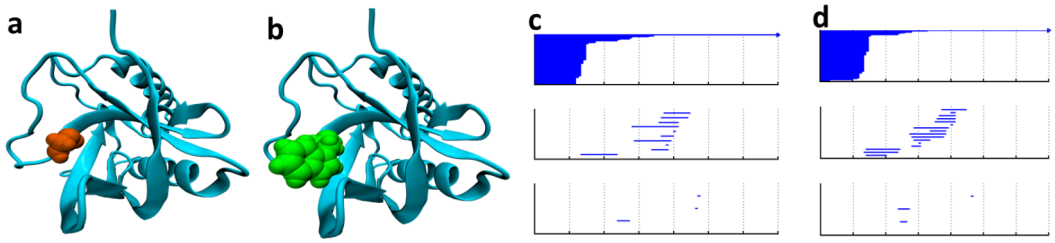

Figure 2: An illustration of persistent homology barcode changes from wild type to mutant proteins (100).

protein mutation impact predictions. To characterize chemical and biological properties of biomolecules, we introduce element specific persistent homology (ESPH). Instead of labeling every atom as in many physics based methods, we distinguish different element types of biomolecules in constructing persistent homology barcodes. For proteins, commonly occurring element types include C;N;O; S and H.

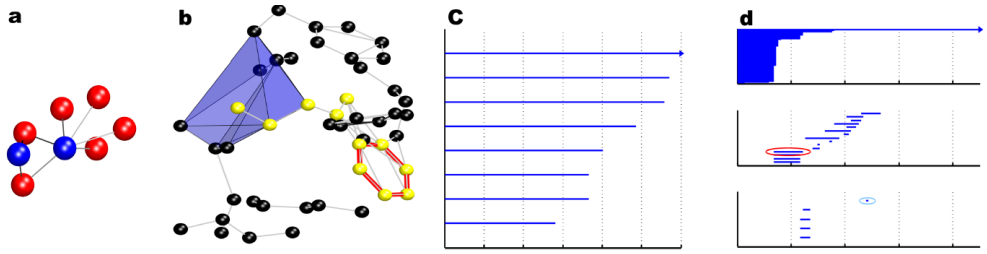

Figure 3: An illustration of element specific persistent homology (ESPH) indicating the hydrophilic network (Left) and hydrophobic network (Right) at a mutation site (100).

The most important issue in protein mutation impact analysis is the interactions between the mutation site and the rest of the protein. To describe these interactions, we propose interactive persistent homology adopting the distance function $DI(A_i; A_j)$ describing the distance between two atoms A_i and A_j defined as

$$DI(A_i; A_j) = \begin{cases} \infty; \text{if} Loc(A_i) = Loc(A_j); \\ DE(A_i; A_j); \text{otherwise}; \end{cases}$$

where $DE(\cdot, \cdot)$ is the Euclidean distance between the two atoms and $Loc(\cdot)$ denotes the location of an atom which is either in a mutation site or in the rest of the protein. In the persistent homology computation, Vietoris- Rips complex (VC) and alpha complex (AC) are used for characterizing first order interactions and higher order patterns respectively. To characterize interactions of different kinds, we construct persistent homology barcodes on the atom sets by selecting one certain type of atoms

in mutation site and one other certain type of atoms in the rest of the protein.

Barcodes computed by persistent homology are capable of revealing the molecular mechanism of protein stability. For example, interactive ESPH barcodes generated from carbon atoms are associated with hydrophobic interaction networks in proteins. Similarly, interactive ESPH barcodes between nitrogen and oxygen atoms correlate to hydrophilic interactions and/or hydrogen bonds as shown in Figure 3. Interactive ESPH barcodes are also able to reveal other bond information; notwithstanding, they can not always be interpreted as covalent bond, hydrogen bonds, or van der Waals bonds in general. In fact, interactive ESPH barcodes provide an entirely new representation of molecular interactions.

While the topological descriptors give a through examination of the atomic arrangements and interactions, some other crucial properties are not explicitly characterized. Additionally, due to the diverse quality of the structures examined, some higher level descriptors such as residue level descriptors can enhance the robustness of the model. Therefore, we include some auxiliary descriptors from the aspect of geometry, electrostatics, amino acid types composition, and amino acid sequence. The geometric descriptors contain surface area and van der Waals interaction. The electrostatics descriptors are consisted of atomic partial charge, Coulomb interaction, and atomic electrostatic solvation energy. The high level descriptors include neighborhood amino acid composition and predicted pKa shifts. The sequence descriptors describe the secondary structure and residue conservation score collected from Position-specific scoring matrix.

The topological features and the auxiliary features are ideally suited for being used as machine learning features to predict protein stability changes upon mutation. We have examined a number of machine learning algorithms, including decision tree learning, random forest, and gradient boosted regression trees (GBRTs).

To demonstrate the power of the proposed T-MP for protein mutation impact predictions, we consider a data set of 2648 mutation instances in 131 proteins, called S2648 data set.9 Additionally, a subset of the S2648 data set involving 67 proteins, named S350 set, is used as a test set.

A comparison of the performances of various methods is summarized in Table 1. Pearson correlations coefficient (RP) and RMSE for test set S350, and five-fold cross validations for training set S2648, are given for various methods, including ours.

A comparison between T-MP-1 and T-MP-2 indicates that geometric, electrostatic and sequence features give rise to approximately 5% improvement over the original topological prediction, indicating the importance of geometric, electrostatic

and sequence information to mutation predictions.

Our topology based approaches significantly outperform other existing physical or empirical methods. When auxiliary features are used together with topological features, a 5% improvement in Pearson correlation coefficient is found. Compared with Rosetta- MP, which achieves the best performance with terms designed for membrane proteins,19 the present T-MP-2 has a 84% higher Pearson correlation coefficient. Nonetheless, Kroncke et als statement about membrane protein mutation impact predictions still holds as the best Pearson correlation coefficient is only 0.57 and the best RMSE is over 1 kcal/mol. We therefore call for further methodology developments to improve membrane protein mutation impact predictions.

This article introduces element specific persistent homology to appropriately simplify biomolecular complexity while effectively retain essential biological information in protein mutation impact predictions. Extensive numerical experiments indicate that element specific persistent homology offers some of the most efficient descriptions of protein mutation impacts that cannot be obtained by other conventional techniques.

References

[100] Z. Cang and G. Wei wei, Analysis and prediction of protein folding energy changes upon mutation by element specific persistent homology. Bioinformatics, 33(22), 3549–3557, 2017.

[101] A. Zomorodian, Topology for Computing, Cambridge University Press, Cambridge, 2005.

همایش ملی ریاضیات زیستی
اولین همایش ملی ریاضیات زیستی
۲۱ و ۲۲ اسفندماه ۱۳۹۷
دانشگاه نیشابور

Modified variational iteration method to solve a model for HIV infection of $CD4^+$T-cells

Omidiniya, Pooneh* and Alipour, Maryam
Department of Mathematics, University of Sistan and Baluchestan, Zahedan Iran

Abstract:

In this paper, the modified variational iteration method (MVIM) is investigated to give an approximate solution of a model for HIV infection of $CD4^+$ T-cells. MVIM cancels all the unsettled terms in variational iteration method (VIM) and the time for doing the calculations is low. The method is very simple and easy

Keywords: Modified variational iteration method; HIV infection model; Numerical solution.

Mathematics Subject Classification (2010): 62N01, 962F10.

1 Introduction

Many researchers have been researching mathematical models for the problem of HIV and its treatment (102). Rocha et al.(103) studied stability and optimal control of a delayed HIV model. Then Perelson et al. modified and generalized this model to new model with four variables by a system of non-linear ordinary differential equations (102). In recent years, several applicable models have been presented based on the Perelsons models (104). The aim of this paper is to solve the Culshaw and Ruans model (104) for HIV infection of$CD4^+$T-cells as

$$\begin{aligned} \frac{dT}{dt} &= s - \mu_T T + rT(1 - \frac{T+I}{T_{max}}) - k_1 VT, \\ \frac{dI}{dt} &= k_1' VT - \mu_I I, \\ \frac{dV}{dt} &= N\mu_b I - k_1 VT - \mu_V V. \end{aligned} \tag{1.1}$$

*Speaker: Pooneh.omidi.710122@gmail.com

Several approximate analytical methods are proposed for solving this system. Some

Table 1: List of variables and parameters (modified from(104)).

Parameters and variables	Meaning
Dependent variables	
T	Uninfected $CD4^+$ T-cell concentration
I	Infected $CD4^+$ T-cell concentration
V	Concentration of HIV RNA
Parameters and constants	
μ_T	Natural death rate of $CD4^+$ T-cell concentration
μ_I	Blanket death rate of infected $CD4^+$ T-cells
μ_b	Lytic death rate for infected cells
μ_V	Death rate of free virus
k_1	Rate $CD4^+$ T-cells become infected with virus
k_1'	Rate infected cells become active
r	Growth rate of $CD4^+$T-cell concentration
N	Number of virion produced by infected $CD4^+$-cells
T_{max}	Maximal concentration of $CD4^+$ T-cells
s	Source term for uninfected $CD4^+$ T-cells
Derived quantities	
T_0	$CD4^+$ T-cell concentration for HIV-negative persons

of these methods are the homotopy perturbation method(105; 106), Adomian decomposition method(107) and etc. In this paper, the Modified variational iteration analysis method (MVIM) is introduced for solving the model for HIV infection of $CD4^+$ T-cells of Culshaw and Ruan described above.

2 The modified variational iteration method

Consider the following differential equations,

$$Lu(t) + Ru(t) + Nu(t) = g(t),$$

$$u(0) = f(t) \tag{2.1}$$

where $L = \dfrac{\partial}{\partial t}$, R is a linear operator, $Nu(t)$ is a nonlinear term and $g(t)$ is an inhomogeneous term. Following the same procedure as done in VIM and using the following iteration formula (2.3) instead of the iteration formula (2.2):

$$U_{n+1} = U_n - \int_0^t \{L(U_n) + R(U_n) + NU_n - g\} d\tau \tag{2.2}$$

$$U_{n+1} = U_n - \int_0^t \{R(U_n - U_{n-1}) + (G_n - G_{n-1}\}d\tau, \tag{2.3}$$

where $U_{-1} = 0$, $U_0 = f(t)$, $U_1 = U_0 - \int_0^t (R(U_0 - U_{-1}) + (G_0 - G_{-1}) - g)d\tau$, and $G_n(t)$ is obtained from $NU_n(t) = G_n(t) + O(t^{n+1})$. Actually, for the nonlinear part we use the Taylor series expansion. Eq. (2.3) can be solved iteratively to obtain an approximate solution that takes the form $u(t) \simeq U_n(t)$, where n is the final iteration step.

3 EXAMPLE

In this section, the MVIM is applied to solve the non-linear system of Eqs. (3.1) for mentioned values of Table 1,

$$\begin{aligned} \frac{dT}{dt} &= s - \mu_T T + rT(1 - \frac{T+I}{T_{max}}) - k_1 VT, \\ \frac{dI}{dt} &= k_1' VT - \mu_I I, \\ \frac{dV}{dt} &= N\mu_b I - k_1 VT - \mu_V V, \end{aligned} \tag{3.1}$$

that $T_0 = 1000$, $I_0 = 0$, $V_0 = 0.001$, $r = 0.03$, $\mu_T = 0.02$, $\mu_I = 0.26$, $\mu_b = 0.24$, $\mu_V = 2.4$, $k_1 = 2.4 * 10^{-5}$, $k_1' = 2 * 10^{-5}$, $N = 500$, $s = 10$, $T_{max} = 1500$. By using Mathematica software, three - term approximations for T, I, and V, were obtained as follows

$$\begin{aligned} T_3 &= 1000. - 0.000024t - 2.4 * 10^{-7}t^2, \\ I_3 &= 0. + 0.00002t + 2.6 * 10^{-6}t^2, \\ V_3 &= 0.001 - 0.002424t - 0.0041088t^2. \end{aligned} \tag{3.2}$$

We substitute Eqs 3.2 into 3.1 and obtain the residual function $ER_i(T, I, V)$, $i = 1, 2, 3$ as follows:

$$\begin{aligned} ER_1(T, I, V) &= \frac{dT_n}{dt} - s + \mu_T T_n - rT_n(1 - \frac{T_n + I_n}{T_{max}}) + k_1 V_n T_n, \\ ER_2(T, I, V) &= \frac{dI_n}{dt} - k_1' V_n T_n + \mu_I I_n, \\ ER_3(T, I, V) &= \frac{dV_n}{dt} - N\mu_b I_n + k_1 V_n T_n + \mu_V V_n, \end{aligned} \tag{3.3}$$

we define the square residual error for the three -order approximation to be:

$$\begin{aligned} RT &= \int_0^1 (ER_1(T,I,V))^2 dt, \\ RI &= \int_0^1 (ER_2(T,I,V))^2 dt, \\ RV &= \int_0^1 (ER_3(T,I,V))^2 dt, \end{aligned} \tag{3.4}$$

then, the minimum values of RT, RI, and RV have been given in table 2.

Table 2: The minimum values of RT, RI, and RV.

	Minimum value
RT	$2.60205 * 10^{-8}$
RI	$2.13071 * 10^{-8}$
RV	$6.30938 * 10^{-4}$

Table 3: The residual errors ER_1, ER_2, and ER_3 fo rvarious $t \in (0,1)$.

t	$ER1(T,I,V)$	$ER2(T,I,V)$	$ER3(T,I,V)$
0.0	$-1.77636 * 10^{-15}$	0.	0.
0.1,	$-7.98617 * 10^{-6}$	$7.71 * 10^{-6}$	$-1.89886 * 10^{-3}$
0.2	$-2.05751 * 10^{-5}$	$1.94485 * 10^{-5}$	$-4.35396 * 10^{-3}$
0.3	$-3.84052 * 10^{-5}$	$3.57921 * 10^{-5}$	$-7.45106 * 10^{-3}$
0.4	$-6.2115 * 10^{-5}$	$5.73176 * 10^{-5}$	$-1.1276 * 10^{-2}$
0.5	$-9.23429 * 10^{-5}$	$8.46017 * 10^{-5}$	$-1.59144 * 10^{-2}$
0.6	$-1.29727 * 10^{-4}$	$1.18221 * 10^{-4}$	$-2.14522 * 10^{-2}$
0.7	$-1.74907 * 10^{-4}$	$1.58752 * 10^{-4}$	$-2.79751 * 10^{-2}$
0.8	$-2.28519 * 10^{-4}$	$2.06773 * 10^{-4}$	$-3.5569 * 10^{-2}$
0.9	$-2.91204 * 10^{-4}$	$2.62858 * 10^{-4}$	$-4.43195 * 10^{-2}$
1	$-3.63599 * 10^{-4}$	$3.27586 * 10^{-4}$	$-5.43124 * 10^{-2}$

4 Conclusion

In this paper, the modified variational iteration method has been successfully developed and applied for solving a model for HIV infection o $CD4^+$ T-cells. The results obtained show that the MVIM is an accurate and effective technique for obtaining the approximate solution of HIV infection of $CD4^+$ T-cells.

References

[102] A. S. Perelson, D. E. Kirschner, R. D. Boer, *Dynamics of HIV infection of $CD4^+$ T-cells*, Math Biosci, 114 (1993), 81–125 .

[103] D. Rocha, C. J. Silva, F. M. Torres, *Stability and optimal control of a delayed HIV model*, Math Methods Appl Sci, doi: 10.1002/mma (2016) .

[104] R. V. Culshaw, S. Ruan, *Adelay-differential equation model of HIV infection of $CD4^+$ T-cells*, Mathematical Biosciences, 165 (2000), 27–39.

[105] M. Merdan, *Homotopy perturbation method for solving a model for hiv infection of $CD4^+$ T-cells*, Istanb. Commerce Uni. J. Sci, 12 (2007), 39–52.

[106] A. Barari, M. Omidvar, Abdoul R. Ghotbi, D. D. Ganji, *Application of homotopy perturbation method and variational iteration method to nonlinear oscillator differential equations*, Acta Appl, Math, 104 (2008), 161–171.

[107] M. Y. Ongun, *The Laplace adomian decomposition method for solving a model for HIV infection of $CD4^+$ T-cells*, Math. Comput. Modelling, 53 (2011), 597–603.

The role of disease in the prey-predator model

Marzieh Shamsabadi*, Mohammad Hossein Rahmani Doust and Mohammad Shirazian
Department of Mathematics, University of Neyshabur, Iran.

Abstract:
The abstract Mathematical ecology and mathematical epidemiology are both major field of studies in both biology and applied mathematics. To describe any type of biological phenomena such as competition, coexistence, reactions between two species and etc. In the present paper a prey- predator model which having disease is studied. In continuity, the said model is constructed. Finally, three theorem are proved.
Keywords: Prey-Predator, Infected Model ,Equilibrium Point, Boundedness, Stability.
Mathematics Subject Classification (2010): 92D40, 92B05.

1 Introduction

To find out more practical application, it is necessary to have good knowledge in mathematics (110). Infectious diseases can be factor in regulating human population sizes. For example, Black Death in Europe in the 14^{th} centur killed up to one-fourth of the human population. European diseases such as smallpox brought by Cortez and others to Mexico decimated the native population there in the 16^{th} century. Rinderpest caused high mortality in wild animals in Africa at the end of the 19^{th} century. Myxomatosis caused enormous decreases in the rabbit population in Australia in the 1950s. In the complex ecosystem predator-prey relationships can be important in regulating the numbers of prey and predators. For example, when a bounty was placed on natural predators such as cougars, wolves and coyotes

*Speaker: mh.rahmanidoust@university.ac.ir

in the Kaibab Plateau in Arizona, the deer population increased beyond the food supply, and then over half of the deer died of starvation in 1923-25 (109).The model we introduce consists of two populations: the prey population and the predator population. Both of the populations have two sub classes: susceptible and infected (108).

2 Modelling

At time T, let $S(T)$ denotes the density of the susceptible prey, and $I(T)$ denotes the density of the infected prey. The susceptible and infected predator densities are denoted by $X(T)$ and $Y(T)$, respectively. We describe some basic assumptions which have been made in the formulating of model.
H_1) In the absence of predator population and with no disease, the prey population grows logistically with intrinsic growth rate γ and environmental carrying capacity κ(which is positive).
H_2) Only the susceptibeie prey can reproduce.
H_3) The disease spreads among the susceptible prey when it comes in contact with the infected one. The prey, once became infected, never recovers. It will either die or will be removed by predation. The infected prey population have a disease induced death rate in excess.
H_4) We assume that the infected predators are unfit to be able to catch a healthy predator only. But an infected prey, being weak and more vulnerable, is available for predation by both susceptible and infected predators.
H_5) The disease spread over predator population by direct contact with an infected predator. An infected predator never becomes recovered or immuneit remains infected or dies out.
H_6) We further assume that the predator population have a natural death, whereas the infected population have a disease induce excess death rate also.
The above consideration motivate us to from the following set of four nonlinear ordinary differential equations:

$$\begin{aligned}
\frac{dS}{dT} &= \gamma S(1-\frac{S+I}{\kappa}) - a_1SI - b_1SX,\\
\frac{dI}{dT} &= a_1SI - d_1I - f_1IX - m_1IY,\\
\frac{dX}{dT} &= c_1SX + g_1IX - e_1XY - \delta_1X,\\
\frac{dY}{dT} &= e_1XY - (\delta_1+\alpha_1)Y + n_1IY. \qquad (2.1)
\end{aligned}$$

Whit $S(0) = S_0 \geqslant 0, I(0) = I_0 \geqslant 0, X(0) = X_0 \geqslant 0, Y(0) = Y_0 \geqslant 0$. Here the parameter a_1 is the infection rate fore prey population, b_1 is the predation rate of susceptible prey by healthy predators.The infected prey population has a disease induced death d_1, alsof_1 and m_1 are respectively the predation rate of infected prey by susceptible and infected predators.The parameters c_1 and g_1 are the conversion rates for healthy and infected preys to healthy predator. δ_1 is the natural death rate for the predator population has disease induced death rate α_1. We e_1 as the infection rate for predator population and n_1 as the conversion rate for infected prey to infected predator. We make an obvious assumption that all the parameters are positive.The model we have just specified has thirteen parameters, which makes analysis difficult.To reduce the number of parameters and to determine which combinations of parameters control the behavior of the system, we non-dimensionalize the system (1) whit the following scaling:
$s = \frac{S}{\kappa}, i = \frac{I}{\kappa}, x = \frac{X}{\kappa}, y = \frac{Y}{\kappa}$ and $t = \gamma T$.
Then (after some simplification) the system (1) leads to the following form:

$$\begin{aligned}
\frac{ds}{dt} &= s(1-s-i) - asi - bsx,\\
\frac{di}{dt} &= asi - di - fxi - miy,\\
\frac{dx}{dt} &= csx + gix - exy - \delta x,\\
\frac{dy}{dt} &= exy - \alpha y + niy. \qquad (2.2)
\end{aligned}$$

In the above system, we have: $a = \frac{a_1\kappa}{\gamma}, b = \frac{b_1\kappa}{\gamma}, c = \frac{c_1\kappa}{\gamma}, d = \frac{d_1}{\gamma}, e = \frac{e_1\kappa}{\gamma}, f = \frac{f_1\kappa}{\gamma}, g = \frac{g_1\kappa}{\gamma}, m = \frac{m_1\kappa}{\gamma}, n = \frac{n_1\kappa}{\gamma}, \alpha = \frac{\delta_1+\alpha_1}{\gamma}, \delta = \frac{\delta_1}{\gamma}$.

Definition 9. *A point $x_e \in R^n$ is called an equilibrium point of equation $\acute{x} = f(t,x)$(at time $t^* \in R^+$) if $f(t,x_e) = 0$ for all $t > t^*$.*

Definition 10. *The solution of equation $\acute{x} = f(t,x)$ is uniformly bounded if for any*

$\alpha > 0$ and $t_0 \in R^+$, there exists a $\beta = \beta(\alpha) > 0$ (independent of t_0) such that if $\mid \xi \mid < \alpha$, then $\mid \phi(t, t_0, \xi) \mid < \beta$ for all $t \geqslant t_0$.

Definition 11. *The equlibrium $x = 0$ is stable for system $x' = f(t, x)$ if for every $\varepsilon > 0$ and any $t_0 \in R^+$ there exists a $\delta(\varepsilon, t_0) > 0$ such that $\mid \phi(t, t_0, \xi) \mid < \varepsilon$ for all $t \geqslant t_0$ whenever $\mid \xi \mid < \delta(\varepsilon, t_0)$.*

3 Main results

First, equilibrium points will be presented, then some theorems will be proved. In the next theorems boundedness, locally asymptotically stability will be studied.
System (2) may have the following equilibrium points:
a) The trivial equilibrium point $E_0(0, 0, 0, 0)$,
b) The axial equilibrium point $E_1(1, 0, 0, 0)$,
c) The disease-free equilibrium point $E_2(s_2, 0, x_2, 0)$,
d) The predator-free equilibrium point $E_3(s_3, i_3, 0, 0)$,
e) The infected-predator-free equilibrium point $E_4(s_4, i_4, x_4, 0)$,
f) The infected-prey-free equilibrium point $E_5(s_5, 0, x_5, y_5)$,
g) The interior equilibrium point $E^*(s^*, i^*, x^*, y^*)$.

Theorem 3.1. *All solutions of system (2) which start in R^4_+ remain positive forever.*

Proof. Since all the parameters are non-negative, the right hand side of (2) is a smooth function of variables (s, i, x, y) in the positive octant, $\Omega = \{(s, i, x, y) | s \geqslant 0, i \geqslant 0, x \geqslant 0, y \geqslant 0\}$. Ω is an invariant set. Since system (2) is homogeneous, we have $s = 0, i = 0, x = 0$ and $y = 0$ is one of the solutions. The uniqueness and existence theorem ensures that any trajectory starting from the first quadrant remains in it that is no trajectory will cross the coordinate planes. □

Theorem 3.2. *All solutions of system (2) are uniformly bounded.*

Proof. Let $(s(t), i(t), x(t), y(t))$ be any solution of the system(2). Since

$$\frac{ds}{dt} \leqslant s(1 - s),$$

we have

$$\limsup_{t \to \infty} s(t) \leqslant 1.$$

Let

$$W = s + i + x + y.$$

Therefore,

$$\begin{aligned}\frac{dW}{dt} &\leqslant s - di - \delta x - \alpha y \\ &\leqslant 2s - RW, R = \min\{1, d, \delta, \alpha\}.\end{aligned}$$

Hence

$$\frac{dW}{dt} + RW \leqslant 2S \leqslant 2.$$

Now, by applying theory of differential inequalities, we obtain

$$0 \leqslant W(s, i, x, y) \leqslant \frac{2}{R} + \frac{W(s(0), i(0), x(0), y(0))}{e^{Rt}},$$

And for $t \to \infty$,

$$0 \leqslant W \leqslant \frac{2}{R}.$$

Thus, all the solutions of system (2) enter into the following region

$$B = \{(s, i, x, y) : 0 \leqslant W \leqslant \frac{2}{R} + \varepsilon, \text{ for any} \varepsilon > 0\}.$$

□

Now we analyze the nontrivial equilibrium point.
The interior equilibrium point $E^*(s^*, i^*, x^*, y^*)$ of system(2) exists if
(i) $|P_2| \geqslant max\{|(1+a)P_1 + bP_3|, |\frac{(c+ac-g)P_1+bcP_3}{c-\delta}|\}$,
(ii) P_1, P_2 and P_3 are of same sign, where P_1, P_2 and P_3 are given by:

$$\begin{aligned}P_1 &= e(ab\alpha + f\alpha + cm + de) - (bcm\alpha + me\delta + ae^2), \\ P_2 &= e(abn + fn + (1+a)cm) - (bcmn + a(1+a)e^2 + meg), \\ P_3 &= (aen + mn\delta + (1+a)cm\alpha) - cmn + den + (1+a)ae\alpha + mg\alpha).\end{aligned}$$

When these conditions are satisfied, the values of s^*, i^*, x^*, y^* are given by

$$
\begin{aligned}
s^* &= \frac{P_2 - (1+a)P_1 - P_3 b}{P_2}, \\
i^* &= \frac{P_1}{P_2}, \\
x^* &= \frac{P_3}{P_2}, \\
y^* &= \frac{(g - c - ac)P_1 + (c - \delta)P_2 - bcP_3}{eP_2}.
\end{aligned}
$$

Theorem 3.3. *Nontrivial equilibrium point E^* is locally asymptotically stable provided $D_1 > 0, D_3 > 0, D_4 > 0$ and $D_1 D_2 D_3 > D_3^2 + D_1^2 D_4$.*

At the interior equlibrium E^*, the Jacobian matrix $J(E^*)$ can be obtained as follows:

$$
J(E^*) = \begin{bmatrix} -s^* & -(1+a)s^* & -bs^* & 0 \\ ai^* & 0 & -fx^* & -mi^* \\ cx^* & gx^* & 0 & -ex^* \\ 0 & ny^* & ey^* & 0 \end{bmatrix}_{4\times 4}
$$

The corresponding characteristic equation is given by

$$\lambda^4 + D_1\lambda^3 + D_2\lambda^2 + D_3\lambda + D_4 = 0,$$

where

$$D_1 = -tr(J(E^*)) = s^*$$

Sum of all the possible second order principal minors is

$$D_2 = e^2 x^* y^* + fg{x^*}^2 + mni^* y^* + a(a+1)s^* i^* + bcs^* x^*,$$

-(Sum of all the possible third order principal minors) is

$$D_3 = \left(e^2 s^* x^* y^* + fgs^* {x^*}^2 + mns^* i^* y^* - enf{x^*}^2 y^* + megi^* x^* y^* + abgs^* i^* x^* - cf(a+1)s^* x^*\right),$$

and $det(J(E^*))$ is

$$D_4 = -enfs^* {x^*}^2 y^* + [emg + a(a+1)e - aben + bcmn - cme(a+1)]s^* i^* x^* y^*.$$

By Routh - Hurwitz criterion, all the eigenvalues of $J(E^*)$ have negative real

parts if

$$\begin{cases} D_i > 0, i = 1, 3, 4, \\ D_1(D_2D_3 - D_1D_4) - D_3^2 > 0. \end{cases}$$

Therefore, if $D_1 > 0, D_3 > 0, D_4 > 0$ and $D_1D_2D_3 > D_3^2 + D_1^2D_4, E^*$ is locally asymptotically stable.

Acknowledgment

Authors would like to express their thanks to University of Neyshabur for supporting the present research.

References

[108] S. P. Bera, A. Maiti , G. P. Samanta, *A prey-predator model with infection in both prey and predator*, Filomat 29:8 (2015) 1753-1767.

[109] H.W. Hethcote, W. Wang, L. Han, Zh. Ma, *A predator-prey model with infected prey*, Theoretical Population Biology. 66 (2004) 259-268.

[110] S. Jana, T. K .Kar, *Modeling and analysis of a prey-predator system with disease in the prey* , Chaos, Solitons & Fractals, 47 (2013), 42-53.

[111] S. Kumar , H. Kharbabda, *Stability analysis of prey-predator model with infection, migration and vaccination in prey*, arXiv preprint arXiv:1709.10319 (2017).

[112] R. K. Miller, A. N. Michel , *Ordinary Differential Equations*, New York, Academic Press (1982).

Comparison of the Euler and Adaptive Runge-Kutta Methods for Solving a HTLVI Mathematical Model

Rezaei. Zeynab,*[1], Karami. Saeed[1] and Dadi. Zohreh[2]
[1]Institute for Advanced Studies in Basic Sciences(IASBS), Zanjan, Iran.
[1]Institute for Advanced Studies in Basic Sciences(IASBS), Zanjan, Iran.
[2] University of Bojnord, Bojnord, Iran.

Abstract:

In the paper [HTLV-Infection: A dynamic struggle between viral persistence and host immunity, Aaron G. Lim, Philip K. Maini, Journal of Theoretical Biology 352 (2014) 92-108], the authors proposed a mathematical model for HTLV-I infection, which is a non-linear ordinary differential system.
In this paper we compare the numerical solution of the Euler method and the adaptive Runge-Kutta methods for this model.

Keywords: HTLV-I Infection, Euler Method, Adaptive Runge- Kutta method, Modified Euler method.
Mathematics Subject Classification (2010): 62N01, 962F10.

1 Introduction

The human T-cell lymphotropic virus, or human T-cell leukemia-lymphoma virus (HTLV) family of viruses are a group of human retroviruses that are known to cause a type of cancer called adult T-cell leukemia/ lymphoma and a demyelinating disease called HTLV-I associated myelopathy/tropical spastic paraparesis (HAM/TSP). For this infection Neither vaccine nor cure has been discovered. HTLV-I is a persistent human retrovirus that infects between 10 and 25 million individuals world-wide. Studies in the infectious mode of transmission of HTLV-I and the risk factors for

*Speaker:zaynab.r@iasbs.ac.ir

HTLV-I-related diseases have been carried out in several countries, and the worldwide differences in the prevalence, age patterns, ethnic groups and clinical presentation of related diseases have been described. Recent experiments on the persistence of HTLV-I have leads to creation mathematical models that reveal interactions between pro-viral latency and activation. Mathematical modeling can help us break a part the complex mechanisms of HTLV-I persistence and identify the underlying principles that govern successful viral propagation in the presence of host immunity. In (114) Li and Lim, formulate a mathematical model which illustrate the balance between latency and activation in the target cell dynamics of the viral infection.
In this paper, we discrete this mathematical model by using Euler method, and then we study the stability of its fixed point.

2 Mathematical model

A mathematical model is offered by Li and Lim (114), in which the interaction between the latent and active in the target cells is shown.
The target cells of this virus are $CD4^+$ helper T-cells that in the first we divided into three different compartment. As mentioned in (113), we define
$y_1(t)$: density of healthy $CD4^+$ helper T-cells at time t,
$y_2(t)$: density of latently infected $CD4^+$ helper T-cells at time t,
$y_3(t)$: density of actively infected $CD4^+$ helper T-cells at time t,
$y_4(t)$: density of HTLV-I-specific $CD8^+$ CTLs at time t.
The proposed mathematical model of HTLV-I infection is as follows:

$$\begin{aligned} dy_1/dt &= \lambda - \beta y_1 y_3 - \mu_1 y_1 \\ dy_2/dt &= \beta y_1 y_3 + r y_3 - (\tau + \mu_2) y_2 \\ dy_3/dt &= \tau y_2 - \gamma y_3 y_4 - \mu_3 y_3 \\ dy_4/dt &= \nu y_3 - \mu_4 y_4 \end{aligned} \tag{2.1}$$

This is a 4-dimensional nonlinear ordinary differential equation. The parameters have been estimated using both experimental and theoretical methods in studies of $CD4^+$ lymphocyte kinetics by Kirschner and Webb (115). We summarize the parameters in the the Table 1, ((113)).

Table 1: Table of biologically relevant dimensional initial conditions and parameter values

Initial condition	Value ($cells/mm^3$)	
$y_1(0)$	~ 850	
$y_2(0)$	0.1	
$y_3(0)$	0.5	
$y_4(0)$	0.1	
Dimensional parameter	Value	Biological meaning
λ	$10cells/mm^3/day$	Rate of production of target cells
β	$0.00110cells/mm3/day$	Infectious transferability coefficient
r	$0.011day^-1$	Selective proliferation rate of actively infected c
τ	$0.003day^{-1}$	Rate of spontaneous Tax expression
γ	$0.029day^-1$	Rate of CTL-mediated lysis of actively infected
ν	$0.036day^-0$	Proliferation rate of CTLs (or CTL responsiven
μ_1	$0.012day^-1$	Natural death rate of healthy cells
μ_2	$0.03day^-1$	Natural death rate of latently infected cells
μ_3	$0.03day^-1$	Natural death rate of actively infected cells
μ_4	$0.03day^-1$	Natural death rate of virus-specic CTLs

3 NUMERICAL METHODS FOR ODE SYSTEM

The initial value problem for a system of m first-order differential equations has the general form

$$\begin{aligned} y_1^{'}(t) &= f_1(t, y_1(t), ..., y_m(t)), \quad y_1(t_0) = y_{1,0}, \\ &\vdots \\ y_m^{'}(t) &= f_m(t, y_1(t), ..., y_m(t)), \quad y_m(t_0) = y_{m,0}. \end{aligned} \tag{3.1}$$

We seek the functions $y_1(t), ..., y_m(t)$ on some interval $t_0 \leqslant t \leqslant T$. Let

$$\mathbf{Y}(t) = \begin{bmatrix} y_1(t) \\ \vdots \\ y_m(t) \end{bmatrix}, \quad \mathbf{Y}_0 = \begin{bmatrix} y_{1,0} \\ \vdots \\ y_{m,0} \end{bmatrix}, \quad \mathbf{f}(t, \mathbf{Y}) = \begin{bmatrix} f_1(t, y_1, ..., y_m) \\ \vdots \\ f_m(t, y_1, ..., y_m) \end{bmatrix} \tag{3.2}$$

Then (3.1) can be rewritten as

$$\mathbf{Y}^{'}(t) = \mathbf{f}(t, \mathbf{Y}(t)), \quad \mathbf{Y}(t_0) = \mathbf{Y}_0. \tag{3.3}$$

Assume that we partition the interval $[t_0, T]$ as $\left\{ t_i : \ t_i = t_0 + ih, \ i = 0, 1, ..., n \ \text{ and } \ h = \dfrac{T - t_0}{n} \right\}$. The Eulers method for solving the system (3.3) has the following vector form:

$$\begin{aligned} \mathbf{Y}(t_{n+1}) &= \mathbf{Y}(t_n) + h\mathbf{f}(t_n, \mathbf{Y}(t_n)) + \mathbf{R}(\mathbf{t}), \ , \quad y(t_0) = y_0, \\ \mathbf{R}(\mathbf{t}) &= \frac{1}{2!}h^2\mathbf{Y}''(\xi), \quad \xi \in (t, t+h) \end{aligned}$$

If a positive number M exists so that $|\mathbf{Y}''(t)| \leqslant M$ for all $t \in (t_0, T)$, it follows that

$$|\mathbf{R}(t)| \leqslant \frac{1}{2}Mh^2$$

therefore $\mathbf{R}(t) = O(h^2)$. The procedure for calculating the numerical solution to the initial value problem via the improved Euler's method. by way of Modified Euler (ME) method, is to first calculate the intermediate value $\hat{y}_{i+1}$ and then the final approximation y_{i+1} at the next integration point.

$$\begin{aligned} \hat{\mathbf{Y}}_{\mathbf{i+1}} &= \mathbf{Y}_i + h\mathbf{f}(\mathbf{t_i}, \mathbf{y_i}), \\ \mathbf{Y}_{i+1} &= \mathbf{Y}_i + \frac{h}{2}\left[\mathbf{f}(\mathbf{t_i}, \mathbf{y_i}) + \mathbf{f}(\mathbf{t_{i+1}}, \hat{\mathbf{y}}_{\mathbf{i+1}})\right]. \end{aligned} \tag{3.4}$$

The general s-stage RK method written in the form

$$\mathbf{Y}_{n+1} = \mathbf{Y}_n + h\sum_{i=1}^{s} b_i\mathbf{K}_i, \tag{3.5}$$

where $\mathbf{K}_i$ are as follow:

$$\mathbf{K}_i = \mathbf{f}(t_n + c_ih, \mathbf{Y}_n + h\sum_{j=1}^{s} a_{i,j}\mathbf{K}_j), \quad i = 1 : \ s, \quad c_i = \sum_{j=1}^{s} a_{i,j}, \quad {\scriptstyle i=1\,:\,s.} \tag{3.6}$$

We can show the coefficient of Runge-Kutta method by the following table, known as Butcher table. The Boucher table is triangular to the top form of explicit RK

Table 2: The Butcher array for a full (implicit) RK method

c_1	$a_{1,1}$	$a_{1,2}$	$\cdots$	$a_{1,s}$
c_2	$a_{2,1}$	$a_{2,2}$	$\cdots$	$a_{2,s}$
$\vdots$	$\vdots$	$\vdots$		
c_s	$a_{s,1}$	$a_{s,2}$	$\cdots$	$a_{s,s}$
	b_1	b_2	$\cdots$	b_s

method.

3.1 Error Control and the Runge-Kutta-Fehlberg Method

One popular adaptive technique for controlling the error is the Runge-Kutta-Fehlberg method (known also as ode45 method in Matlab). This technique uses a Runge-Kutta method with local truncation error of order five,

$$\mathbf{Y}_{i+1} = \mathbf{Y} + \frac{16}{135}K_1 + \frac{6656}{12825}K_3 + \frac{28561}{56430}K_4 - \frac{9}{50}k_5 + \frac{2}{55}K_6, \tag{3.7}$$

to estimate the local error in a Runge-Kutta method of order four given by

$$\mathbf{Y}_{i+1} = \mathbf{Y}_i + \frac{25}{216}k_1 + \frac{1408}{2565}k_3 + \frac{2197}{4104}k_4 - \frac{1}{5}k_5, \tag{3.8}$$

where

$$\begin{aligned}
k_1 &= h\mathbf{f}(t_i, \mathbf{Y}_i),\\
k_2 &= h\mathbf{f}(t_i + \frac{h}{4}, \mathbf{Y}_i + \frac{1}{4}\mathbf{k}_1),\\
k_3 &= h\mathbf{f}(t_i + \frac{3h}{8}, \mathbf{Y}_i + \frac{3}{32}\mathbf{k}_1 + \frac{9}{32}\mathbf{k}_2),\\
k_4 &= h\mathbf{f}(t_i + \frac{12h}{13}, \mathbf{Y}_i + \frac{1932}{2197}\mathbf{k}_1 - \frac{7200}{2197}\mathbf{k}_2 + \frac{7296}{2197}\mathbf{k}_3),\\
k_5 &= h\mathbf{f}(t_i + h, \mathbf{Y}_i + \frac{439}{216}\mathbf{k}_1 - 8\mathbf{k_2} + \frac{3680}{513}\mathbf{k}_3 - \frac{845}{4104}\mathbf{k}_4),\\
k_6 &= h\mathbf{f}(t_i + \frac{h}{2}, \mathbf{Y}_i - \frac{8}{27}\mathbf{k}_1 + 2\mathbf{k_2} - \frac{3544}{2565}\mathbf{k}_3 + \frac{1859}{4104}\mathbf{k}_4 - \frac{11}{40}\mathbf{k_5}).
\end{aligned}$$

We solve the model of (2.1) by the Matlab code 'ode45' which use Runge-Kutta-Fehlberg method and then plot the functions $y_i(t), i = 1, 2, 3, 4$ in the Figure 1.

Since 'ode45' uses a method of oder 5, we assume the solutions of ode45 as exact solution of the model (2.1). Then fo comparing the Euler and Modified Euler methods we solve (2.1) by Euler method with time step size $h = 1$ day and also by the Modified Euler (ME) method with time step size $h = 5$ day. The results ae presented in Table 3 and 4.

4 Corollary

Our numerical experiments show that for solving mathematical models such as (1), the Modified Euler (ME) method (even by larger step size) is more accurate than Euler method.

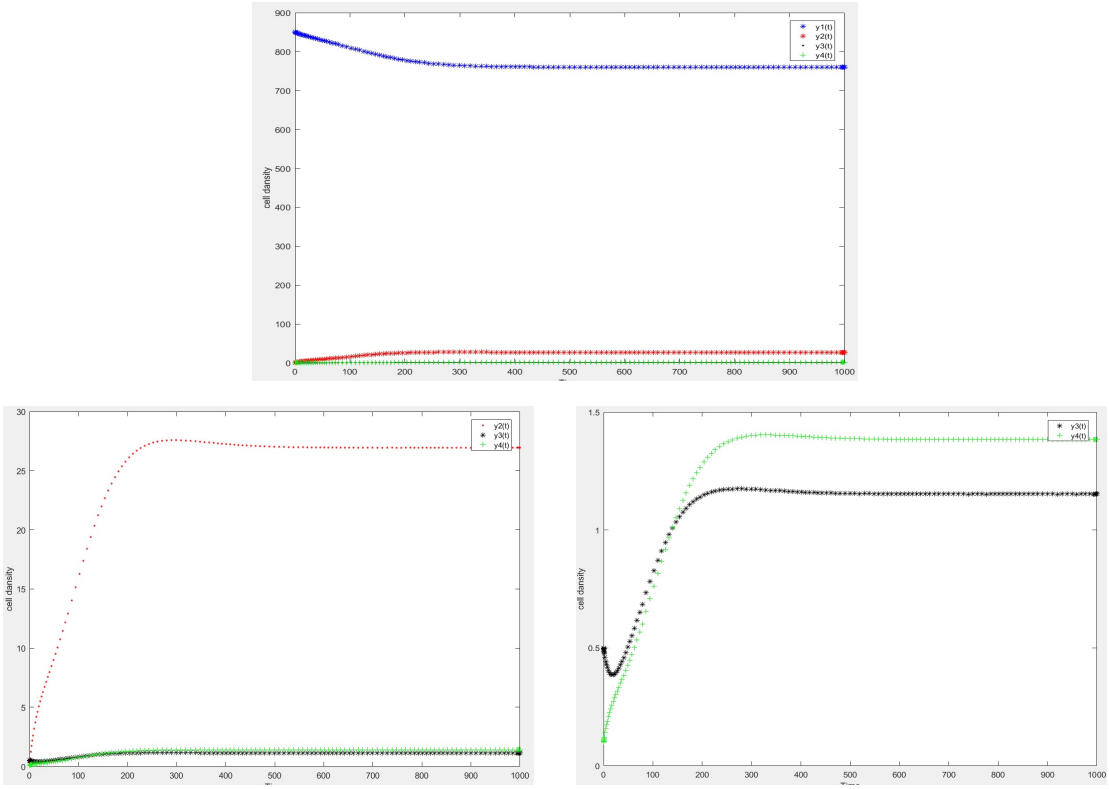

Figure 1: Numerical solution of model (2.1) with initial conditions and parameter values as in Table (1) The level of healthy $y_1(t)$, latently infected $y_2(t)$, and actively infected $y_3(t)$ target cells are shown in blue, red, and black, respectively, and the level of HTLV-I-specific CTLs $y_4(t)$ is shown in green. (a) The full dimensional range showing all cell populations and highlighting their relative abundances. $(b) - (c)$ A closer examination of the behaviour of $y_2(t)$, $y_3(t)$ and $y_4(t)$ in model (2.1).

Table 3: Numerical solution obtained by Euler and ode45 methods at different times

T	y_1^{Euler}	y_2^{Euler}	y_3^{Euler}	y_4^{Euler}	y_1^{ode45}	y_2^{ode45}	y_3^{ode45}	y_4^{ode45}
$T = 0$	850	0.1	0.5	0.1	850	0.1	0.5	0.1
$T = 25$	838.1986	5.9675	0.3920	0.3049	838.2361	5.9316	0.3953	0.3040
$T = 250$	769.0396	27.3701	1.11735	1.3736	769.1160	27.3480	1.1730	1.3724
$T = 500$	760.2673	27.0242	1.1547	1.3876	760.2737	27.0276	1.1547	1.3877
$T = 1000$	760.2941	26.9440	1.1528	1.3834	760.2909	26.9483	1.1525	1.3836

References

[113] Aaron G. Lim and Philip K. Maini, *HTLV- Infection: A dynamic struggle between viral persistence and host immunity*, Journal of Theoretical Biology 352 (2014), pp.92–108.

[114] M.Y. Li and A. G. Lim, *Modeling the role of Tax expression in HTLV-I per-*

Table 4: Numerical solution obtained by Modified Euler (ME) and ode45 methods at different times

T	y_1^{ME}	y_2^{ME}	y_3^{ME}	y_4^{ME}	y_1^{ode45}	y_2^{ode45}	y_3^{ode45}	y_4^{ode45}
$T = 0$	850	0.1	0.5	0.1	850	0.1	0.5	0.1
$T = 25$	838.2700	5.8871	0.3979	0.3023	838.2361	5.9316	0.3953	0.3040
$T = 250$	769.1289	27.3426	1.1729	1.3721	769.1160	27.3480	1.1730	1.3724
$T = 500$	760.2756	27.0273	1.1548	1.3877	760.2737	27.0276	1.1547	1.3877
$T = 1000$	760.2941	26.9439	1.1528	1.3834	760.2909	26.9483	1.1525	1.3836

sistence in vivo, Bull.Math.Biol, 73 (2011), pp 3008–3029.

[115] D. Kirschner and G. F. Webb, *A model for treatment strategy in the chemotherapy of AIDS*, Bull.Math.Bio, 58 (1996), pp.367–390.

[116] Griffiths, David F. Desmond J. Higham, *Numerical methods for ordinary differential equations: initial value problems*. Springer Science, Business Media, 2010.

[117] Burden, Richard L, and J. Douglas Faires, *Numerical analysis. 2001.* Brooks/Cole, USA (2001).

[118] Atkinson, Kendall, Weimin Han, and David E. Stewart, *Numerical solution of ordinary differential equations*. Vol. 108. John Wiley, Sons, 2011.

Optimal control of chemotherapy on a cancer-obesity model

Mohammad Shirazian and Somayyeh Beheshti*
Department of Mathematics, University of Neyshabur, Iran.

Abstract:

Obesity as a risk factor has been found in dierent types of cancers such as breast cancer and colorectal cancer among others. This challenges us to study the cancer-obesity relationship and the tumor response to chemotherapy. In this work, we study and analyze an improved optimal control protocols for chemotherapy treatments for a mathematical model of cancerous growing tumor that is interacting with the healthy cells, the immune system cells and the stored fat in the organism.

Keywords: Optimal control, Chemotherapy ,Equilibrium points, Stability.
Mathematics Subject Classification (2010): 49J15, 34H15.

1 Introduction

In this work, we propose and analyze a cancer-obesity model for the growth of a tumor where chemotherapy schedules are obtained using optimal control techniques. Our aim is to study how the diet can affect different tumor growth scenarios when chemotherapy is applied. This is motivated by the reported relationship between obesity and cancer in several experimental studies such as (119). Our model includes an equation for the stored fat in the organism based on logistic growth which includes a parameter to model the carrying capacity of the system. We claim that this parameter, the carrying capacity, is related to anthropometric measurements of in-body fat such as the Body Mass Index (BMI) and Waist-to-Hip ratio.

The use of optimal control to model a chemotherapy treatment is not a new idea, but it is a well known tool to study chemotherapy protocols with constrains. For example, in (122) it is used optimal control chemotherapy treatments to study the

*Speaker: somayebeheshte812@gmail.com

resistance to a drug in a heterogeneous cancerous tumor. There, it is concluded that the drug must be given at the maximum rate in order to reduce the resistance. An overview of chemotherapy models using optimal control is presented in (121) and a discussion of the potential of application of this technique is given in (120). Our model proposal is based on the De Pillis and Radunskaya model, reported in (121) which also models the chemotherapy treatment using control theory. Their goal is to minimize the tumor cells while keeping the healthy cells above a predetermined level.

2 The cancer-obesity model description

Consider the following control model (121),

$$\dot{I} = s + \frac{\rho IT}{\alpha + \mu F + T} - c_1 IT - d_1 I - a_1(1 - e^{-u})I \tag{2.1}$$

$$\dot{T} = r_1 T(1 - b_1 T) - c_2 IT - c_3 TN + c_5 TF - a_2(1 - e^{-u})T \tag{2.2}$$

$$\dot{N} = r_2 N(1 - b_2 N) - c_4 TN - a_3(1 - e^{-u})N \tag{2.3}$$

$$\dot{F} = r_3 F(1 - b_3 F) - c_6 FT - a_4(1 - e^{-u})F \tag{2.4}$$

$$\dot{u} = v - d_2 u, \tag{2.5}$$

where $I(t)$ denotes the number of immune cells at time t, $T(t)$ the tumor cells at time t, $N(t)$ the normal cells at time t, $F(t)$ the fat stored in adipocytes at time t, and $u(t)$ the drug in the organism. The function $v(t)$ models the application protocol of chemotherapy, while d_2 is the constant related to the natural decay of the drug. The parameters associated to immune system are: s the basal response, ρ the immune response stimulated by the cancer cells, α and μ are constants that model the immune response caused by tumor in a form of a saturation term. The constants r_1, r_2 and r_3 are the growth rates for the tumor cells, the normal cells and the fat, respectively. Also, the constants b_1, b_2 and b_3 are the inverses of the carrying capacity of the populations of T, N and F, respectively. The coefficients of the competition terms among the different populations are the constants c_1, c_2, c_3, c_4, c_5, and c_6 is the coefficient of the term that models the contribution of F to the tumor growth rate. The constants a_1, a_2, a_3, and a_4 model the kill effectiveness of the drug on I, T, N and F populations, respectively.

The equilibrium points of this model can be presented for two cases: no fat ($F = 0$) and fat present ($F \neq 0$).

2.1 No fat in adipocytes, $F = 0$

When $F = 0$ in our model without chemotherapy, all the equilibria are unstable. We have named the points based on their biological interpretation as:

- *Death*: We name this point in this way because there are no normal cells ($N = 0$) and the only present population is the immune cell population, $P1 = (\frac{s}{d_1}, 0, 0, 0)$.
- *Total cancer invasion*: We call this point this way because $N = 0$ and the tumor cell density is not zero, $T \neq 0$. This means that the tumor has invaded the organ because only the immune cells and cancer cells remain. This also implies the death of the organism.The point has the form $P_2 = (I, T, 0, 0)$.
- *Tumor-free point*: As the name indicates, in this point the tumor has been eradicated because the variable $T = 0$ and we still have healthy cells. This state represents the healthy equilibrium where only normal cells and immune cells remain. It have the form $P_3 = (\frac{s}{d_1}, 0, \frac{1}{b_2}, 0)$.
- *Coexistence equilibrium*: We name an equilibrium point of coexistence whenever all its rst three entries are non-zero, so we have these three populations coexisting. We can nd one, two or three points of this type depending on the parameter values, $P_4 = (I, T, N, 0)$.

2.2 Equilibria with fat in adipocytes $F \neq 0$

For the following equilibrium points the existing fat in the organism is $F \neq 0$. These points play a important role because they could change their stability. These equilibrium points are named using the same terminology of the previous equilibria and they are:

- *Death*: $PO_1 = (\frac{s}{d_1}, 0, 0, \frac{1}{b_3})$. Only immune cells and fat are present. It is easy to verify that this equilibrium point is always unstable. This state can not be achieved in reality because it would imply that there are not healthy cells in the organism.
- *Total cancer invasion*: $PO_2 = (I, T, 0, F)$ is a state of death because there are not normal cells. The stability of the equilibrium point changes depending on the parameter values.
- *Tumor-free*: $Po_3 = (\frac{s}{d_1}, 0, \frac{1}{b_2}, \frac{1}{b_3})$ is a healthy state because the tumor cell population is zero. This point is stable when $r_1 + \frac{c_5}{b_3} < \frac{c_2 s}{d_1} + \frac{c_3}{b_2}$. Its stability

depends on the tumor growth rate, the interaction coecients and the source rate of the immune system.

- *Coexistence*: $PO_4 = (I, T, N, F)$ is a state where all types of cells coexist. It is possible to nd zero, one, two or three points of this type depending on the parameter values. The stability depends on the parameter values.

3 Optimal control and chemotherapy

In this section, we briefly describe the optimal control approach and its relationship with the chemotherapy. The optimal control problem consists of forcing the solution of a system out an undesirable set at a given time. Let us denote the state variables by $(I, T, N, F, u) = (x_1, x_2, x_3, x_4, x_5)$.
In (121), the authors considered the objective functional as:

$$\min \quad J(x, v) = x_2(t_f), \tag{3.1}$$

which minimizes the final tumor size but not the total tumor size at the time interval. Hence, we propose another objective which minimizes the total tumor size along with the costs of chemotherapy, as:

$$\min \quad J(x, v) = \int_{t_0}^{t_f} \left(x_2(t) + \frac{1}{2}\epsilon v^2(t) \right) dt, \tag{3.2}$$

where ϵ is the cost of chemotherapy per a unit of v. Moreover, in (121), the time interval considered as $[0, t_f]$, i.e. the chemotherapy should be started before any change in organism. As simulation results show, the tumor size is constant for the first 5 days, i.e. $t \in [0, 5]$. Thus, we assume $t_0 = 5$ days for starting the chemotherapy treatment.
Now, the problem is minimizing the objective function in (3.2), subject to the equation system (2.1) and the constraint:

$$k(x, t, v) = x_3(t) - 0.75 \geqslant 0, \quad t_0 \leqslant t \leqslant t_f \tag{3.3}$$

which keeps the normal cells above a minimum level of 75% of its normalized total amount.
Following the classical control theory, we derive the associated hamiltonian for the

optimal control problem:

$$H = x_2(t) + \frac{1}{2}\epsilon v^2(t) + \sum_{i=1}^{5}(p_i(t)\dot{x}_i(t)) + \eta(t)k(t),$$

where the functions $p_i(t)$, are called the co-state variables, which satisfy $\dot{p}_i = \frac{\partial H}{\partial x_i}$, or explicitly:

$$\dot{p}_1 = -p_1\left(\frac{\rho x_2}{\alpha + x_2 + \mu x_4} - c_1 x_2 - d_1 - a_1(1 - e^{-x_5})\right) + c_2 p_2 x_2 \tag{3.4}$$

$$\dot{p}_2 = -1 - p_1\left(\frac{(\alpha + \mu x_4)\rho x_1}{(\alpha + x_2 + \mu x_4)^2} - c_1 x_1\right) - p_2(r_1 - 2r_1 b_1 x_2 - c_2 x_1 - c_3 x_3 + c_5 x_4 \tag{3.5}$$

$$- a_2(1 - e^{-x_5})) + p_3 c_4 x_3 + p_4 c_6 x_4 \tag{3.6}$$

$$\dot{p}_3 = p_2 c_3 x_2 - p_3(r_2 - 2r_2 b_2 x_3 - c_4 x_2 - a_3(1 - e^{-x_5})) - \eta(t) \tag{3.7}$$

$$\dot{p}_4 = p_1\frac{\rho x_1 x_2 \mu}{(\alpha + x_2 + \mu x_4)^2} - p_2 c_2 x_2 - p_4(r_3 - 2r_3 b_3 x_4 - c_6 x_2 - a_4(1 - e^{-x_5})) \tag{3.8}$$

$$\dot{p}_5 = e^{-x_5}(p_1 a_1 x_1 + p_2 a_2 x_2 + p_3 a_3 x_3 + p_4 a_4 x_4) + p_5 d_2, \tag{3.9}$$

where $\eta(t) \leqslant 0$ with $\eta(t)k(t) = 0$ and

$$\eta(t) = \begin{cases} -1, & \text{if} \quad x_3(t) \leqslant 0.75 \\ 0, & \text{otherwise.} \end{cases} \tag{3.10}$$

Foregoing costate system have the following boundary conditions:

$$p_i(t_f) = 0, \quad i = 1, 2, \cdots, 5.$$

Finally, the optimal control law is given by,

$$\frac{\partial H}{\partial v} = \epsilon v(t) + p_5(t) = 0,$$

which yields

$$v^*(t) = -\frac{p_5(t)}{\epsilon} \tag{3.11}$$

Acknowledgment

Authors would like to express their thanks to University of Neyshabur for supporting the present research.

References

[119] G. An and S. Kulkarni. *An agent-based modeling framework linking inammation and cancer using evolutionary principles: Description of a generative hierarchy for the hallmarks of cancer and developing a bridge between mechanism and epidemiological data*, Mathematical biosciences, 260 (2015) 1624.

[120] M. Engelhart, D. Lebiedz, and S. Sager. *Optimal control for selected cancer chemotherapy ode models: a view on the potential of optimal schedules and choice of objective function*, Mathematical biosciences, 229(1) (2011) 123134.

[121] R.A. Ku-Carrillo, S.E. Delgadillo-Aleman and B.M. Chen-Charpentier, *Effects of the obesity on optimal control schedules of chemotherapy on a cancerous tumor*, Journal of Computational and Applied Mathematics, 309 (2017) 603-610.

[122] J. Murray, *The optimal scheduling of two drugs with simple resistance for a problem in cancer chemotherapy*, Mathematical Medicine and Biology, 14(4) (1997) 283303.

Numerical solutions of mathematical model on fractional Lotka-Volterra equations

Haleh Tajadodi*
Department of Mathematics, University of Sistan and Baluchestan, Zahedan, Iran

Abstract:

In this paper, we present the solutions of fractional Lotka-Volterra equations with the help of linear B-spline polynomials. The key-idea is to expand unknown function in terms of the B-spline polynomials. In this way, we use the operational matrices of fractional integration and multiplication. By using these matrices, the given problem can be changed to the system of algebraic equations, and by solving this system, we obtain the solutions of problem. Numerical results are demonstrated the efficiency and simplicity of this technique for this historical biological model.

Keywords: Fractional differential equations; Lotka-Volterra model; B-spline.
Mathematics Subject Classification (2010): 34A08, 26A33.

1 Introduction

Fractional Calculus generalizes to real order the well known concept of derivative and integral of integer order. Even if the birth of fractional calculus can be set at the beginning of the 18th century, its use for the modeling of real-life problems is very recent. Nevertheless, in the last decades the interest in fractional differential and integral equations is rapidly growing and models involving fractional derivatives and/or integrals are widely used in several fields. The reason why the fractional derivative is more suitable to model real-world problems is related to its non-local behavior that is able to introduce in a elegant way into the model, either memory effects in time or non-locality in space. Systems of nonlinear differential equations

*Speaker: tajadodi.h@gmail.com,tajadodi@math.usb.ac.ir

arise in many scientific models such as biological systems and are used in various fields as engineering, chemistry, and ecology. In 1925, Lotka (125) developed the motion of an evolutionary system based on two fundamental changes, those involving matter between components of a system and those involving exchanges of energy. Unlike being grounded in chemistry, Lotka believed that these ideas could be applied to any biological system. In 1926, Volterra (127) developed the well-known mathematical models of multispecies interaction. These models, the predator, prey and competition models are known today as Lotka-Volterra models. In this paper, we consider numerical solutions of fractional Lotka-Volterra models using B-spline functions as:

$$\begin{aligned} D^{\alpha}x(t) &= a(t)x(t) - b(t)x(t)y(t) \\ D^{\beta}y(t) &= c(t)x(t)y(t) - d(t)y(t) \end{aligned} \tag{1.1}$$

where $0 < \alpha \leqslant 1, 0 < \beta \leqslant 1$ and $a(t), b(t), c(t), d(t)$ are, respectively, the growth rate of prey,the efficiency of the predators ability to capture theprey, the growth rate of prey and the death rate of predator. D^{α} is the differential operator of order α in the sense of Caputo as following:

$$D_t^{\alpha}x(t) = \begin{cases} \frac{1}{\Gamma(n-\alpha)}\int_0^t \frac{x(\tau)}{(t-\tau)^{1+\alpha-n}}d\tau, & n-1 < \alpha < n, \quad n \in I\!N, \\ \\ \dfrac{d^n}{dt^n}x(t), & \alpha = n. \end{cases} \tag{1.2}$$

Also I_t^{α} the fractional Riemann-Liouville integral, namely (126):

$${}_0I_t^{\alpha}x(t) = \frac{1}{\Gamma(\alpha)}\int_0^t \frac{x(\tau)}{(t-\tau)^{1-\alpha}}d\tau, \quad \alpha > 0. \tag{1.3}$$

B-spline function is divided the interval into a collection of subintervals and construct a different approximating polynomial on each subinterval. unknown function is approximated with a linear B-spline functions. To this end, we use Operational matrix of integration. In consequence, the diven problems convert to systems of algebraic equations. Solutions of problem is obtained by solving the aforesaid systems .

2 Linear cardinal B-spline function on [0,1]

Boor et al. (123) define the explicit expression of $N_2(t)$ (the linear B-spline function) in the following form:

$$N_2(t) = \sum_{k=0}^{2} \binom{2}{k} (-1)^k (t-k)_+ = \begin{cases} t & t \in [0,1) \\ 2-t & t \in [1,2) \\ 0 & otherewise \end{cases} \tag{2.1}$$

Suppose $N_{j,k}(t) = N_2(2^j t - k),\ j,k \in Z$ and $B_{j,k} = supp[N_{j,k}] = close\,\{t\ :\ N_{j,k} \neq 0\}$. By inspection we have that

$$B_{j,k} = [2^{-j}k, 2^{-j}(2+k)], \quad j,k \in Z \tag{2.2}$$

The support of $N_{j,k}(t)$ can be outside of $[0,1]$,therefore we have to define $N_{j,k}(t)$ on $[0,1]$. Thus, we conclude that

$$\phi_{j,k} = N_{j,k}(t)\chi_{[0,1]}(t), \quad j \in Z \tag{2.3}$$

As a result for $k = 0, 1, \cdots, 2^j - 2$ we have

$$\phi_{j,k} = \sum_{i=0}^{2} \binom{2}{i} (-1)^i (2^j t - (k+i))_+ = \begin{cases} 2^j t - k & \frac{k}{2^j} \leqslant t < \frac{k+1}{2^j} \\ 2 - (2^j t - k) & \frac{k+1}{2^j} \leqslant t < \frac{k+2}{2^j} \\ 0 & otherewise \end{cases} \tag{2.4}$$

Also, left and right boundary scaling functions for $k = -1, 2^j - 1$ are, respective:

$$\phi_{j,-1} = \begin{cases} 1 - 2^j x, & 0 \leqslant t < \frac{1}{2^j}, \\ 0, & otherewise, \end{cases} \tag{2.5}$$

and

$$\phi_{j,2^j-1} = \begin{cases} 2^j t - 2^j + 1, & 1 - \frac{1}{2^j} \leqslant t < 1, \\ 0, & otherewise. \end{cases} \tag{2.6}$$

2.1 The function approximation

For a fixed $j = J$, a function $x(t)$ is defined over $[0, 1]$ can be represented by B-spline scaling functions as

$$x(t) \simeq \sum_{k=-1}^{2^j-1} c_k \phi_{j,k}(t) = C^T \Phi_J(t) \tag{2.7}$$

where

$$C = [c_{-1}, c_0, \ldots, c_{2^j-1}]^T \tag{2.8}$$
$$\Phi_J(t) = [\phi_{j,-1}(t), \phi_{j,0}(t), \ldots, \phi_{j,2^j-1}(t)]^T \tag{2.9}$$

Then, c_k can be obtained by

$$c_k^T = \int_0^1 x(t) \widetilde{\phi}_{j,k}^T(t) dt, \quad k = -1, \ldots, 2^j - 1, \tag{2.10}$$

where $\widetilde{\phi}_{j,k}$ is the vector of dual basis of Φ_J. By using the linear combinations of $\phi_{j,k}$, the $\widetilde{\phi}_{j,k}$ are obtained as:

$$\widetilde{\phi}_{j,k} = P^{-1} \Phi_J \tag{2.11}$$

where

$$P = \int_0^1 \Phi_J(t) \Phi_J^T(t) dt = \frac{1}{2^{J-2}} \begin{bmatrix} \frac{1}{12} & \frac{1}{24} & & & \\ \frac{1}{24} & \frac{1}{6} & \frac{1}{24} & & \\ & \ddots & \ddots & \ddots & \\ & & \frac{1}{24} & \frac{1}{6} & \frac{1}{24} \\ & & & \frac{1}{24} & \frac{1}{12} \end{bmatrix} \tag{2.12}$$

where P is a symmetric $(2^J + 1) \times (2^J + 1)$ matrix. Replacing (2.11) in (2.10) we get

$$c_k^T = \left(\int_0^1 x(t) \phi_J^T(t) dt \right) P^{-1}. \tag{2.13}$$

2.2 Fractional integration within the operational matrix

The fractional integration of ϕ_J with respect to RiemannLiouville is given by

$${}_0I_t^\alpha \Phi_J(t) \simeq I^\alpha \Phi_J(t), \tag{2.14}$$

where I^α is the $(2^J+1)\times(2^J+1)$ fractional operational matrix of integration for B-spline function.
Proof: See (124).

2.3 The operational matrix of product

The operational matrices for the product $\hat{C}$ using linear B-spline function is given by

$$C^T\Phi_J(x)\Phi_J(x)^T \simeq \Phi_J(x)^T\hat{C}, \tag{2.15}$$

where $\hat{C}$ is an $(2^J+1)\times(2^J+1)$ matrix.
Proof: For more information about operational matrix of product, refer to (124).

3 Numerical solutions of the problem

In this section, consider the fractional Lotka-Volterra equation (1.1) with intial conditions

$$x(0)=\delta, \qquad y(0)=\gamma. \tag{3.1}$$

We expand the fractional derivative in Eq.(1.1) by linear B-spline function Φ_J as follows:

$$D^\alpha x(t) \simeq X^T\Phi_J(t), \qquad D^\beta y(t) \simeq Y^T\Phi_J(t) \tag{3.2}$$

Applying the fractional integral operator on the both sides of Eq. (3.2) and by replacing initial condition, we can obtain:

$$x(t) \simeq X^T{}_0I_t^\alpha + \Phi_J(t) + \delta = (X^TI^\alpha + e_1^T)\Phi_J(t) = X_\alpha^T\Phi_J(t), \tag{3.3}$$
$$y(t) \simeq Y^T{}_0I_t^\beta + \Phi_J(t) + \gamma = (Y^TI^\beta + e_2^T)\Phi_J(t) = Y_\alpha^T\Phi_J(t) \tag{3.4}$$

where I^α, I^β are operational matrix of fractional integration and

$$e_1 = [e_{1-1}, e_{10}, \ldots, e_{12^j-1}]^T \tag{3.5}$$
$$e_2 = [e_{2-1}, e_{20}, \ldots, e_{22^j-1}]^T \tag{3.6}$$

Also using (2.7), we approximate functions $a(t), b(t), c(t), d(t)$ by the linear B-spline basis as:

$$a(t) \simeq A^T \Phi_J(t), \qquad b(t) \simeq B^T \Phi_J(t), \qquad c(t) \simeq C^T \Phi_J(t), \qquad d(t) \simeq D^T \Phi_J(t) \tag{3.7}$$

Now, by substituting (3.3)-(3.7) into (1.1), we obtain

$$\begin{aligned} X^T \Phi_J(t) &= A^T \Phi_J(t) \Phi_J^T(t) X_\alpha^T - B^T \Phi_J(t) X_\alpha^T \Phi_J(t) \Phi_J^T(t) Y_\beta^T \\ Y^T \Phi_J(t) &= C^T \Phi_J(x) X_\alpha^T \Phi_J(t) \Phi_J^T(t) Y_\beta^T - D^T \Phi_J(t) \Phi_J^T(t) Y_\beta^T \end{aligned} \tag{3.8}$$

Then, from (2.15) we have

$$\begin{aligned} &A^T \Phi_J(t) \Phi_J(t)^T X_\alpha^T \simeq \Phi_J(t)^T \hat{A} X_\alpha^T = X_\alpha \hat{A}^T \Phi_J(t), \\ &B^T \Phi_J(t) X_\alpha^T \Phi_J(t) \Phi_J^T(t) Y_\beta^T \simeq B^T \Phi_J(t) \Phi_J(t)^T \hat{X}_\alpha Y_\beta^T = Y_\beta \hat{X_\alpha}^T \hat{B}^T \Phi_J(t) \\ &C^T \Phi_J(t) X_\alpha^T \Phi_J(t) \Phi_J^T(t) Y_\beta^T \simeq C^T \Phi_J(t) \Phi_J(t)^T \hat{X}_\alpha Y_\beta^T = Y_\beta \hat{X_\alpha}^T \hat{C}^T \Phi_J(t) \\ &D^T \Phi_J(t) \Phi_J(t)^T Y_\beta^T \simeq \Phi_J(t)^T \hat{D} Y_\beta^T = Y_\beta \hat{D}^T \Phi_J(t) \end{aligned} \tag{3.9}$$

where $C_\alpha = C^T I^\alpha$, Now substituting Eqs. (3.9) in Eq. (3.8) we obtain:

$$\begin{aligned} X^T \Phi_J(t) &= X_\alpha \hat{A}^T \Phi_J(t) - Y_\beta \hat{X_\alpha}^T \hat{B}^T \Phi_J(t) \\ Y^T \Phi_J(t) &= Y_\beta \hat{X_\alpha}^T \hat{C}^T \Phi_J(t) - Y_\beta \hat{D}^T \Phi_J(t) \end{aligned} \tag{3.10}$$

or

$$\begin{aligned} (X^T - X_\alpha \hat{A}^T + Y_\beta \hat{X_\alpha}^T \hat{B}^T) \Phi_J(t) = 0 \\ (Y^T - Y_\beta \hat{X_\alpha}^T \hat{C}^T + Y_\beta \hat{D}^T) \Phi_J(t) = 0 \end{aligned} \tag{3.11}$$

Finally,

$$\begin{aligned} X^T - X_\alpha \hat{A}^T + Y_\beta \hat{X_\alpha}^T \hat{B}^T = 0 \\ Y^T - Y_\beta \hat{X_\alpha}^T \hat{C}^T + Y_\beta \hat{D}^T = 0 \end{aligned} \tag{3.12}$$

The vector X, Y can be obtained by solving the above system. Consequently determine the approximate value of $X(t), Y(t)$ can be calculated from (3.3). We solve the fractional Lotka-Volterra predator-prey system (1.1) with initial conditions $x(0) = 1.3, y(0) = 0.6$ and $a(t) = t, b(t) =, c(t) = t, d(t) = 1$. Fig. 1 is shown numerical results for $J = 3$ and different values of $\alpha = \beta = 1, 0.95, 0.9$.

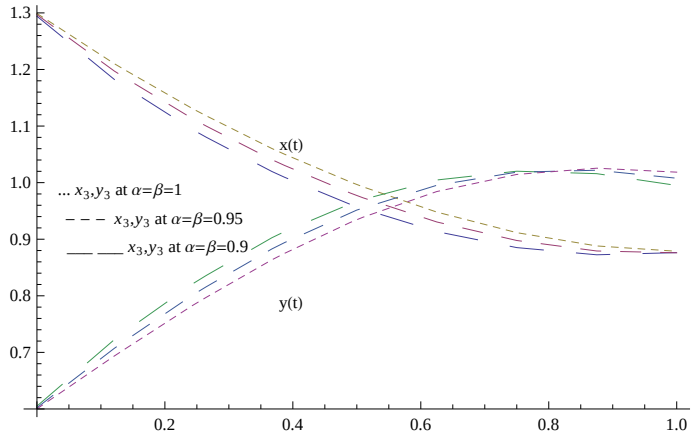

Figure 1: Numerical solutions $x(t), y(t)$ for different values of α, β

References

[123] C. de Boor, *A Practical Guide to Spline*, Springer-Verlag, Berlin, 1978.

[124] H. Jafari, H. tajadodi, *New Method for Solving a Class of Fractional Partial Differential Equations with Applications*, Thermal Science, (22) 1, pp. 277-286, 2018.

[125] A. J. Lotka, *Elements of Physical Biology*, William and Wilkins, Baltimore, Md, USA, 1925.

[126] I. Podlubny, *Fractional Differential Equations*, Academic Press, New York, USA, 1999.

[127] V. Volterra, *Variazioni e fluttuazioni del numero dindividui in specie animali conniventi*, Memorie della Reale Accademia Nazionale delle Scienze, vol. 2-3, pp. 30-111, 1926.